Coordination chemistry of heavy polychalcogenide ligands

Mercouri G. Kanatzidis and Song-Ping Huang

Department of Chemistry and Center for Fundamental Materials Research, Michigan State University, East Lansing, MI 48824 (USA)

(Received 4 January 1993; accepted 24 February 1993)

CONTENTS

Correspondence to: M.G. Kanatzidis, Department of Chemistry and Center for Fundamental Materials Research, Michigan State University, East Lansing, MI 48824, USA.

0010-8545/94/$26.00

ABSTRACT

The coordination complexes of polychalcogenide ligands with metal ions are reviewed. In the past two decades, the chemistry of metal polysulfides has been extensively studied, while a great deal of attention is currently being paid to metal polyselenides and polytellurides. Compounds of metal heavy polychalcogenides are primarily of interest regarding their structure and reactivity, but they also provide potential for being used as soluble precursors to some technologically relevant metal chalcogenides. This article focuses on coordination compounds of metal polyselenides and polytellurides, both homoleptic species and organometallic complexes with heavy polychalcogenide co-ligands, from the synthetic and structural point of view. After giving a comprehensive survey of the compounds known to date according to the periodic table, some applications and an outlook in this research area are discussed.

ABBREVIATIONS

acac	acetylacetonate anion, $[CH_3C(O)CHC(O)CH_3]^-$
Bu_4N^+	tetrabutylammonium cation
Bu_3P	tributylphosphine
Cp	cyclopentadienyl, C_5H_5
crypt	4,7,13,16,21,24-hexaoxa-1,10-diazabicyclo[8,8,8]hexacosane, $N(CH_2CH_2OCH_2CH_2OCH_2CH_2)_3N$
DMAD	dimethyl acetylene dicarboxylate
DMF	*N,N*-dimethylformamide, $HC(O)N(CH_3)_2$
dmos	dimethyloctylsilyl, $(C_7H_{15}CH_2)Si(CH_3)_3$
dmpe	1,2-bis(dimethylphosphino)ethane, $(CH_3)_2PCH_2CH_2P(CH_3)_2$
DMSO	dimethylsulfoxide, $(CH_3)_2SO$
dppe	1,2-bis(diphenylphosphino)ethane, $Ph_2PCH_2CH_2PPh_2$
en	ethylenediamine, $H_2NCH_2CH_2NH_2$
Et_4N^+	tetraethylammonium cation
Me_4N^+	tetramethylammonium cation
N-MeIm	*N*-methylimidazole
OTf	trifluoromethanesulfonate or triflate, $CF_3SO_3^-$
Ph_3P	triphenylphosphine
Ph_4P^+	tetraphenylphosphonium cation
PPN^+	bis(triphenylphosphino)iminium cation, $[(Ph_3P)_2N]^+$
THF	tetrahydrofuran, C_4H_8O
tmeda	*N,N,N',N'*-tetramethylethylenediamine, $(CH_3)_2NCH_2CH_2N(CH_3)_2$
triphos	1,1,1-tris(diphenylphosphinomethyl)ethane, $(Ph_2PCH_2)_3CCH_3$

A. INTRODUCTION

All three elements of Group 16, S, Se and Te, have a tendency to catenate. This results not only in rings or chains of their several elemental forms [1], but also in the polychalcogenide Q_n^{2-} (Q = S, Se, Te; n = 2–6) ions that can exist in solutions [2,3] or in the solid-state [4–22] in various sizes. The versatile chelating abilities of these polyhomoatomic anions towards virtually all metal ions have and continue to breed a new branch of coordination chemistry which is largely characterized by extensive structural diversity. In the past two decades, the coordination chemistry of metal polysulfides has been extensively studied because this system is believed to be relevant to many important processes, such as hydrodesulfurization (HDS) of crude oil [23], hydrogenation of unsaturated and aromatic hydrocarbons [24], biosynthesis of metalloproteins [25], and even the hydrothermal conversion of metals to their binary chalcogenide minerals in nature [26]. The chemistry of metal polysulfides is rich and diverse. Interested readers are encouraged to consult any of the comprehensive review articles available in the literature [27,28]. However, until ca. 1987, the chemistry of metal heavy polychalcogenides (i.e. polyselenides and polytellurides) failed to keep abreast with that of metal polysulfides, as witnessed by the very few sporadic reports of metal compounds containing polyselenide or polytelluride ligands, namely $MeC(CH_2PPh_2)_3Co(Se_4)$ (1) [29], $[(dmpe)_2Ir(Se_4)]Cl$ (2) [30], $(\eta^5\text{-}Cp)_2Ti(Se_5)$ (3) [31], $(\eta^5\text{-}Cp)_2V(Se_5)$ (4) [32], $(\eta^5\text{-}Cp)_2M(Se_4)$ (M = Mo, W) (5,6) [33], $(Ph_4P)_2[Fe_2Se_2(Se_5)_2]$ (7) [34], $(Bu_4N)_4[Hg_4(Te)_2(Te_2)_2(Te_3)_2]$ (8) [35] and $(Ph_4P)_2[Hg_2(Te)(Te_2)_2]$ (9) [35]. Two reasons seem to be primarily responsible for this delayed development. First, the most convenient method for synthesizing metal polysulfide complexes involved the use of H_2S, and this was found to be unattractive for the polyselenide or polytelluride systems (H_2Se is extremely poisonous and H_2Te is highly unstable). Second, initial perception that the chemistry of metal heavy polychalcogenides would more or less parallel that of metal polysulfides had greatly hindered research enthusiasm in this area. As a result, much of our understanding of metal polychalcogenide chemistry up to the mid-1980s had been derived from the metal polysulfide system.

The synthesis, characterization and chemistry of M/Se_x^{2-} and M/Te_x^{2-} compounds became an active area of research with the use of non-aqueous solvents (i.e. DMF, CH_3CN and en, etc.), and the extraction of so-called Zintl phases of polychalcogenides (M_2Se_n or M_2Te_n, M = alkali metal, n = 2–6) in such solvents as the starting materials[36–38]. The initial synthetic efforts in this field were mostly invested on broad exploration throughout the periodic table in order to establish the feasibility of different approaches to new compounds. Three review articles summarizing the various activities of specific research interests have already appeared [39–41]. Since then, investigations have covered almost every group of p-block and d-block elements with a fair degree of success at least for the polyselenide system. Thus, it becomes timely to comprehensively review the state of the art at this stage of its development. The compounds known to date are surveyed according to the periodic table. In addition to covering homoleptic complexes, for the first time, organometallic complexes (mainly Cp- and/or CO-containing com-

pounds) in which the metal centers have a partial polychalcogenide environment are also included. This reflects our own interest as well as the considerable research that is being carried out in this particular field of organometallic chemistry [42–45], and the fact that there appears to be no fundamental change in the behavior of Q_x^{2-} ligands in going from homoleptic, to mixed ligand and to organometallic complexes.

Research in polychalcogenide chemistry has been mostly driven by the motivation to expand our knowledge of structural and bonding principles in these ligands. Therefore, the emphasis is primarily placed on fundamental chemistry rather than on practical applications. However, the potential of using some of these compounds as soluble low temperature precursors to solid-state materials should not be overlooked [46–48]. To illustrate how this can provide practical incentives for the study of these complexes, a few examples of using such soluble complexes to fabricate solid-state thin films or nanoclusters of technologically relevant binary and ternary metal chalcogenides are given [49–53].

We must clarify at this point which compounds qualify to be included in this review. The term "soluble" for describing the molecular complexes formed between metal ions and polychalcogenide ligands has been used extensively, and this convention is also followed here. However, the solubility of these compounds varies greatly, ranging from soluble to completely insoluble in common organic solvents. Actual solubility is apparently not the qualification for the compound to be included in this review. Furthermore, compounds are found to have polymeric frameworks, so even "molecular" is invalid as the term "soluble" often implies in this field. On the other hand, solid state compounds that contain extensive Q–Q bonds are included, as they are distinct from the extended solids of binary or ternary monochalcogenides. In metal polychalcogenide networks, coordination forces are usually responsible for the stabilization of recognizable localized structural units, which are linked via bridging interactions to give rise to polymeric entities. Sometimes, van der Waals forces or ionic interactions are responsible for the formation of such solid-state structures. Our coverage of extended structures is not comprehensive, but rather they are included when deemed relevant to the discussion regarding corresponding molecular species. While such species are included in the same category with coordination compounds, monochalcogenides, the classical pyrite-type dichalcogenides MQ_2 (Q = S, Se and Te; M = Fe, Ru, Os) [54] and trichalcogenides MQ_3 (Q = S and Se; M = Ti, Zr, Hf, Nb and Ta) [55] are not discussed.

B. SURVEY OF SYNTHESES AND STRUCTURES OF SOLUBLE METAL POLYSELENIDES AND POLYTELLURIDES

(i) Homoleptic complexes

Most main group or transition metal ions can form coordination complexes with the polychalcogenide Q_n^{2-} anions being the only ligands. Such compounds are often called "homoleptic" complexes. The synthesis and structural characterization of these compounds are given here in sequence according to the new notation of the periodic table. For

the purposes of this review, Groups 1 and 2 polychalcogenides are not considered coordination complexes and they are only discussed briefly.

(a) The chemistry of Group 1 and Group 2 elements (alkali and alkaline-earth metals)

It has been known since the turn of the century that the electropositive elements, such as alkali or alkaline-earth metals, can partially reduce elemental chalcogens forming polyhomoatomic chalcogen anions [2]. Among the earliest systematic investigators to study the solution chemistry of the electropositive metals and many post-transition nonmetals were Zintl, Klemm and their co-workers [2e,f]. Thus, compounds like A_2Q_n (A = alkali metal) or BQ_n (B = alkaline earth metal) are often referred to as Zintl phases . By using cryptands to sequester the alkali ions, Corbett and co-workers were able to isolate some of these compounds in single-crystal form, and studied their structures by X-ray diffraction [19,20a,56]. The interactions between the electropositive metal ions and the polychalcogenide anions are mostly ionic. The only exception to this may be $[Li(tmeda)]_2[S_6]$ where the S_6^{2-} acts as a bridging ligand, along with two amine molecules, to form coordinative bonds to two Li^+ centers [57]. Studies of the free polychalcogenide ligands themselves are found in these references [5–8,9a–b,11,12,13b,c,14a,c,f,g, 19,20c,21b,c,22a,b]. The predominantly ionic bonding between the alkali metals and chalcogens in these species renders them good starting materials for synthesizing other metal polychalcogenide complexes. Two simple methods for making these materials are (a) heating the stoichiometric amount of metal and chalcogen at elevated temperatures (usually below 500°C), and (b) allowing them to react in liquid ammonia, respectively. A detailed discussion on preparing these materials and their use as reagents is given in the synthetic section of this review.

(b) The chemistry of Group 3 elements (lanthanides and actinides)

Due to the high oxophilicity of the lanthanide and actinide metals, homoleptic complexes cannot be easily prepared in polar organic solvents. The use of molten alkali metal polychalcogenides as both reactants and reaction media provides the great advantage of eliminating possible oxygen sources from the solvent [58]. However, such reactions often give solid-state compounds rather than molecular species. With the reaction temperatures kept within the range of 200–400°C, where most alkali metal polychalcogenides melt, meta-stable phases including some molecular species can be obtained. This is best illustrated by the synthesis of the first example of an f-block metal polyselenide compound, $K_4[U(Se_2)_4]$ (**10**) [59]. Compound **10** was synthesized from a mixture of K_2Se, U and Se in 2:1:8 ratio. The reaction was conducted in a sealed Pyrex ampoule at 300°C for 10 days (cooling 2°C/h). The structure of $[U(Se_2)_4]^{4-}$ anion is shown in Fig. 1. The most conspicuous feature of this molecule is that the entire anion forms a triangulated dodecahedron (see Fig. 2). Eight Se atoms are located at the corners of two trapezoids which lie orthogonal to each other. However, the $[U(Se_2)_4]^{4-}$ is distorted from an ideal dodecahedron in two respects. First, the bases of the Se trapezoids intersect at the U center, leaving the four basal Se atoms in a nearly square-planar arrangement; in an ideal

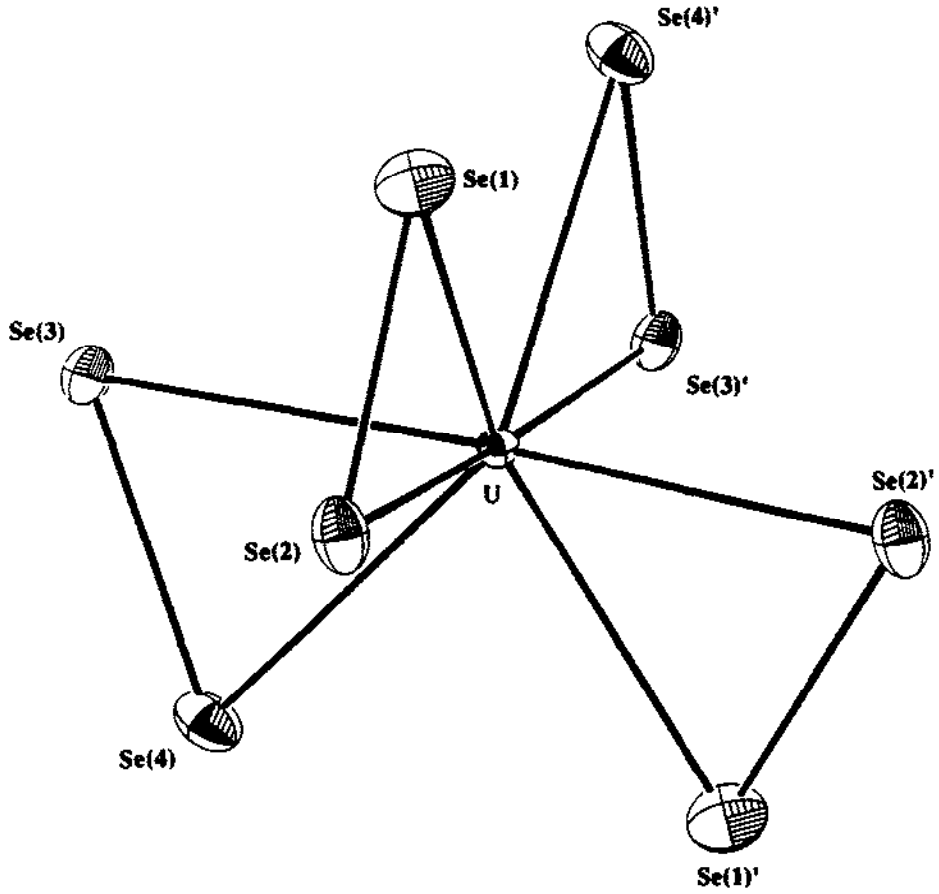

Fig. 1. The structure of $[U(Se_2)_4]^{4-}$.

dodecahedron, the trapezoids slice further into each other. Secondly, the presence of the Se–Se bonds necessitates that the corresponding Se–U–Se angle be smaller than in an ideal dodecahedron (49.05° versus 73.69°). The U–Se bond distances are in the range of 2.840(3) to 2.923(3) Å, while the Se–Se bond distances are 2.385(4) and 2.401(4) Å. Strong paramagnetic behavior, conforming to the Curie–Weiss law, was observed for $K_4[U(Se_2)_4]$ from 120 K upwards. Below this region, a transition is observed at ca. 90 K, and is then followed by antiferromagnetic ordering which has a critical temperature of 65 K. The μ_{eff} at 300 K is $3.82\mu_B$, consistent with an f^2 (U^{4+}) configuration where $L \neq 0$.

No other f-metal polychalcogenides with molecular structures are known to date. As mentioned above, the molten salt synthesis often produces solid-state compounds. For example, under the same conditions, the molten salt synthesis with Ce in place of U gave a solid-state compound, $K[Ce(Se_2)_2]$ (11), which has a two-dimensional structure containing eight-coordinated Ce^{3+} centers bridged by the Se_2^{2-} ligands [60].

(c) The chemistry of Group 4 elements (Ti, Zr and Hf)

To the best of our knowledge, no molecular homoleptic compounds of polyselenides or polytellurides containing any of these elements have been reported.

(d) The chemistry of Group 5 elements (V, Nb and Ta)

Compound $(Et_4N)_2[V_2(Se_2)_4(Se_5)]$ (**12**), formed by the reaction of NH_4VO_3 with $(dmos)_2Se$ in a toluene/acetonitrile solution in the presence of Et_4NCl and Et_3N [61], was the first vanadium polyselenide. The generation of diselenide and pentaselenide ligands in this molecule is believed to be achieved by the redox reaction between V^{5+} and the "selenization" agent $(dmos)_2Se$. The formal oxidation state of the vanadium in the structure is 4+. The structure of the diamagnetic $[V_2(Se_2)_4(Se_5)]^{2-}$ anion is shown in Fig. 3. Four Se_2^{2-} ligands are split into two different groups according to their coordination modes. Two of these act as μ–η^2-type ligands to bridge the vanadium centers, others are each chelated to a vanadium atom. Finally, a Se_5^{2-} chain spans two metal centers, completing the heptacoordination at the vanadium atoms. In addition, the V–V distance of 2.779(5) Å suggests a single metal–metal bond. The molecule possesses a pseudo-, seven-membered V_2Se_5 ring which adopts a chair conformation (Fig. 3). The average V–Se bond distances are 2.518(6) Å to the μ–η^2 Se_2^{2-} units, 2.350(11) and 2.428 Å to the terminal Se_2^{2-} ligands, and 2.505(2) Å to the Se_5^{2-} chain.

Methanothermal reactions of vanadium metal with K_2Se_4 at 135°C lead to the formation of two dimeric compounds $K_4[V_2O_2Se_2(Se_4)_2]\cdot 2MeOH$ (**13**) and $K_4[V_2O_2Se_2(Se_2)(Se_4)]\cdot 0.65MeOH$ (**14**) [62]. Compound **13** was prepared by carrying out the reaction in a sealed Pyrex tube for 4 days, while **14** was obtained when the reaction was run in an autoclave for 30 days. Although not strictly homoleptic, the obvious structural and electronic relationship of these compounds to homoleptic W/Se and Mo/Se

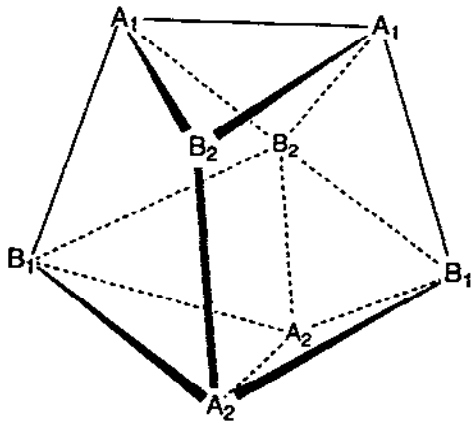

Fig. 2. An ideal triangulated dodecahedron. The intersecting trapezoids are bounded by A_n, apex positions, and B_n, basal positions. In the case of $[U(Se_2)_4]^{4-}$, the center of the dodecahedron and the points B_1, B_1, A_1, and A_1 lie in the same plane.

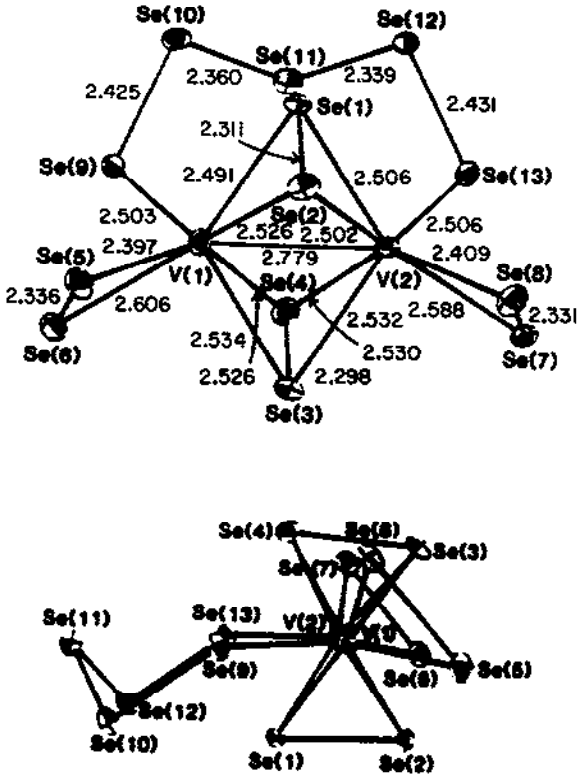

Fig. 3. Two views of $[V_2(Se_2)_4(Se_5)]^{2-}$.

complexes (vide infra) makes it useful to discuss these complexes here. Compound **13** crystallizes in the space group *Pnc*2 (No. 30) with two crystallographically independent, but structurally similar $[V_2O_2Se_2(Se_4)_2]^{4-}$ anions. Figures 4 and 5 depict the structures of the anions $[V_2O_2Se_2(Se_4)_2]^{4-}$ (two independent molecules) and $[V_2O_2Se_2(Se_2)(Se_4)]^{2-}$, respectively. In both compounds the vanadium is coordinated in a square-pyramidal fashion by a bidentate tetraselenide Se_4^{2-} (or a Se_2^{2-}), two μ_2-Se^{2-} and an apical O^{2-} ligand. The oxygen atoms are thought to originate from MeOH or trace H_2O. The average V–Se bond distances are 2.459 Å in **13** and 2.451 Å in **14**, and the average V–O bond distances are 1.61 Å in **13** and 1.64 Å in **14**. The V–V distances of 2.93(1) Å in **13** and 2.958(7) Å in **14** are much longer than that found in **12**, suggesting significantly weaker V–V interactions. It is found that, in the competition between oxygen, sulfur, selenium or tellurium for the apical positions in this type of compounds, oxygen often wins [63–65]. For the significantly oxophilic vanadium, this tendency is even greater. Although compounds of this type are rather common in the Mo(W) polychalcogenide chemistry, which displays a homologous family with the formula $[M_2X_2(Q_x)(Q_y)]^{2-}$ (M = Mo, W; X = O, S, Se; Q = S, Se) [63,64a,66–67], this is the first time such a compound is observed for a metal outside Group 6. With V^{4+} replacing Mo^{5+} (W^{5+}) in the structure, the d^1 electronic configuration

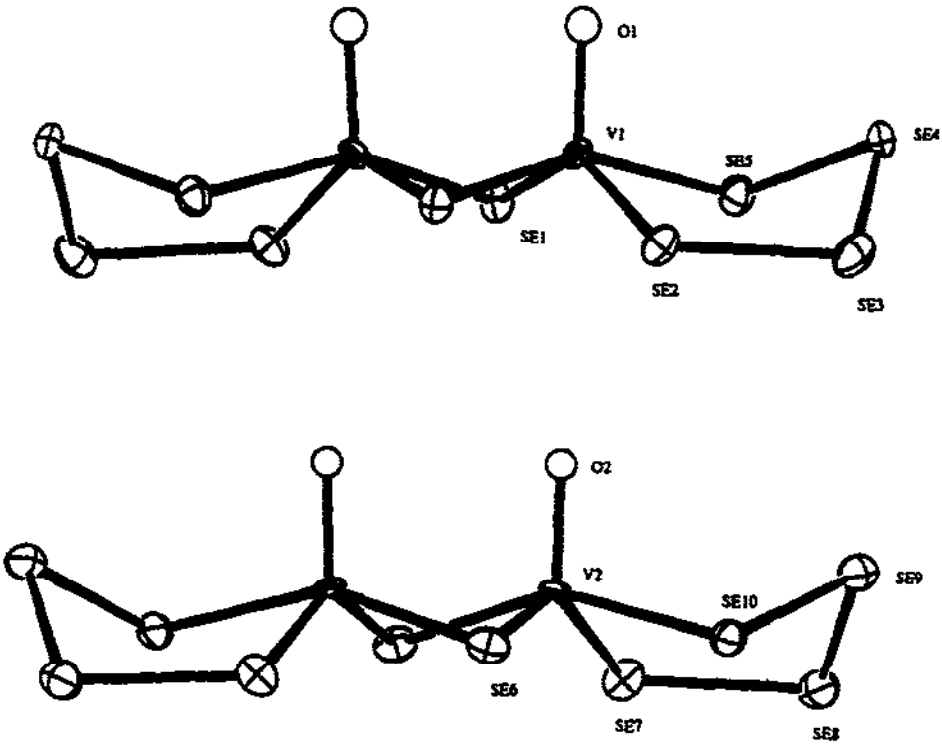

Fig. 4. Structures of the two $[V_2O_2Se_2(Se_4)_2]^{4-}$ anions found in the $K_4[V_2O_2Se_2(Se_4)_2]\cdot 2MeOH$ crystal lattice.

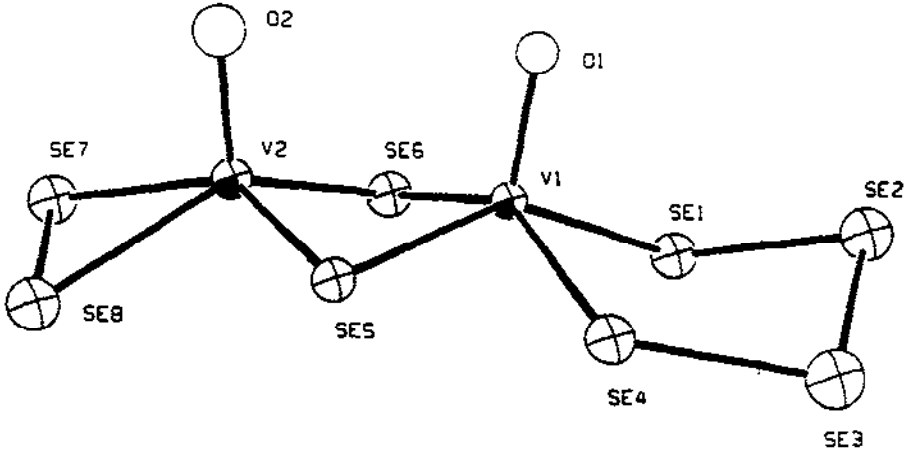

Fig. 5. The structure of $[V_2O_2Se_2(Se_2)(Se_4)]^{4-}$.

is retained, but the molecule becomes a tetraanion. Having twice the negative charge of its Mo analog, the V complexes are less likely to crystallize readily with four of the same large organic cations except perhaps with a great deal of solvent co-crystallization. On this account, the use of a small alkali ion such as K^+, coupled with the methanothermal technique, has allowed for the isolation of these two compounds.

Niobium also forms a cluster with polyselenide ligands. $K_6[Nb_4Se_4(Se_2)_9]$ (**15**), synthesized through the reaction of K_2Se, Nb and Se in a 3:1:10 ratio at 375°C for 100 h [68]. The $[Nb_4Se_4(Se_2)_9]^{6-}$ anion is a tetramer, consisting of two $[Nb_2Se_2(Se_2)_4]^{2-}$ dimers linked by a *trans*-$\mu-\eta^1,\eta^1$-Se_2 unit, as shown in Fig. 6. Each niobium is surrounded by seven selenium atoms of either terminal Se^{2-}, side-on Se_2^{2-}, bridging *trans*-$\mu-\eta^1,\eta^1$-Se_2 or $\mu-\eta^1,\eta^2$-Se_2 ligands. All metal centers have a formal oxidation state 5+, which accounts for the observed long Nb···Nb distance (i.e. 3.679(3) Å). The Nb–Se and Se–Se bond distances average 2.683(3) and 2.358(3) Å, respectively.

The reaction of $NbCl_5$ with K_2Te_4 in DMF in the presence of Ph_4PBr afforded an unusual tellurium-rich complex $(Ph_4P)_3[NbTe_{10}]$-DMF (**16**) [36a]. This molecule is peculiar in that the decatelluride ligand forms a "teepee" of tellurium inside which a niobium atom is nested as shown in Fig. 7. First, three tellurium atoms constitute a Te_3 ring at the base of the teepee. They are each bound to another tellurium atom, giving a second triangular layer, lying slightly above the first. A third layer is obtained by three more tellurium atoms eclipsed to the second one. Finally, an apical tellurium atom closes the teepee at the top. Thus, the molecule possesses a pseudo-C_3 axis running through the apex and the center of the Te_3 base. The niobium atom is coordinated by seven tellurium ligands, three from each of the second and third tellurium layers and one apical tellurium. The geometry around this atom is best described as a capped trigonal prism. Unlike ordinary polychalcogenide ligands where each atom is usually defined as either "internal" or "terminal" for bookkeeping purposes on the formal charge, simple valence bond theory seems to produce little information on the formal charge of this polytelluride ligand. This makes it difficult to clarify the oxidation state of the niobium in this structure. The compound is

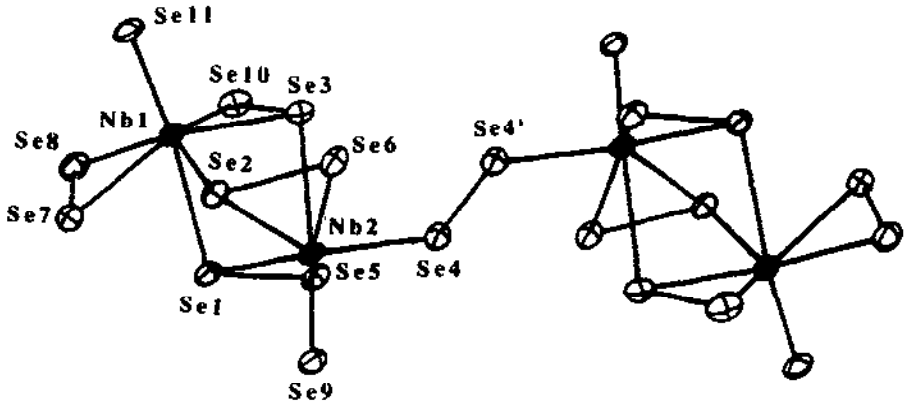

Fig. 6. The structure of $[Nb_4Se_4(Se_2)_9]^{6-}$.

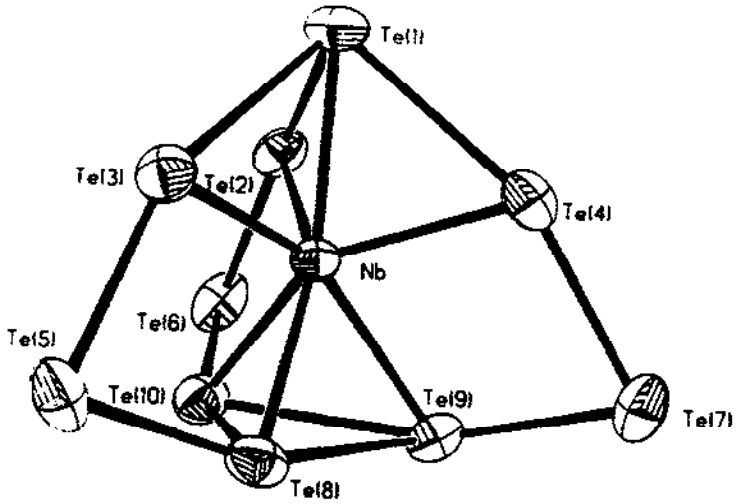

Fig. 7. The structure of $[NbTe_{10}]^{3-}$.

found to be diamagnetic in the solid state. So any bonding consideration for this molecule should be consistent with this observed magnetic behavior. The Nb–Te bond distances vary from 2.757(2) to 2.857(2) Å, while the Te–Te distances exhibit considerable discrepancy throughout the structure, ranging from 2.818(2) to 3.161(2) Å. Recently, an extended Hückel calculation on this molecule has shed some light on its electronic structure [69]. Complementary to the localized bonding picture described above, the calculation did suggest that strong mixing between Te and Nb orbitals, caused by the similar electronegativities of the two elements (i.e. 2.1 versus 1.8), is the most important factor for stabilizing the cluster. Te–Te antibonding interactions are responsible for the observed long Te–Te bond distances. It is also pointed out that two-electron oxidation of this species might be possible, which should result in shorter bonds in the base of the Te_{10} cage.

(e) The chemistry of Group 6 elements (Cr, Mo and W)

A number of monomeric compounds in the family of $[MX(Q_4)_2]^{2-}$, whereby M is molybdenum or tungsten, X can be oxygen, sulfur or selenium, and Q selenium or tellurium, are readily accessible by simple synthetic methods. These complexes are analogous to the known polysulfide ions $[MX(S_4)_2]^{n-}$ (X = O, S; M = Mo, $n = 2$ [63], M = Re, $n = 1$ [70]). So far, the structurally characterized species include $[MoSe(Se_4)_2]^{2-}$ (**17**) obtained by reacting $[MoSe_4]^{2-}$ with grey [71] or red [64b] elemental selenium, $[MoO(Se_4)_2]^{2-}$ (**18**) [64b] obtained by reacting $[MoSe_4]^{2-}$ with $(NC_5H_{10})_2Se_2$, $[WS(Se_4)_2]^{2-}$ (**19**) [64b] obtained by reacting $[WSe_4]^{2-}$ with SeS_2, $[MoO(Te_4)_2]^{2-}$ (**20**) [72], and $[WO(Te_4)_2]^{2-}$ (**21**) [72] by reacting K_2Te_2 with $MoCl_5$ or WCl_5, respectively. In addition, $[WSe(Se_4)_2]^{2-}$ (**22**), $[WO(Se_4)_2]^{2-}$ (**23**) and $[MoS(Se_4)_2]^{2-}$ (**24**) were also prepared in a similar manner [64b]. Scheme 1 depicts the structure of these ions. They all show a square-pyramidal

Scheme 1. Structure of the $[MX(Q_4)_2]^{2-}$, where M = Mo or W; X = O, S or Se and Q = Se or Te.

metal center surrounded by two Se_4^{2-} (or Te_4^{2-}) ligands along with a terminal atom of selenium, sulfur or oxygen. The metal centers are often displaced from the basal planes towards the apical atoms. In almost all structures, the Mo–X_{apical} bond distances are shorter than expected, suggesting a significant multiple bond character [64b,71,72]. The MSe_4 in **17**, **18** and **19** rings are all puckered while the MTe_4 rings in **20** and **21** have an envelope conformation.

Formation of the five-membered MQ_4 rings in this monomeric series may prove to be thermodynamically favored. No matter what polychalcogenide is involved, the molecule invariably contains tetrachalcogenide ligands. Furthermore, the apical positions of all structures are readily susceptible to oxygen attack.

It is found that the Q–Q bond distances in the above structures alternate within each MQ_4 ring. Typically, the internal Q–Q bonds are somewhat shorter than the external ones [73]. This is very common for five-membered metal-polychalcogenide rings, with some more pronounced than others. A plausible explanation may be that M($d\pi$)–Q($d\pi$) interactions depopulate the HOMO of the Q_4^{2-} ligand, and therefore decrease the antibonding effect between the two internal chalcogen atoms[74,75]. From this point of view, the degree of alternation in the Q–Q bond distances is the consequence of certain $d\pi$ orbital overlap between the metal and chalcogen, thus it is subject to variation from compound to compound. Generally, complexes of d^2 and d^8 metals show a pronounced Q–Q bond alternation whereas d^{10} metal complexes do not. Table 1 compares the distances of the internal and external Q–Q bonds in various compounds containing MQ_4 rings.

A common phenomenon observed in tungsten polyselenide chemistry is that different species often co-crystallize from the same reaction solution due to the complex equilibria involving multiple components. This is also prevalent in many polysulfide systems of this group [63,66a]. When a methanol solution of $[WSe_4]^{2-}$ was acidified by CH_3COOH, a co-crystallizate of $(Ph_4P)_2[(W_3Se_9)_{0.46}(W_3OSe_8)_{0.54}]$ (**25**) was obtained with the ratio derived from the X-ray crystallographic results [64a,76]. The presence of oxygen was also qualitatively confirmed by Auger spectroscopy. Longer reaction times seemed to increase the proportion of $(Ph_4P)_2[W_3OSe_8]$ in the product. Pure $(Ph_4P)_2[W_3Se_9]$ (**26**) can be prepared by refluxing $[WSe_4]^{2-}$ in acetonitrile [64a]. When this thermal reaction was carried out in DMF at 85°C, the product contained pure **26** (35% yield) and another co-crystallizate $(Ph_4P)_2[\{W_2Se_4(Se_2)(Se_3)\}_{0.66}\{W_2Se_4(Se_2)(Se_4)\}_{0.34}]$ (**27**) (45% yield) [64a,76]. If $[WSe_4]^{2-}$ is refluxed with elemental selenium in acetonitrile, two isomers of $(Ph_4P)_2[W_2Se_{10}]$, i.e. $(Ph_4P)_2[W_2Se_4(Se_2)(Se_4)]$ (**28**) and $(Ph_4P)_2[W_2Se_4(Se_3)_2]$ (**29**), are

TABLE 1

Comparison of the Q–Q bond distances in the MQ_4-containing compounds

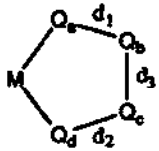

Compound	d_1 and d_2 (Å)	d_3 (Å)	Reference
$[V_2O_2Se_2(Se_2)(Se_4)]^{4-}$	2.385(4), 2.473(5)	2.338(5)	[62]
$[V_2O_2Se_2(Se_4)_2]^{4-}$	A: 2.385(6), 2.447(6)	A: 2.342(7)	[62]
molecules A and B	B: 2.376(6), 2.424(6)	B: 2.342(6)	
$[MoSe(Se_4)_2]^{2-}$	2.384(5), 2.461(5)	2.291(5)	[71]
	2.395(5), 2.446(5)	2.307(5)	
$[MoO(Se_4)_2]^{2-}$	2.390(1), 2.446(2)	2.303(2)	[64b]
	2.399(2), 2.425(1)	2.304(2)	
$[WS(Se_4)_2]^{2-}$	2.416(2), 2.514(2)	2.300(2)	[64b]
	2.419(2), 2.458(2)	2.301(2)	
$[MoO(Te_4)_2]^{2-}$	2.763(2), 2.838(2)	2.686(2)	[72]
$[WO(Te_4)_2]^{2-}$	2.778(2), 2.858(2)	2.682(2)	[72]
$[CpMo(Se_4)_2]^{-}$	2.381, 2.399	2.310	[135b]
	2.365, 2.419	2.342	
$[Cr(CO)_4(Te_4)]^{2-}$	2.705(1), 2.750(1)	2.717(1)	[153]
$[W(CO)_4(Te_4)]^{2-}$	2.703(1), 2.764(2)	2.719(1)	[153]
$[W_2Se_4(Se_2)(Se_4)]^{2-}$	2.314, 2.327	2.282	[76]
$[Mn(Se_4)_2]^{2-}$	A: 2.325(5), 2.328(5)	A: 2.339(5)	[85]
molecules A and B	2.318(6), 2.333(5)	2.346(5)	
	B: 2.336(5), 2.338(5)	B: 2.340(5)	
	2.329(6), 2.365(8)	2.395(7)	
$[Fe(CO)_2(Se_4)_2]^{2-}$	2.354(5), 2.357(8)	2.316(9)	[171]
	2.323(9), 2.327(9)	2.325(9)	
$[Ru(CO)_2(Se_4)_2]^{2-}$	2.346(1), 2.353(1)	2.323(1)	[176]
	2.339(1), 2.369(1)	2.3 15(1)	
$[(dmpe)_2Ir(Se_4)]^{2-}$	A: 2.340(3), 2.340(3)	A: 2.301(5)	[30]
molecules A and B	B: 2.305(4), 2.305(4)	B: 2.251(7)	
$[Ni(Se_4)_2]^{2-}$	2.344(1), 2.398(1)	2.321(1)	[86]
$[Pd(Se_4)_2]^{2-}$	2.340(2), 2.352(2)	2.329(3)	[14d]
	2.353(3), 2.362(2)	2.330(3)	
$[Pt(Se_4)_3]^{2-}$	2.330(5), 2.337(5)	2.342(2)	[98]
	2.342(5), 2.343(5)	2.342(5)	
	2.338(5), 2.342(5)	2.3 15(5)	
$[Pd(Te_4)_2]^{2-}$	2.754(2), 2.764(2)	2.705(2)	[94a]
	2.763(2), 2.768(2)	2.695(2)	
$[Au_2Se_2(Se_4)_2]^{2-}$	2.332(3), 2.357(3)	2.304(2)	[108]
$[Cu_2(Te_4)_3]^{4-}$	A: 2.722(4), 2.722(4)	A: 2.743(4)	[105]
molecules A and B	2.716(4), 2.726(4)	2.774(4)	
	B: 2.713(4), 2.746(4)	B: 2.722(4)	

TABLE 1 (*continued*)

Compound	d_1 and d_2 (Å)	d_3 (Å)	Reference
$[Ag_2(Te_4)_3]^{4-}$ molecules A and B	A: 2.732(2), 2.743(2) 2.725(2), 2.732(2) B: 2.733(2), 2.741(2)	A: 2.750(2) 2.780(2) B: 2.745(2)	[105]
$[Zn(Se_4)_2]^{2-}$	2.323(3), 2.323(3) 2.338(3), 2.338(3)	2.334(5) 2.321(4)	[115]
$[Cd(Se_4)_2]^{2-}$	2.332(4), 2.332(4) 2.344(4), 2.344(4)	2.340(8) 2.321(6)	[115]
$[Hg(Se_4)_2]^{2-}$	2.313(4), 2.313(4) 2.331(3), 2.331(3)	2.341(5) 2.324(4)	[115]
$[In_2Se_2(Se_4)_2]^{2-}$	2.320(3), 2.325(3)	2.340(4)	[130]
$[In_2(Se_4)_4(Se_5)]^{4-}$	2.245(6), 2.412(6) 2.177(6), 2.251(7)	2.446(6) 2.436(7)	[127]
$[In_3Se_3(Se_4)_3]^{3-}$	2.337(4), 2.346(4) 2.343(7), 2.419(5) 2.328(4), 2.369(4)	2.330(4) 2.319(7) 2.320(4)	[130]
$[Tl_3Se_3(Se_4)_3]^{3-}$	2.323(8), 2.351(8) 2.324(8), 2.359(8) 2.265(12), 2.371(10)	2.333(8) 2.325(8) 2.271(13)	[130]
$[NaIn_6Se_6(Se_4)_6]^{5-}$	2.345(6), 2.351(6)	2.314(7)	[131]
$[Ti_4Se_4(Se_2)_2(Se_4)_2]^{4-}$	2.300(10), 2.351(9)	2.319(8)	[133]
$[Sn(Se_4)_3]^{2-}$	2.327(4), 2.341(4) 2.320(4), 2.337(4) 2.308(4), 2.319(4)	2.302(4) 2.328(4) 2.332(4)	[135a]

obtained in a ratio of 73% to 27% [64a,76]. The formation of four-membered MSe_3 rings in **29** seems to be unique because it only occurs in the M^{n+}/Se_x^{2-} system. No metal polysulfide compounds containing MS_3 rings are known. Attempts to separate these two isomers were said to be unsuccessful. The structures of all these anions are reproduced in Fig. 8. The representative bond distances and bond angles are given in each drawing. Except for **25** which contains no Se–Se bonds, these molecules only differ in the size of their MSe_x rings. Again, all metal centers have a distorted square-pyramidal coordination geometry. In addition, there are metal–metal bonds in all structures.

Compared to the tungsten system, little is known about the oligomeric molybdenum polyselenide chemistry. This may be attributed to the fact that under the same conditions molybdenum polychalcogenide compounds are more difficult to crystallize than their tungsten analogs. The following compound seems to be the only isolated and structurally characterized molybdenum species in the above family. $Cs_2[Mo_2O_2Se_2(Se_2)_2]$ (**30**) was prepared by the hydrothermal method at 110°C [77]. Figure 9 shows the structure of the $[Mo_2O_2Se_2(Se_2)_2]$ anion.

Recently, the application of the hydrothermal technique to the synthesis of transition metal polychalcogenide compounds has suddenly opened up a new avenue to the

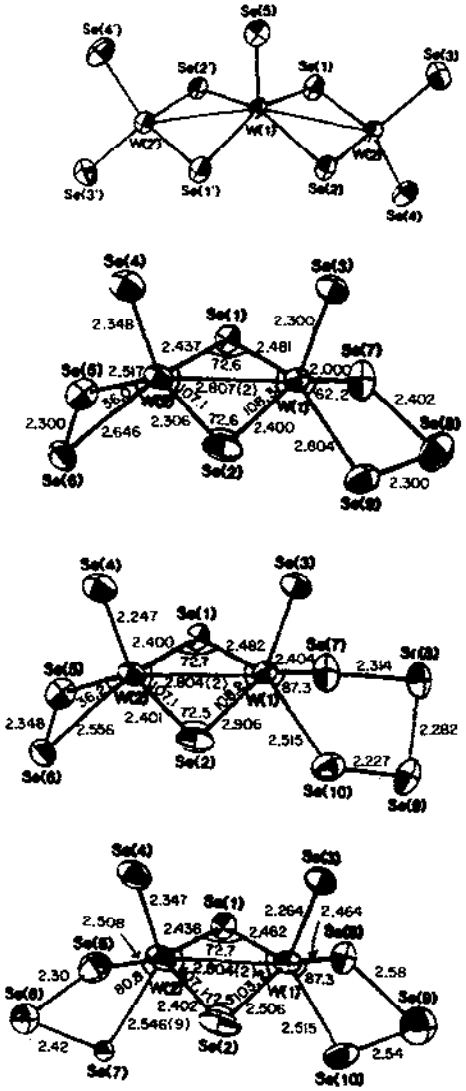

Fig. 8. The structures of $[W_3Se_9]^{2-}$, $[W_2Se_4(Se_2)(Se_3)]^{2-}$, $[W_2Se_4(Se_2)(Se_4)]^{2-}$ and $[W_2Se_4(Se_3)_2]$.

cluster chemistry of molybdenum polyselenides. This was first demonstrated by the preparation of a large cluster $K_{12}[Mo_{12}Se_8(Se_2)_{18}(Se_3)_4]$ (31) as the prelude [78,79]. Compound 31 was prepared by reacting Mo metal (0.5 mmol) with 2 equiv. of K_2Se_4 and 0.3 ml of water in a sealed Pyrex tube at 140°C for 60 h. The structure of $[Mo_{12}Se_8.(Se_2)_{18}(Se_3)_4]^{12-}$ is shown in Fig. 10. It is a cluster made up of four smaller trinuclear sub-

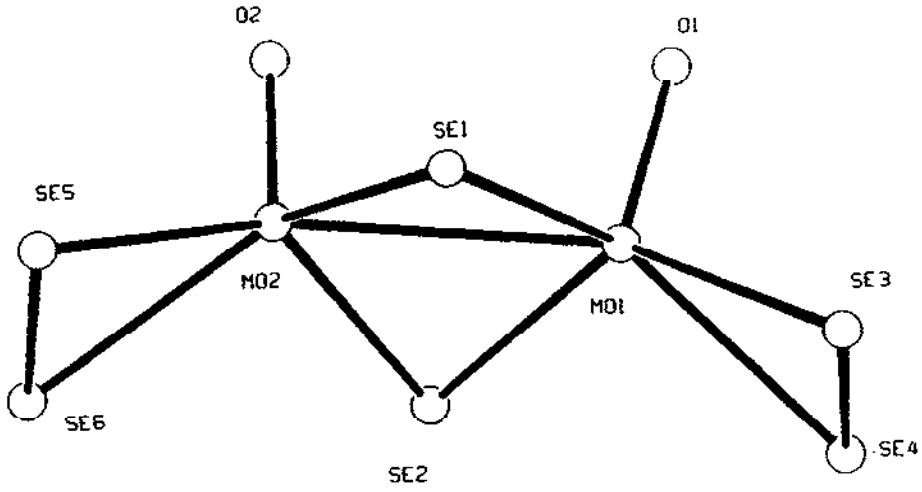

Fig. 9. The structure of $[Mo_2O_2Se_2(Se_2)_2]^{2-}$.

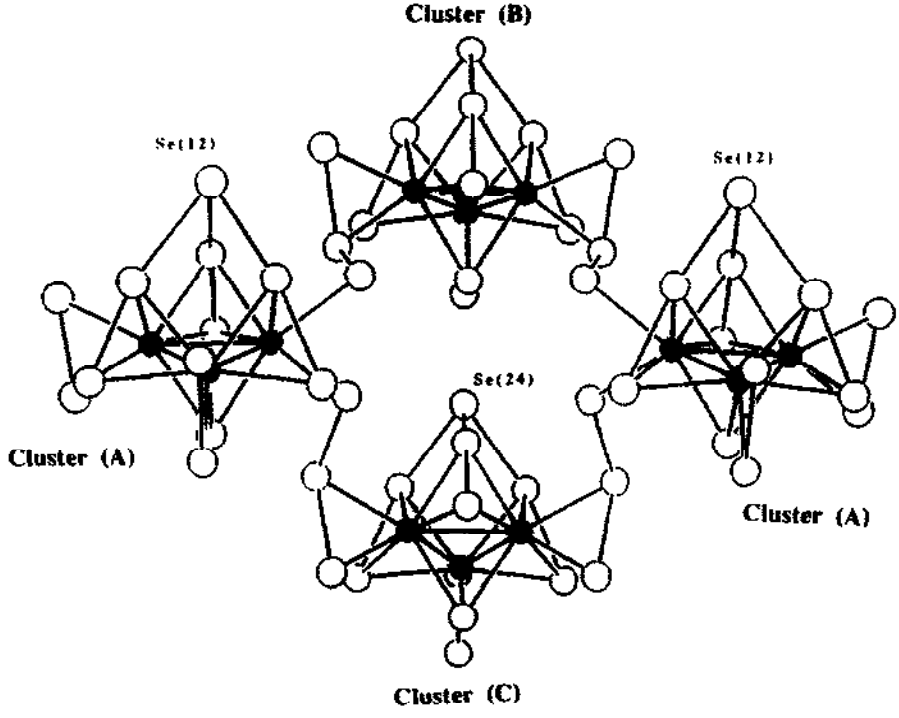

Fig. 10. The structure of $[Mo_{12}Se_8(Se_2)_{18}(Se_3)_4]^{12-}$. The black circles represent Mo atoms. The open circles represent Se atoms.

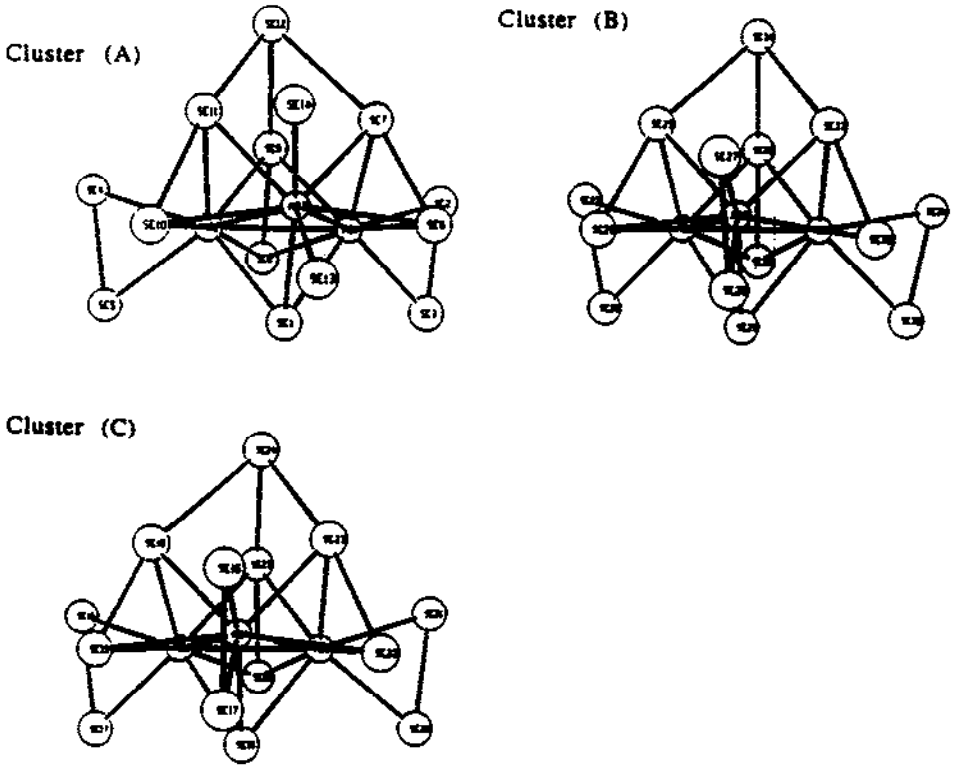

Fig. 11. The structures of three different subclusters in the $[Mo_{12}Se_8(Se_2)_{18}(Se_3)_4]^{12-}$ anion.

clusters with slightly different structures. These subclusters can be divided into three different types, i.e. A, B and C, whose structures are shown in Fig. 11. Since B and C are both connected to A and also bisected by a crystallographic mirror plane, the main cluster $[Mo_{12}Se_8(Se_2)_{18}Se_3)_4]^{12-}$ contains two A units, one B and one C unit connected together in the sequence of A–B–A–C. There is extensive M–M bonding in each Mo_3 units with an average Mo–Mo distance of 2.75(2) Å. If we neglect the Mo–Mo bonds, the molybdenum atoms have heptacoordination with a formal oxidation state of 4+. The most striking feature of these subclusters is that an extra selenium atom interacts with the selenium atoms of the three Se_2^{2-} ligands as shown in Fig. 10 and Scheme 2, forming a $[Se_7]^{8-}$ umbrella-

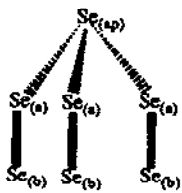

Scheme 2. Structure of the umbrella-like $[Se_7]^{8-}$ fragment in **31**.

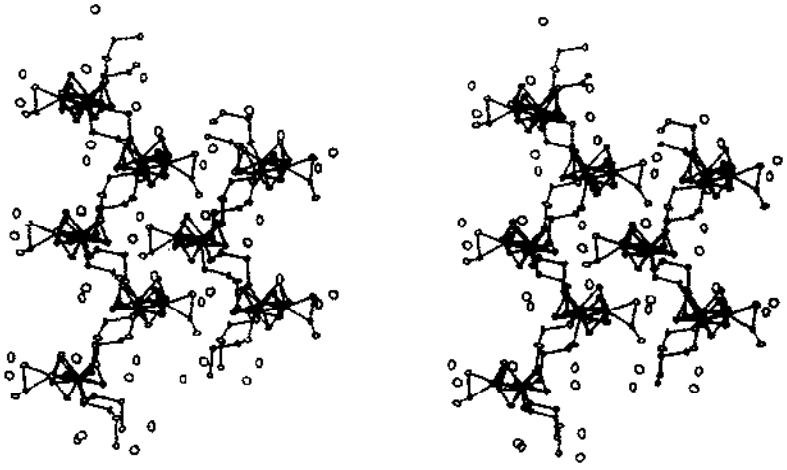

Fig. 12. A stereoview of two "interlocking" zigzag chains in $[Mo_3Se(Se_2)_3(Se_3)(Se_4)_2]_n^{2n-}$. The isolated circles are K atoms.

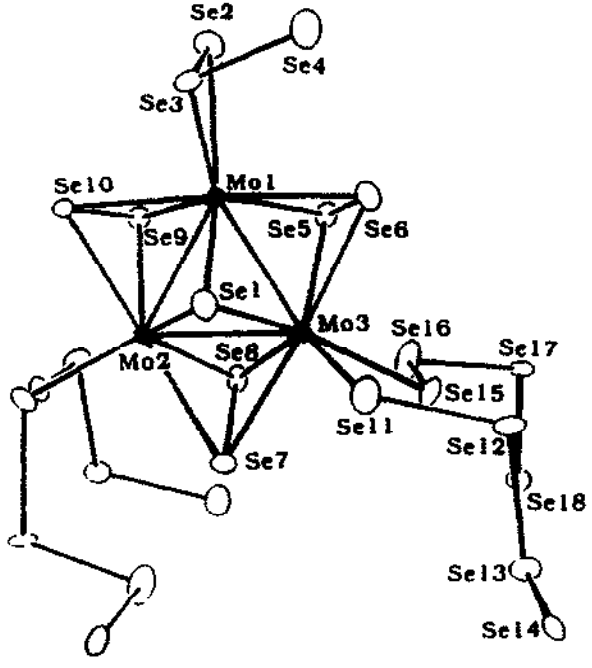

Fig. 13. Structure of the repeating unit $[Mo_3Se(Se_2)_3(Se_3)(Se_4)_2]^{2-}$.

like fragment with the $Se_{(ap)}$–$Se_{(a)}$ distances ranging from 2.56(1) to 3.03(1) Å (average 2.76(15) Å).

Further exploration of this system under hydrothermal conditions revealed that this is a very fertile area in metal polychalcogenide chemistry. For instance, the reaction of Mo metal, K_2Se_4 and H_2O in 1:1.5:222 ratio at 135°C for 3 days yielded $K_2[Mo_3Se(Se_2)_3(Se_3)(Se_4)_2]$ (**32**) [80]. The reaction of MoO_3, K_2Se_2 and H_2O in 1:2:222 ratio under the same conditions as above yielded $K_8[Mo_9(Se)_4(Se_2)_{18}]\cdot 4H_2O$ (**33**) [80]. Compound **32** is the first known molybdenum polyselenide polymer.

The structure of $[Mo_3Se(Se_2)_3(Se_3)(Se_4)_2]_n^{2n-}$ is illustrated in Fig. 12. It consists of a zigzag chain structure made up of the repeating unit shown in Fig. 13. In this unit, the same trinuclear $[Mo_3(\mu_3\text{-}Se)(\mu_2\text{-}Se_2)_3]^{4+}$ cluster core, as found in **31** is also recognizable as a building block. The one-dimensional chain is formed through the cross-linking at Mo(2) and Mo(3) by bridging Se_4^{2-} ligands. In addition, a terminal selenium atom from the Se_3^{2-} ligand at Mo(1) stretches out to the center of three selenium atoms of three μ_2-Se_2^{2-} ligands of the $[Mo_3(\mu_3\text{-}Se)(\mu_2\text{-}Se_2)_3]^{4+}$ cluster in a neighboring chain, as shown in Fig. 14. This generates a similar $[Se_7]^{8-}$ "umbrella" as shown in Scheme 3. Such an un-

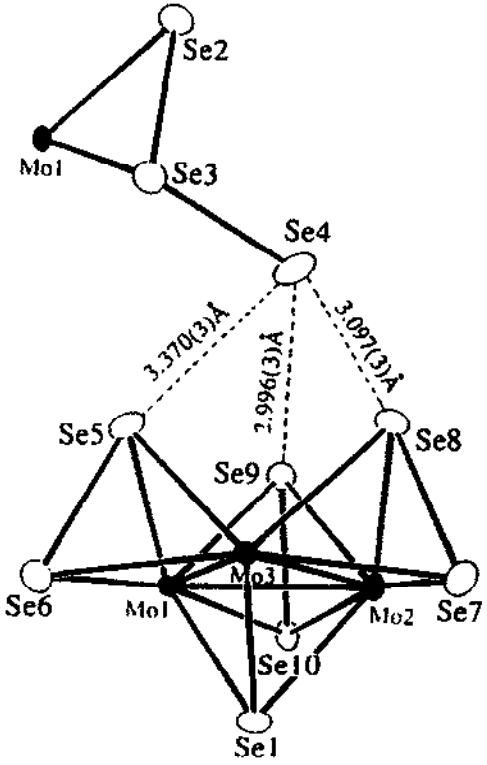

Fig. 14. Interaction between the Se_3^{2-} ligand and the $[Mo_3(\mu_3\text{-}Se)(\mu_2\text{-}Se_2)_3]^{4+}$ core in $[Mo_3Se(Se_2)_3(Se_3)(Se_4)_2]_n^{2n-}$.

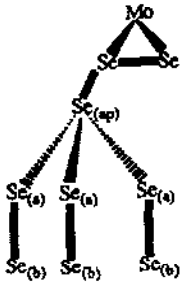

Scheme 3. Structure of a different type of the umbrella-like $[Se_7]^{8-}$ fragment in **32**.

usual bridging interlocks the different chains, and gives the structure a two-dimensional character. The average distance between Se and Se is 3.15(16) Å, while the average Mo–Mo distance is 2.77(1) Å with the molybdenum atoms all in the 4+ oxidation state.

The $[Mo_9(Se)_4(Se_2)_{18}]^{8-}$ anion is also assembled with the same trinuclear $[Mo_3(\mu_3\text{-}Se)(\mu_2\text{-}Se_2)_3]^{4+}$ core. It contains a linear array of three such clusters designated as A, B and C along with an encapsulated selenium atom sitting in a pocket created by two triangular rings of six selenium atoms from each three μ_2-Se_2^{2-} ligands in E and F, as shown in Fig. 15. Such an interaction creates an intriguing $[Se_{13}]^{x-}$ "double-umbrella" as shown in Scheme 4.

On the other hand, the μ_3-Se^{2-} ligand from B now acts as an apical selenium atom to the triangular ring of three selenium atoms from the three μ_2-Se_2^{2-} ligands in A, resulting in yet another type of $[Se_7]^{8-}$ "umbrella", as shown in Scheme 5. Finally, there is an unusually short intercluster Se(28)···Se(28) distance of 2.98(1) Å between two different $[Mo_9(Se)_4(Se_2)_{18}]^{8-}$ clusters involving a terminal diselenide ligand in C. These two clusters are related by a crystallographically imposed inversion center as shown in Fig. 16. The distance between the $Se_{(ap)}$ atom and the six Se atoms in the double umbrella ranges from 2.80(2) to 3.182(9) Å, while that between the $Se_{(ap)}$ atom and the three Se atoms in the single umbrella has an average value of 3.13(6) Å. The average Mo–Mo distance in all clusters is 2.77(1) Å.

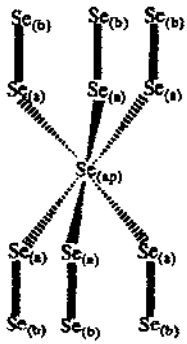

Scheme 4. Structure of the double umbrella-like $[Se_{13}]^{x-}$ fragment in **33**.

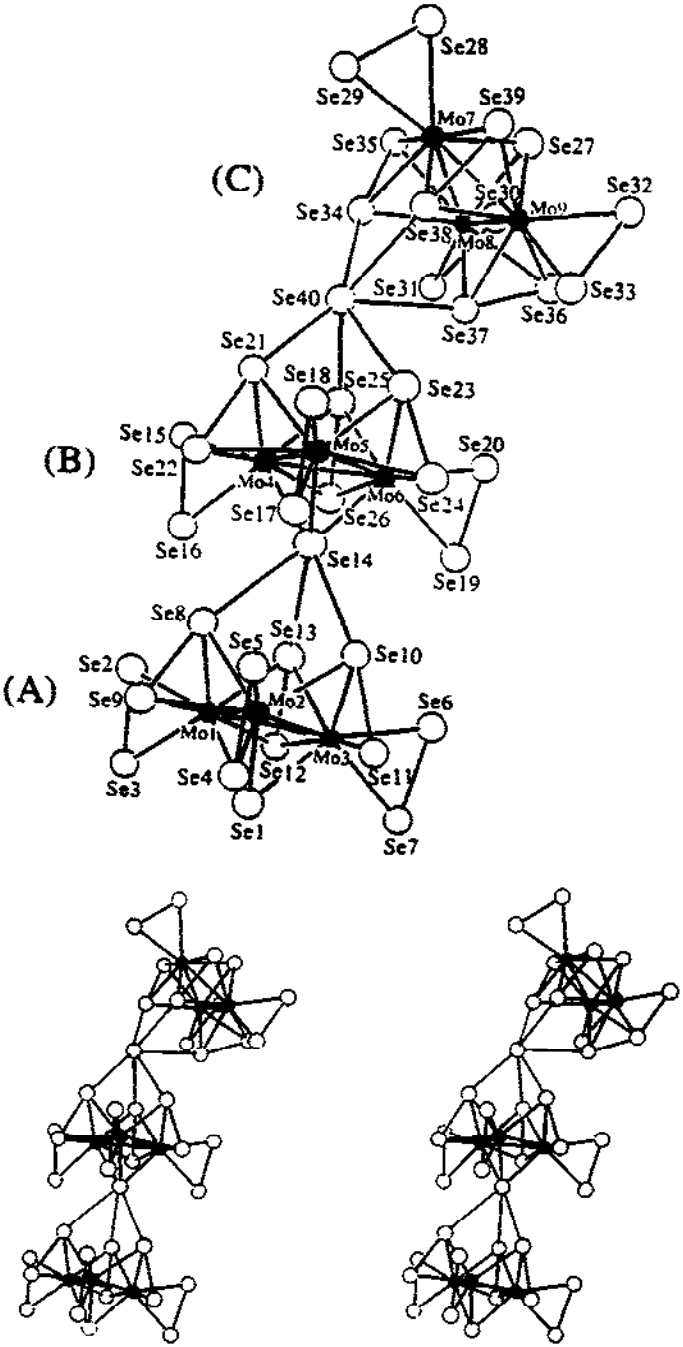

Fig. 15. The structure of $[Mo_9(Se)_4(Se_2)_{18}]^{8-}$. Top: ORTEP representation and labeling scheme of the $[Mo_9(Se)_4(Se_2)_{18}]^{8-}$ anion. Bottom: stereoview of the $[Mo_9(Se)_4(Se_2)_{18}]^{8-}$ anion. Black circles represent Mo atoms.

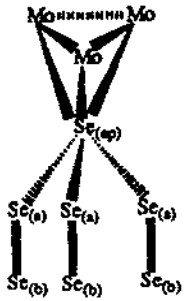

Scheme 5. Structure of a third type of the umbrella-like $[Se_7]^{8-}$ fragment in **33**.

Slight variation of the reaction conditions in the $MoO_3/K_2Se_2/H_2O$ system leads to the isolation of different clusters. For example, increase in the reaction time gives rise to $K_6[Mo_6(Se)_3(Se_2)_{12}]\cdot 4H_2O$ (**34**) [81], which can be thought of as an excised fragment

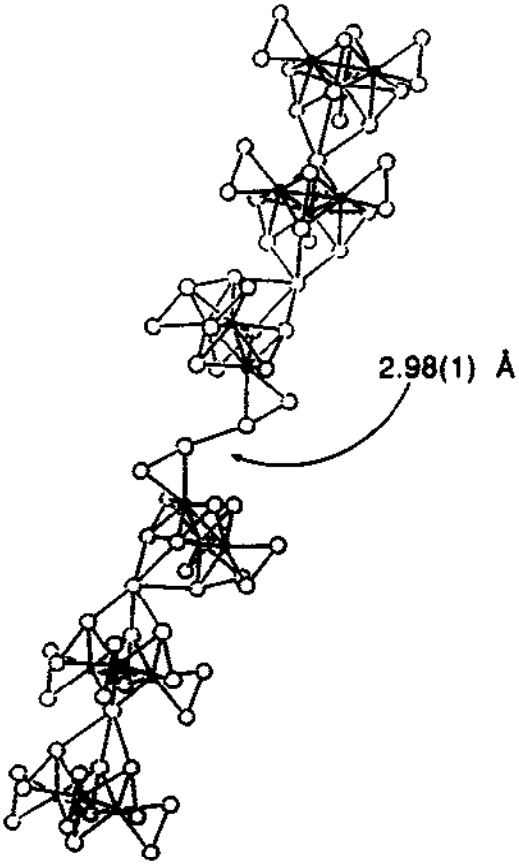

Fig. 16. The intercluster relationship between two $[Mo_9(Se)_4(Se_2)_{18}]^{8-}$ anions.

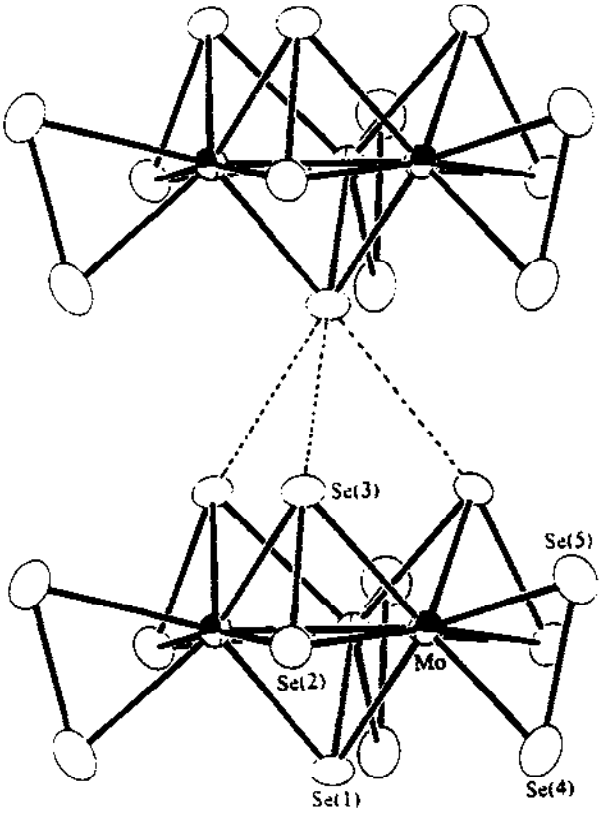

Fig. 17. The structure of $[Mo_6(Se)_3(Se_2)_{12}]$.

from 33. This cluster simply contains the same subclusters found in 33 without any intercluster Se···Se interaction (Fig. 17). Prolonged heating (up to 30 days) will eventually degrade the product to the isolated trinuclear cluster $K_2[Mo_3(Se)(Se_2)_6]$ (35). Figure 18 shows the structure of $[Mo_3(Se)(Se_2)_6]^{2-}$. The sulfur analog of this cluster has been known for some time [82]. It is found that the cluster $[Mo_3(Se)(Se_2)_6]^{2-}$ can best be made with Me_4N^+ as the counterion [81].

The reaction of $Mo_2(OOCH_3)_4$ with K_2Te_4 in en in the presence of cryptand results in the very interesting cluster compound $[K(crypt)]_2[Mo_4(Te_2)_5(Te_3)_2(en)_4]$ (36) [37] which contains two face-sharing $Mo{\equiv}Mo^{6+}$ subunits connected together by a μ_4-Te_2^{2-} and two μ_2-Te_3^{2-} ligands as illustrated in Fig. 19. Between each $Mo{\equiv}Mo^{6+}$ subunit reside two μ_2,η^1-Te_2^{2-} ligands. The octahedral coordination of the molybdenum is completed by a bidentate en molecule. The cluster possesses virtual C_{2h} symmetry with a crystallographically imposed inversion center at the midpoint of the μ_4-Te_2^{2-}. The Mo–Mo bond distances are 2.469(3) Å in the $Mo{\equiv}Mo^{6+}$ subunits.

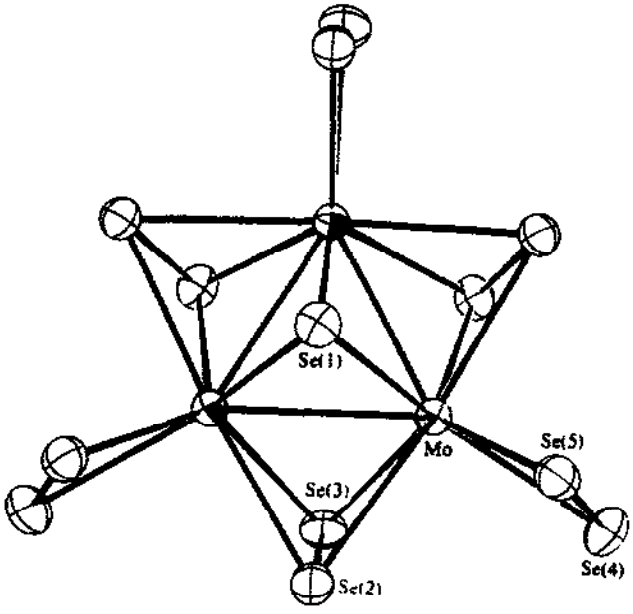

Fig. 18. The structure of $[Mo_3(Se)(Se_2)_6]^{2-}$.

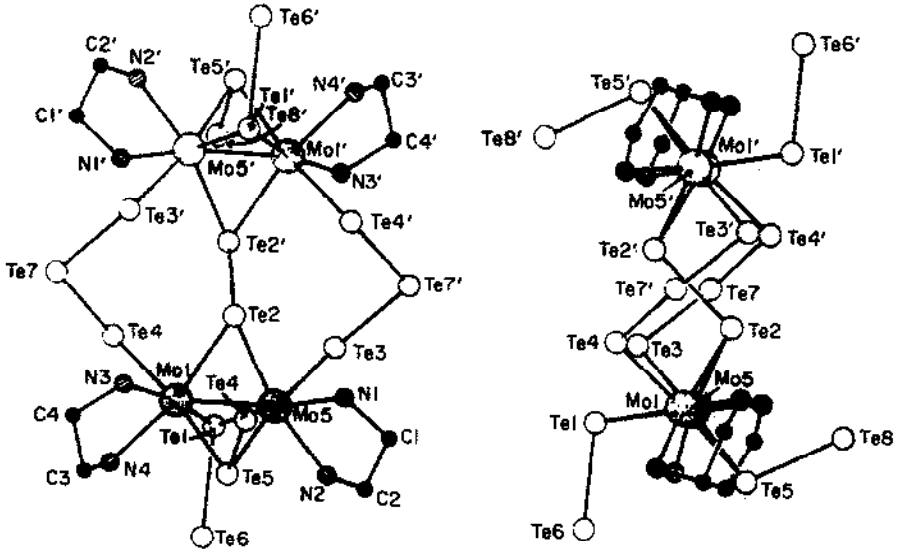

Fig. 19. Two different views of $[Mo_4(Te_2)_5(Te_3)_2(en)_4]^{2-}$

The chemistry of chromium appears to be profoundly different. Thus far, analogs of the aforementioned compounds that contain high-valent metal centers have not been obtained with chromium. Instead, chromium forms two trinuclear clusters with the heavy polychalcogenides in which the metal is found to be invariably in the 3+ oxidation state [36b]. Compounds $(Ph_4P)_3[Cr_3(Se_4)_6]$ (37) and $(Ph_4P)_3[Cr_3(Te_4)_6]$ (38) have a similar structure, although they crystallize in different unit cells. They were prepared by reacting $CrCl_3$ with K_2Se_3 or K_2Te_2 in DMF. Figure 20 shows the structure of the

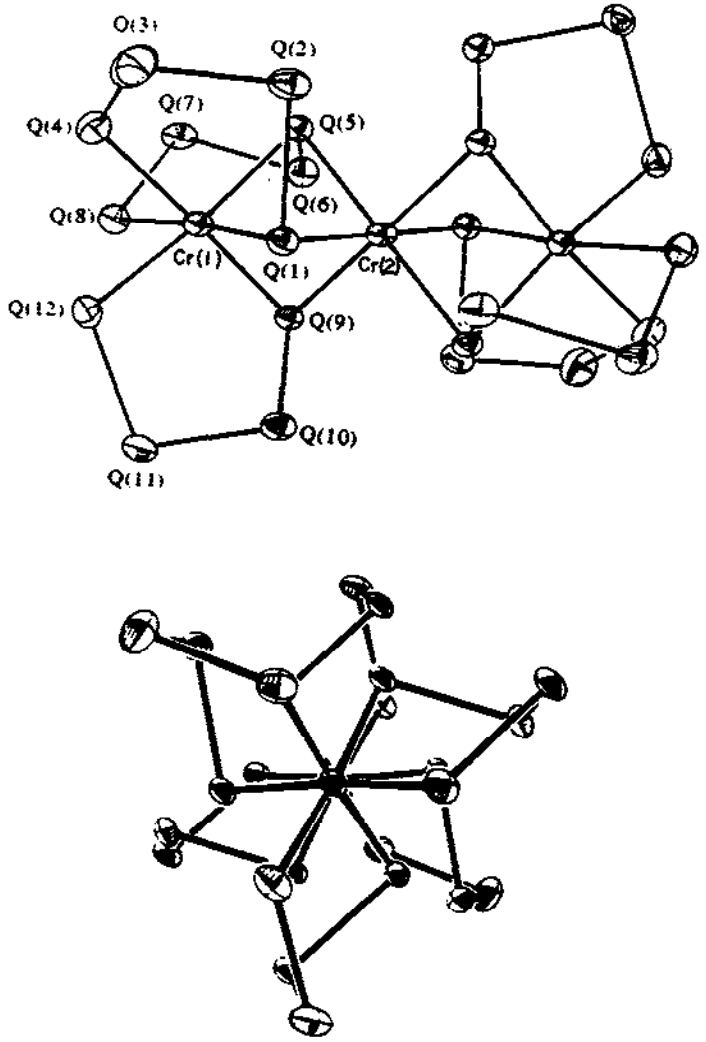

Fig. 20. The structure of $[Cr_3(Q_4)_6]^{3-}$ (O = Se or Te). The top view emphasizes the metal coordination and the bottom view shows the S_6 molecular symmetry.

$[Cr_3(Q_4)_6]^{3-}$ (Q = Se or Te) anion. With Q = Se, two crystallographically independent anions were found in the same unit cell. These linear clusters can be viewed as being formed by two $[Cr(Q_4)_3]^{3-}$ molecules coordinating to a third Cr^{3+} each through one of the triangular Q_3 faces defined by three adjacent terminal atoms in the chelating Q_4^{2-} ligands. All chromium atoms are thus octahedrally coordinated. Both compounds are paramagnetic with $\mu_{eff} = 5.25\mu_B$ for **37** and $5.74\mu_B$ for **38** at 300 K, respectively, consistent with a $S = 3/2$ spin system with reasonably strong antiferromagnetic coupling in each case. It is noteworthy that $[Cr(Q_4)_3]^{3-}$ belongs to the $[M(bidentate)_3]$ system, and should give rise to optical isomerism [83]. With an inversion center located at the central metal atom in **37** and **38**, the molecules possess S_6 symmetry with the improper axis running through the chromium atoms. Thus, these compounds are two rare examples of purely inorganic meso compounds. The Cr–Cr distances of 3.20 Å in **37** and 3.41 Å in **38** rule out any possibility for metal–metal bonding in these two structures. Interestingly, homoleptic chromium polysulfide complexes have not been reported to date [27,28].

(f) The chemistry of Group 7 elements (Mn and Re)

The only homoleptic compound found in this group is $(Ph_4P)_2[Mn(Se_4)_2]$ (**39**) [84–86]. This compound is either isostructural, or has a structurally similar anion to the

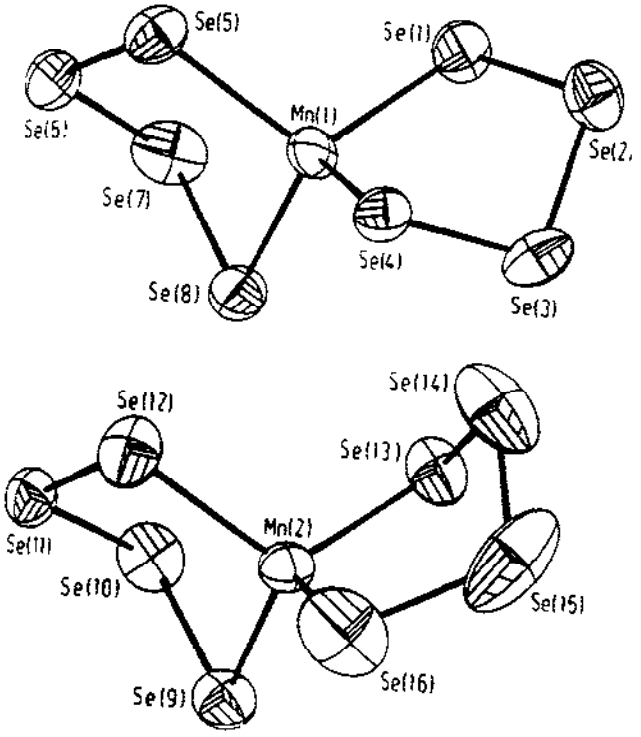

Fig. 21. Structures of the two $[Mn(Se_4)_2]^{2-}$ anions found in the $(Ph_4P)_2[Mn(Se_4)_2]$ crystal lattice.

many metal octachalcogenide analogs in which the divalent transition-metal atoms have a tetrahedral or square-planar coordination with two bidentate Q_4^{2-} (Q = S, Se or Te) ligands (vide infra) [87]. Compound **39** can be readily prepared by reacting $MnCl_2 \cdot 4H_2O$ with Li_2Se_6 in DMF [85], or by reacting anhydrous $MnCl_2$ with K_2Se_5 in the same solvent [86]. In addition, the complete oxidative decarbonylation of $Mn_2(CO)_{10}$ by K_2Se_3 also provides a convenient access to this compound [84]. This compound, regardless of its preparation route, crystallizes in the space group $P2_1$ (No. 4) with two crystallographically independent anions in the same unit cell. Figure 21 shows the two structurally similar anions found in the crystal lattice. The metal centers are each tetrahedrally coordinated by two Se_4^{2-} ligands with all the MSe_4 rings having an envelope conformation. The average Mn–Se bond distance is 2.545 Å, while the Se–Se distances range from 2.292 to 2.327 Å [84].

(g) The chemistry of Group 8 elements (Fe, Ru and Os)

Compound $(Ph_4P)_2[Fe_2Se_2(Se_5)_2]$ (7) is among the first homoleptic species of transition metal heavy polychalcogenides whose structures have been authenticated early by X-ray single-crystal analysis [34]. Compound 7 was prepared by reacting $FeCl_2$ with 6 equiv. of elemental selenium in the presence of sodium metal in DMF at 70°C. This compound was found to have almost the same structure as its sulfur analog $(Ph_4P)_2[Fe_2S_2(S_5)_2]$ (**40**) [88]. The structure of $[Fe_2Se_2(Se_5)_2]^{2-}$ anion is shown in Fig. 22. This spiro-tricyclic molecule consists of a central Fe_2Se_2 rhomb and two $FeSe_5$ rings. The former is situated on a crystallographic inversion center giving rise to a perfectly planar Fe_2S_2 ring. The six-membered $FeSe_5$ rings have a chair conformation with a dihedral angle of 72.3°. Two Fe^{III} atoms are tetrahedrally coordinated by monoselenide Se^{2-} and pentaselenide Se_5^{2-} ligands. The molecule possesses idealized C_{2h} symmetry. The Fe–Se bond distances are Fe–Se(1) 2.329(2), and Fe–Se(1') 2.317(2) Å. The average Se–Se distance is 2.337 Å, while the Fe···Fe distance is 2.787 Å. Recently, this $[Fe_2Se_2(Se_5)_2]^{2-}$ molecule has been obtained again as the PPN^+ salt through the reaction between

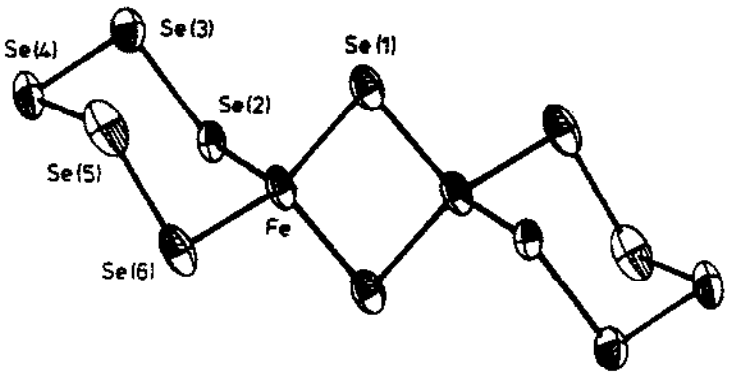

Fig. 22. The structure of $[Fe_2Se_2(Se_5)_2]^{2-}$ anion found in the $(Ph_4P)_2[Fe_2Se_2(Se_5)_2]$.

FeCp(CO)I and Li_2Se_6 in DMF at 100°C [89]. $(PPN)_2[Fe_2Se_2(Se_5)_2]\cdot 2DMF$ (**41**) contains the same anion as found in **7**.

The easy isolation of the Fe^{III} complex from the above two redox reactions between the Fe^{II} salt and polyselenide ligands might have suggested that Fe^{III} is the only "compatible" oxidation state with exclusively polyselenide ligands. Thus, the Fe^{II} species had not been seriously sought until recent careful scrutiny on this system in our laboratory revealed that the Fe^{II} does form a stable homoleptic polyselenide compound, under proper conditions [90]. The $(Ph_4P)_2[Fe(Se_4)_2]$ (**42**) can be readily obtained by reacting $FeCl_2$ with 2 equiv. of Na_2Se_2 in DMF at room temperature and crystallizes in two different space groups. α-$(Ph_4P)_2[Fe(Se_4)_2]$ is isostructural with the $(Ph_4P)_2[Mn(Se_4)_2]$ (**39**) (space group $P2_1$ (No. 4); vide supra), having two crystallographically independent $[Fe(Se_4)_2]^{2-}$ anions in the same unit cell, while the β-form crystallizes in the space group $P\bar{1}$ (No. 2) with only one $[Fe(Se_4)_2]^{2-}$ anion in the asymmetric unit. Nevertheless, X-ray single-crystal structure studies show that all $[Fe(Se_4)_2]^{2-}$ anions have a similar structure as illustrated in Fig. 23. The compound is paramagnetic, obeying Curie–Weiss law in the temperature range of 10 K to 300 K. The μ_{eff} is consistent with a high spin tetrahedral d^6 configuration.

Numerous unsuccessful attempts have been made in our laboratory to prepare homoleptic polysulfido(selenido) complexes of ruthenium by using various ruthenium salts such as $RuCl_3$, $Ru(DMSO)_2Cl_2$ or $Ru(acac)_3$, etc. as starting materials [91]. Due to complex electron transfer processes between Ru^{n+} and Q_x^{2-} (Q = S or Se, $x = 2$–4), these reactions often yielded very ill-defined mixtures possibly containing ruthenium in different oxidation states. Furthermore, pure species could not be extracted from such mixtures by fractional crystallization. So far, there are no reports of homoleptic complexes of polychalcogenides for ruthenium or for its heavy congener osmium [27,28]. The first Ru/Se_x^{2-} complex contains CO co-ligands and it is described elsewhere in this review.

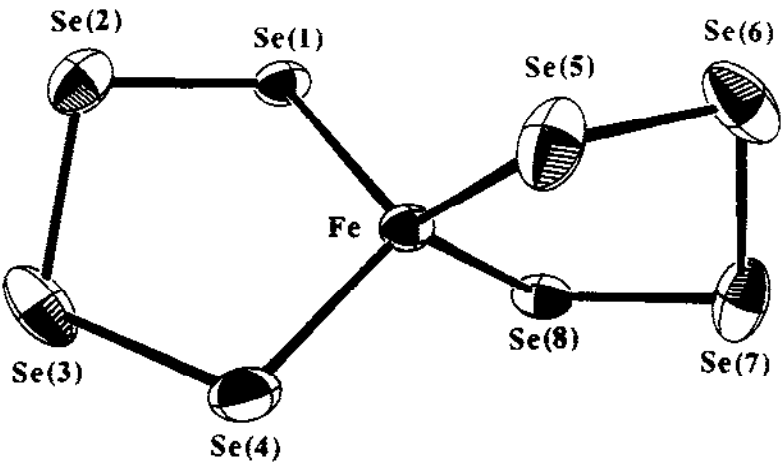

Fig. 23. The structure of $[Fe(Se_4)_2]^{2-}$ anion found in β-$(Ph_4P)_2[Fe(Se_4)_2]$.

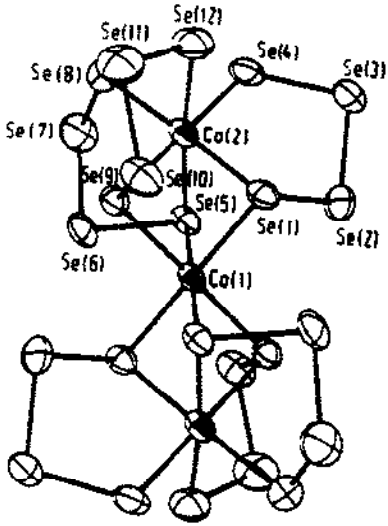

Fig. 24. The structure of $[Co_3(Se_4)_6]^{3-}$.

(h) The chemistry of Group 9 elements (Co, Rh and Ir)

From the three elements in this group, only cobalt forms a homoleptic complex. $(PPN)_3[Co_3(Se_4)_6]\cdot 2DMF$ (**43**) can be prepared by reacting $CoCl_2\cdot 6H_2O$ with Li_2Se_6 in DMF in the presence of PPNCl at 100°C [89]. The structure of $[Co_3(Se_4)_6]^{3-}$, as shown in Fig. 24, is analogous to the two Cr^{3+} polychalcogenides, $[Cr_3(Q_4)_6]^{3-}$ (Q = Se or Te, vide supra). The average Co–Se distance is 2.37 Å, and the average Se–Se distance 2.36 Å.

(i) The chemistry of Group 10 elements (Ni, Pd and Pt)

In this group we find a rare example in which polysulfides, polyselenides and polytellurides form analogous isostructural complexes of the type $[M(Q_4)_2]^{2-}$ (M = Zn, Cd, Hg, Mn, Ni or Pd, vide infra). Otherwise, such a similarity is rather an exception than a rule in M^{n+}/Q_x^{2-} systems. The representative structure formed by the elements of this group with polychalcogenide ligands is the square-planar assembly shown in Scheme 6 with the formula $[M(Q_4)_2]^{2-}$ (when Q = S or Se, M = Ni or Pd and when Q = Te, M = Pd). Thus, along with the known $[Ni(S_4)_2]^{2-}$ [87a,b] and $[Pd(S_4)_2]^{2-}$ [87a], the $[Ni(Se_4)_2]^{2-}$ [86,92], $[Pd(Se_4)_2]^{2-}$ [14d,86] and $[Pd(Te_4)_2]^{2-}$ [93,94] were synthesized and structurally characterized. All of these anions have essentially the same structure which contains a square-planar metal center chelated by two Q_4^{2-} ligands. $(Ph_4P)_2[Ni(Se_4)_2]$ (**44**) [92a] and

Scheme 6. The structure of the $[M(Q_4)_2]^{2-}$ anions, where M = Ni or Pd; Q = Se or Te.

$(Ph_4P)_2[Pd(Se_4)_2]$ (45) [14d] are isostructural to each other (space group $P21$ (No. 4)), but $(Ph_4P)_2[Pd(Te_4)_2]$ (46) [93] crystallizes in a different space group ($P\bar{1}$ (No. 2)). In 44, both MSe_4 rings have the half-chair conformation [92a]. In $(PEtPh_3)_2[Ni(Se_4)_2]$ (47) [86], the molecule is situated on an inversion center and the $NiSe_4$ ring has a distorted envelope conformation. In $(Ph_4P)_2[Pd(Se_4)_2]$ (45), both $PdSe_4$ rings have the half-chair conformation [14d]. In 46, both $PdTe_4$ rings have the half-chair conformation while in $(Ph_4P)_2[Pd(Te_4)_2]\cdot DMF$ (48) [94] both $PdTe_4$ rings have the envelope conformation.

The existence of polyselenide species containing the square-planar Pt^{2+} is nebulous although claims have been made, based on spectroscopic data and elemental analyses, that $[Pt(Se_4)_2]^{2-}$ [14d,86] are stable in both solution and in the solid state. In the polysulfide system, X-ray diffraction studies confirmed that all $[Pt(S_5)_3]^{2-}$ [95,96], $[Pt_4S_4(S_3)_6]^{4-}$ and $[Pt(S_4)_2]^{2-}$ [97] are stable compounds. To date, only the high-valent platinum polyselenide complexes $[Pt(Se_4)_3]^{2-}$ [98] and $[Pt_4Se_4(Se_3)_6]^{4-}$ [97] are structurally confirmed. The $(Ph_4P)_2[Pt(Se_4)_3]\cdot DMF$ (49) can be prepared by reacting $Pt(xanthate)_2$ with Li_2Se_5 (generated in situ) in DMF in the presence of Ph_4PCl [98]. The structure of the $[Pt(Se_4)_3]^{2-}$ anion consists of a central Pt^{4+} ion chelated by three Se_4^{2-} ligands as shown in Fig. 25. The coordination geometry of Pt^{4+} in this complex is octahedral approaching D_3 symmetry, with the Pt–Se bond distance varying from 2.479(4) to 2.491(4) Å. All $PtSe_4$ rings have the envelope conformation. The Pt^{4+} center in the molecule was generated by the redox reaction between the Pt^{2+} and the polyselenide. It should be noted that this molecule can give rise to optical isomerism. The above compound is a racemic mixture similar to the $[M(bidentate)_3]$ class of complexes [83].

It is now generally recognized that polyselenide ligands are more tolerant than their sulfur counterparts towards the different oxidation states of metal centers to which they are bound. The ability of polyselenides to stabilize the higher oxidation state as well as

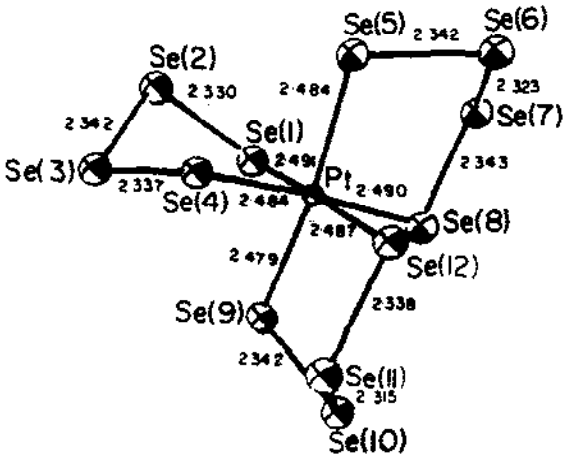

Fig. 25. The structure of $[Pt(Se_4)_3]^{2-}$.

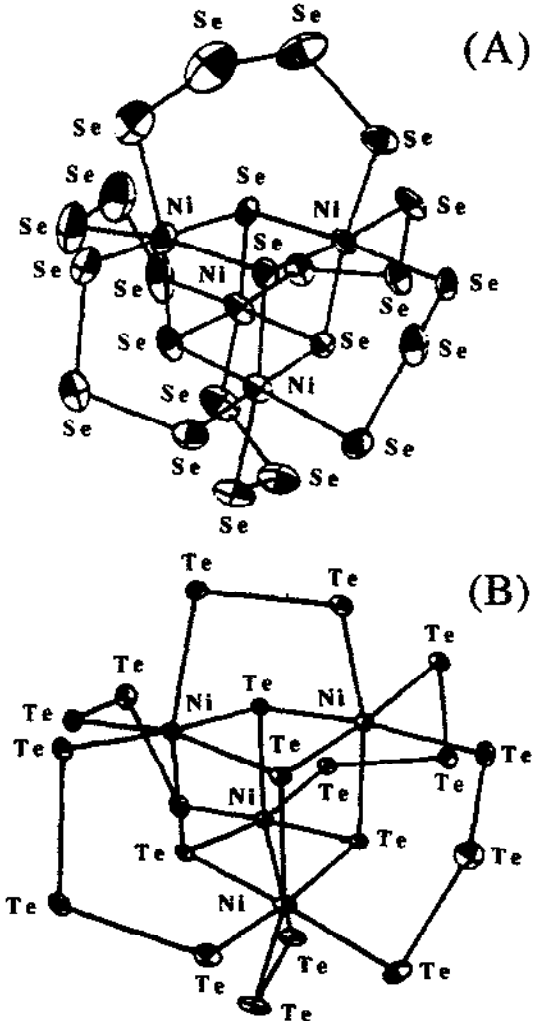

Fig. 26. The structures of (A) $[Ni_4Se_4(Se_3)_5(Se_4)]^{4-}$ and (B) $[Ni_4Te_4(Te_2)_2(Te_3)_4]^{4-}$.

the "normal" oxidation state of the transition metal is manifested by the formation of compounds where the metal centers can adopt different oxidation states. In the systems Au^{n+}/Se_x^{2-} ($n = 1,3$) (vide infra), Fe^{n+}/Se_x^{2-} ($n = 2,3$) (vide supra), and Ni^{n+}/Se_x^{2-} ($n = 2,4$), complexes with the metal in either oxidation state can form. In the corresponding polysulfides, only one oxidation state of the metal is found to form a stable complex. This is best illustrated by the existence of two Ni^{4+}/Q_x^{2-} clusters. The $(Et_4N)_4[Ni_4Se_4(Se_3)_5(Se_4)] \cdot xEt_4NCl$ ($x = 0, 1$) (**50**) can be obtained by a spontaneous assembly reaction involving a redox process between Ni^{2z+} ($z = 1$ or 2) and Se_x^{2-} [99]. The $[Ni_4Se_4(Se_3)_5(Se_4)]^{4-}$ anion, whose structure is shown in Fig. 26(A), consists of four dis-

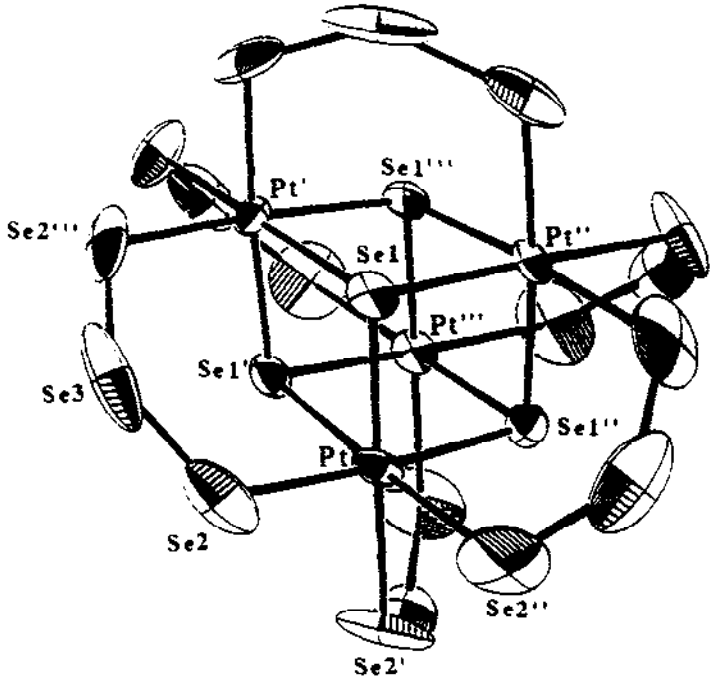

Fig. 27. The structure of $[Pt_4Se_4(Se_3)_6]^{4-}$.

torted octahedral Ni^{4+} centers (d^6 configuration) each bridged by three μ_3-Se^{2-} ligands in the cubane framework and three terminal selenium atoms of the Se_3^{2-} chelating chains (or the Se_4^{2-} chain between Ni(2) and Ni(4)) that span each two nickel centers. The Ni–Se bond distances range from 2.338(8) to 2.442(8) Å. This cubane-like structure is adopted in the polytelluride analog, $(Et_4N)_4[Ni_4Te_4(Te_2)_2(Te_3)_4]$ (**51**) from similar reaction conditions [99b]. In $[Ni_4Te_4(Te_2)_2(Te_3)_4]^{4-}$, two Te_2^{2-} ligands are on opposite faces of the cubane while four Te_3^{2-} ligands criss-cross the reset of the cubane faces as shown in Fig. 26(B). The Ni–Te bond distances range from 2.492(2) to 2.667(2) Å. The average Ni–Ni distances of 3.50(6) Å in **50** and 3.7(1) Å in **51** indicate that there is no Ni–Ni metal bonding. However, the presence of the Se_4^{2-} in **50** and the Te_2^{2-} in **51** imposes distortion on these two cubanes. This structure is also found in $[Pt_4Q_4(Q_3)_6]^{4-}$ (Q = S (**52**), Se (**53**)) [97]. Both compounds are prepared similarly by hydrothermal reactions. Compared to **50**, these two cubanes are less distorted because all bridging ligands are Q_3^{2-}. Figure 27 shows the structure of $[Pt_4Se_4(Se_3)_6]^{4-}$.

The structural diversity of the polychalcogenide chemistry of this group is not limited to the above examples. One notable compound is $(NH_4)_2[PdS_{11}]$ (**54**) [100] which was reported to have a polymeric layered structure containing S_5^{2-} and disordered S_6^{2-} ligands. A salient feature of this compound is that it has a small counterion which is probably responsible for its structural departure from the typical molecular motif. We explored a similar behavior by using small alkali ions such as Na^+, K^+ and Cs^+ as counterions, coupled with the hydrothermal technique (for overcoming the solubility problem of the

alkali salts in organic solvents). Based on our previous experience, the counterions used to crystallize the labile anionic complexes formed between metal ions and polychalcogenide ligands often have a most profound influence on the structures of the crystallized products (vide infra).

The hydrothermal reaction of $PdCl_2$ with K_2Se_4 in the presence of KOH and H_2O in the 1:5:5:40 ratio in a sealed Pyrex tube at 110°C for 1 day produced $K_2[PdSe_{10}]$ (**55**) [101]. This compound is polymeric, featuring interpenetrating frameworks formed by two remarkable macroanions of $[Pd(Se_4)_2]^{2-}$ and $[Pd(Se_6)_2]^{2-}$. In these two macroanions, palladium atoms still have the square-planar geometry. However, both Se_4^{2-} and Se_6^{2-} ligands, instead of being chelated to the same metals, are now acting as extended zigzag chains to bridge different metal centers. Figure 28 shows the repeating units $[Pd(Se_4)_2]^{2-}$ and $[Pd(Se_6)_2]^{2-}$. The frameworks thus formed penetrate into each other's voids with the $PdSe_4$ square planes from one framework stacking directly above and below those of the other (6.44 Å apart). Figure 29 depicts this interpenetrating behavior. There are no covalent or ionic bonds rather than van der Waals interactions between the two frameworks. However, it is almost impossible to describe the complex arrangement of the Se_x^{2-} ($x = 4$

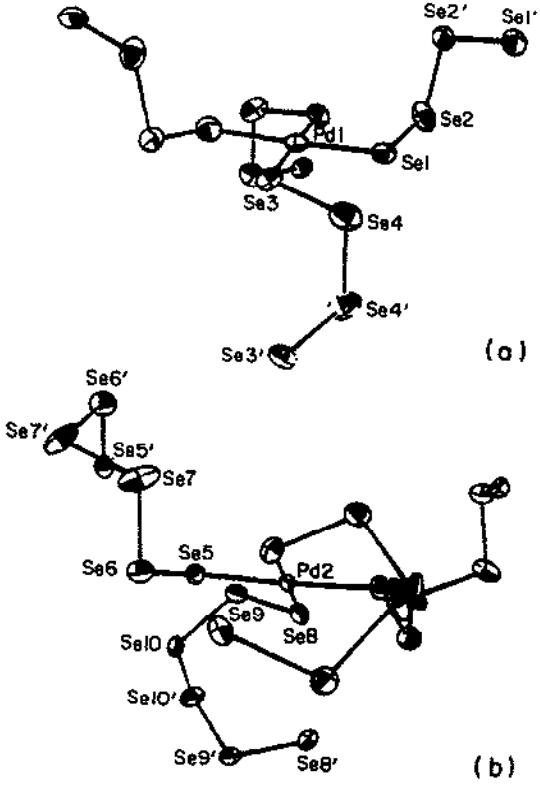

Fig. 28. Structures of the repeating units $[Pd(Se_4)_2]^{2-}$ and $[Pd(Se_6)_2]^{2-}$ in $K_2[PdSe_{10}]$.

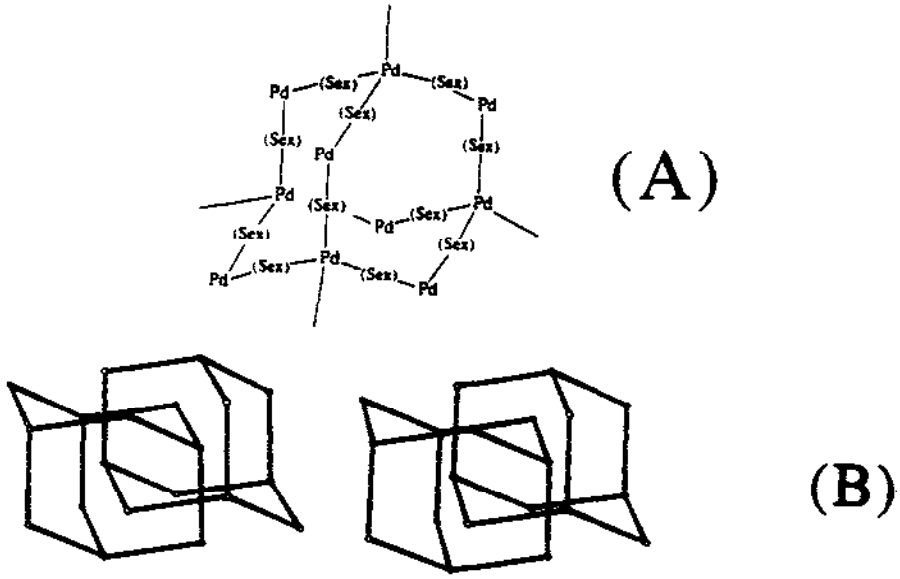

Fig. 29. Schematic view of the interpenetrating behavior of $[Pd(Se_4)_2]^{2-}$ and $[Pd(Se_6)_2]^{2-}$ frameworks.

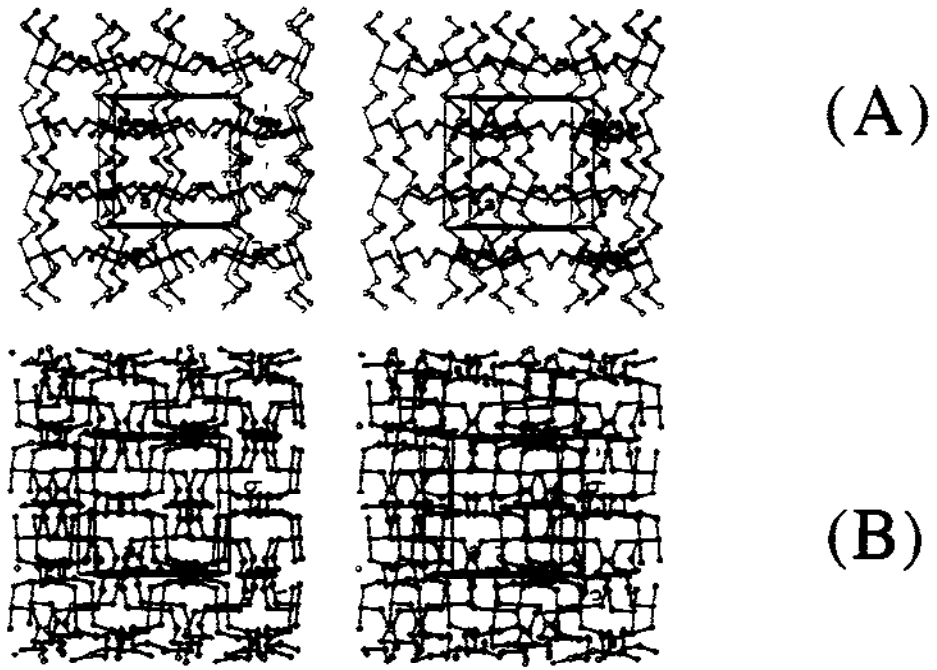

Fig. 30. Stereoview of the individual substructures of (A) $[Pd(Se_4)_2]^{2-}$ and (B) $[Pd(Se_6)_2]^{2-}$ frameworks looking down the c-axis. Filled circles are Pd atoms.

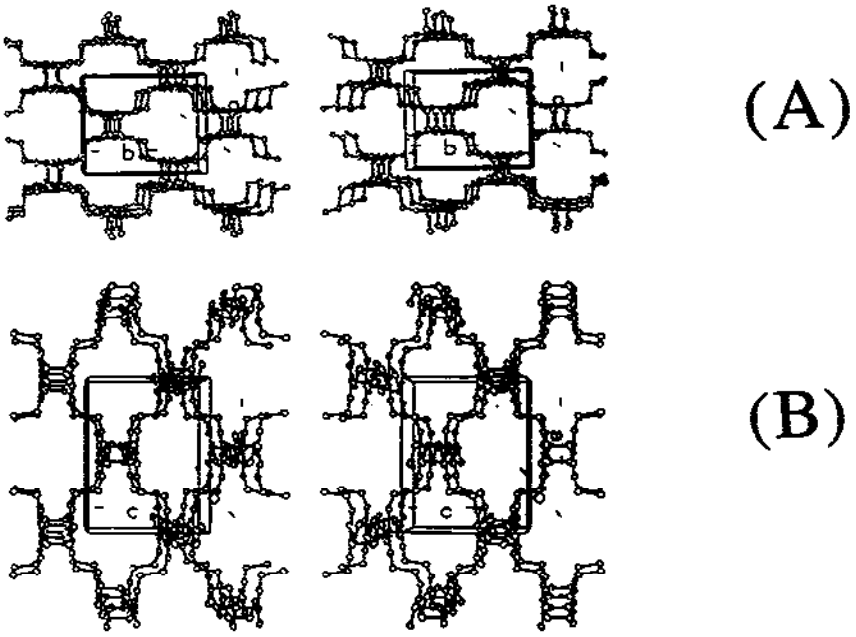

Fig. 31. Stereoview of the $[Pd(Se_4)_2]^{2-}$ substructures looking down (A) the *a*-axis and (B) the *b*-axis, illustrating the large one-dimensional channels.

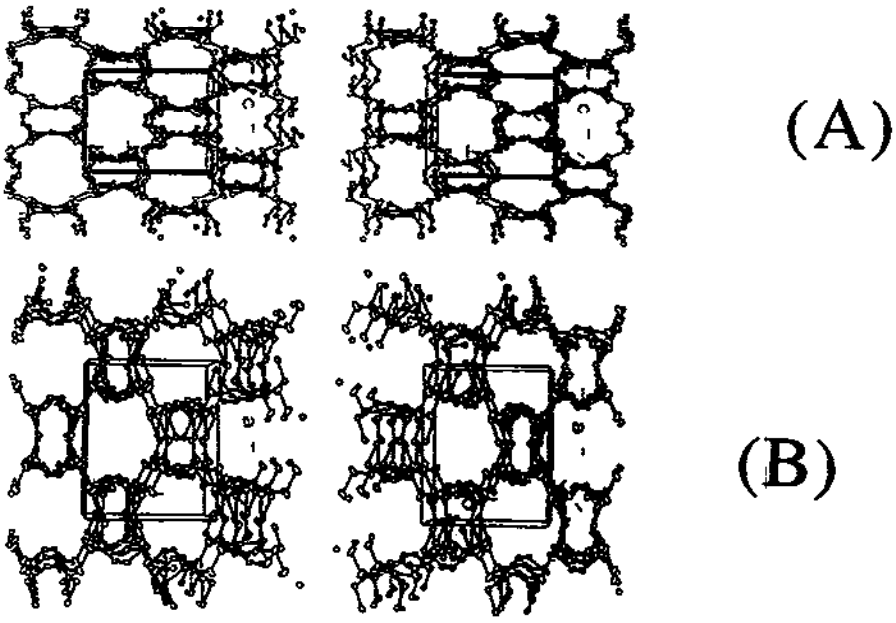

Fig. 32. Stereoview of the $[Pd(Se_6)_2]^{2-}$ substructures looking down (A) the *a*-axis and (B) the *b*-axis illustrating the large one-dimensional channels.

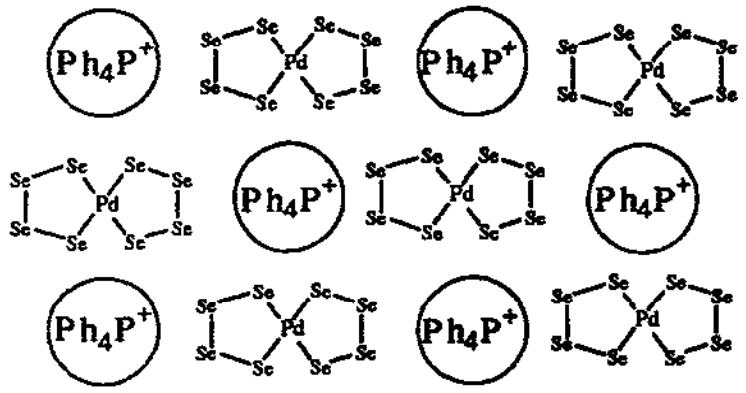

(A)

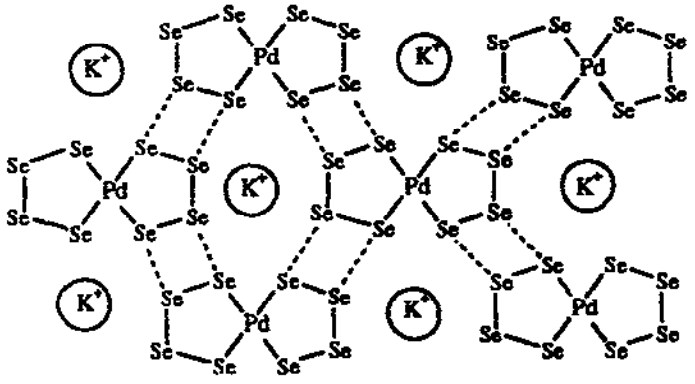

(B)

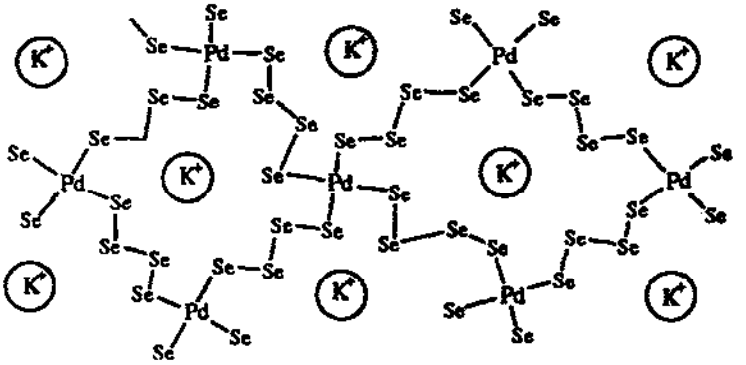

(C)

Scheme 7. (A) Stable assembly of mutually screened Ph_4P^+ cations and $[Pd(Se_4)_2]^{2-}$ anions. (B) Substitution of large Ph_4P^+ for K^+ results in short anion–anion contacts developing destabilizing repulsive interactions. The latter are represented by dotted lines. (C) A stable assembly is possible by converting chelating Se_x^{2-} ligands to bridging.

or 6) chains and Pd atoms in 55 by verbal expression. Thus, we show three figures in the following to illustrate the individual structures of $[Pd(Se_4)_2]^{2-}$ and $[Pd(Se_6)_2]^{2-}$ (Fig. 30), large one-dimensional tunnels in the frameworks of $[Pd(Se_4)_2]^{2-}$ (Fig. 31) and $[Pd(Se_6)_2]^{2-}$ (Fig. 32), respectively. The average Pd–Se distance is 2.462(5) Å, and the average Se–Se distance 2.35(2) Å. The angles around palladium atoms are 90°.

The fact that the same anion $[Pd(Se_4)_2]^{2-}$ can be either discrete molecular (when crystallized with Ph_4P^+) or polymeric (when crystallized with K^+) illustrates the importance of the counterion size in determining the structures of many of these anionic complex species. This can be explained by the "ion screening effect" in the crystal lattice. As shown in Scheme 7, when the large Ph_4P^+ cation is replaced by the much smaller K^+, the $[Pd(Se_4)_2]^{2-}$ anions can no longer be effectively screened, resulting in destabilizing repulsions. One way in which the system responds to such a change is to convert the Se_4^{2-} ligands from chelating one palladium center to bridging two neighboring palladium atoms, thus leading to elimination of Coulombic repulsions and a decrease in the lattice energy. The $K_2[PdSe_{10}]$ is a semiconductor material with a well defined optical band gap of 1.5 eV. The solid state optical absorption spectrum of this compound is shown in Fig. 33.

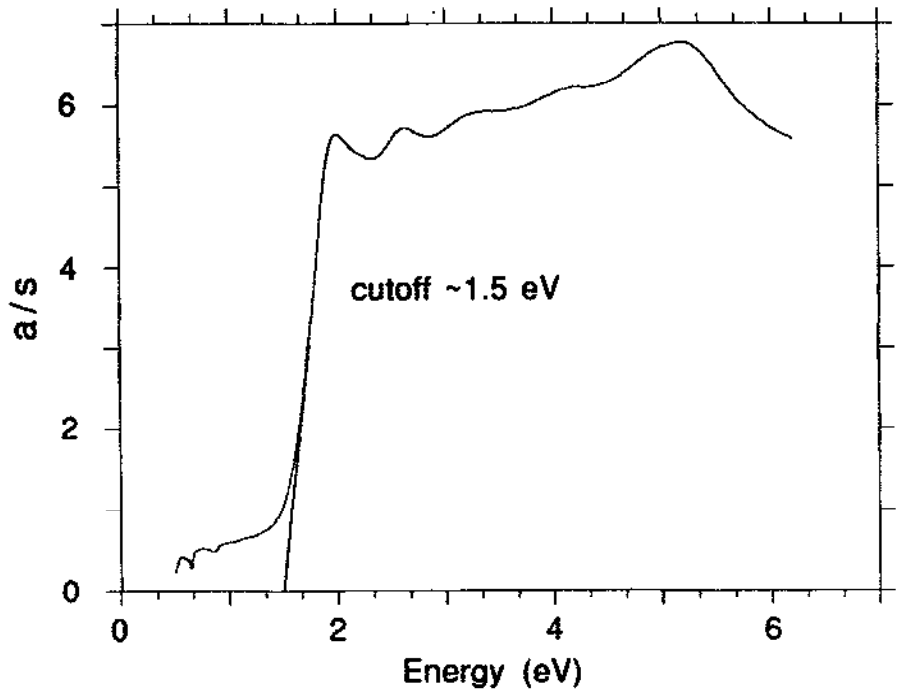

Fig. 33. Solid-state optical absorption spectrum of $K_2[PdSe_{10}]$.

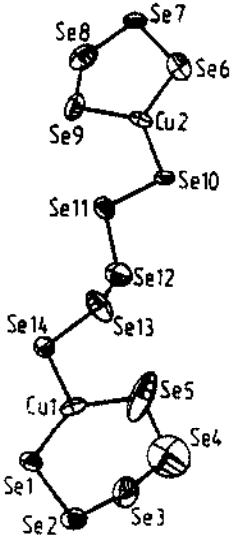

Fig. 34. The structure of $[Cu_2(Se_4)(Se_5)_2]^{4-}$.

(j) The chemistry of Group 11 elements (Cu, Ag and Au)

Compared to the plethora of polysulfide complexes known for copper [102], the number of corresponding polyselenide and polytelluride compounds that have been isolated and structurally characterized is small. There are four complexes known so far, $(Ph_4P)_4[Cu_2(Se_4)(Se_5)_2]$ (**56**) [103], $(Ph_4P)_2[Cu_4(Se_4)_{2.4}(Se_5)_{0.6}]$ (**57**) [104], $(Ph_2P)_4[Cu_2(Te_4)_3]$ (**58**) [105] and $(Me_4N)[Cu(Te_4)]$ (**59**) [106]. Compound **56** was prepared by reacting CuCl with 2 equiv. of Li_2Se_6 (generated in situ) in the presence of Ph_4PBr in DMF at 120°C [103]. The structure of the $[Cu_2(Se_4)(Se_5)_2]^{4-}$ anion, as shown in

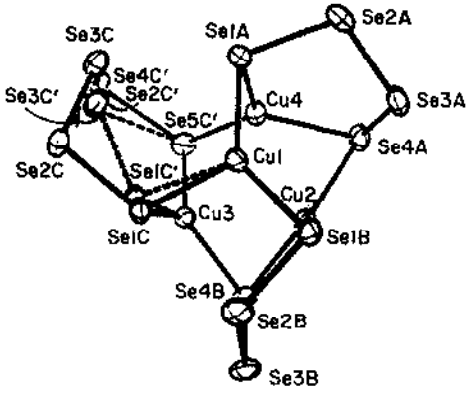

Fig. 35. The structure of $[Cu_4(Se_4)_{2.4}(Se_5)_{0.6}]^{2-}$.

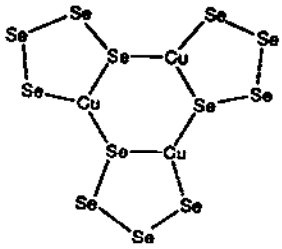

Scheme 8. Structure of the hypothetical $[Cu_3(Se_4)_3]^{3-}$ trimer.

Fig. 34, consists of a five-membered $CuSe_4$ ring and a six-membered $CuSe_5$ ring bridged by a Se_5^{2-} chain. Both copper atoms have a trigonal planar geometry. The Cu–Se bond distances range from 2.26(1) to 2.38(1) Å. Compound **57** was prepared from the reaction of mixing $CuCl_2 \cdot 2H_2O$, Na, Se and Ph_4PBr (in the ratio 1.9:10.4:30.4:3.8) in a DMF/CH_3CN solution at 60°C [104]. The anion $[Cu_4(Se_4)_{2.4}(Se_5)_{0.6}]^{2-}$ is a cluster, featuring a tetrahedral array of copper atoms held together by three Se_4^{2-} ligands, as shown in Fig. 35. It thus contains a highly distorted Cu_4Se_6 central adamantane-like core in which all copper atoms assume trigonal planar coordination. It is noticeable in this figure that ring C is disordered, being either Se_5^{2-} (59%) or Se_4^{2-} (41%). Otherwise, all $CuSe_4$ rings have an envelope conformation. Alternatively, the structure can be regarded as being derived from the cyclic $[Cu_3(Se_4)_3]^{3-}$ trimer shown in Scheme 8 by folding up the terminal selenium atoms to bind to the fourth copper atom which approaches the trimer from the direction of the C_3-axis.

The $(Ph_4P)_4[Cu_2(Te_4)_3]$ (**58**), obtained from the reaction of CuCl with Na_2Te_3 in the presence of Ph_4PBr in DMF [105], has a similar structure to $(Ph_4P)_4[Cu_2(Se_4)(Se_5)_2]$ (**56**). However, two five-membered $CuTe_4$ rings are now bridged by a Te_4^{2-} instead of Te_5^{2-} chain, as shown in Fig. 36. Copper atoms again have a trigonal planar geometry. The Cu–Te bond distances range from 2.465(5) to 2.520(4) Å. When Me_4NCl was used as the counterion in the reaction of $(Ph_3P)_3CuCl$ with K_2Te_4 in DMF, a polymeric copper tetratelluride compound, $(Me_4N)[Cu(Te_4)]$ (**59**), was obtained [106]. Compound **59** is a two-dimensional compound, composed of $[Cu(Te_4)]^-$ layers and non-interacting Me_4N^+ cations situated between the layers, as shown in Fig. 37. Figure 38 is a close look at an individual layer. Also shown in this figure are the layers formed by interconnection of the basic building blocks, five-membered $CuTe_4$ rings. These $CuTe_4$ rings are connected to each other through an unusual bridging mode, for a Te_4^{2-} ligand, as shown below:

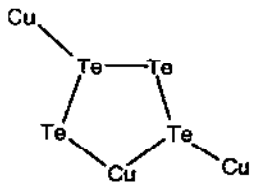

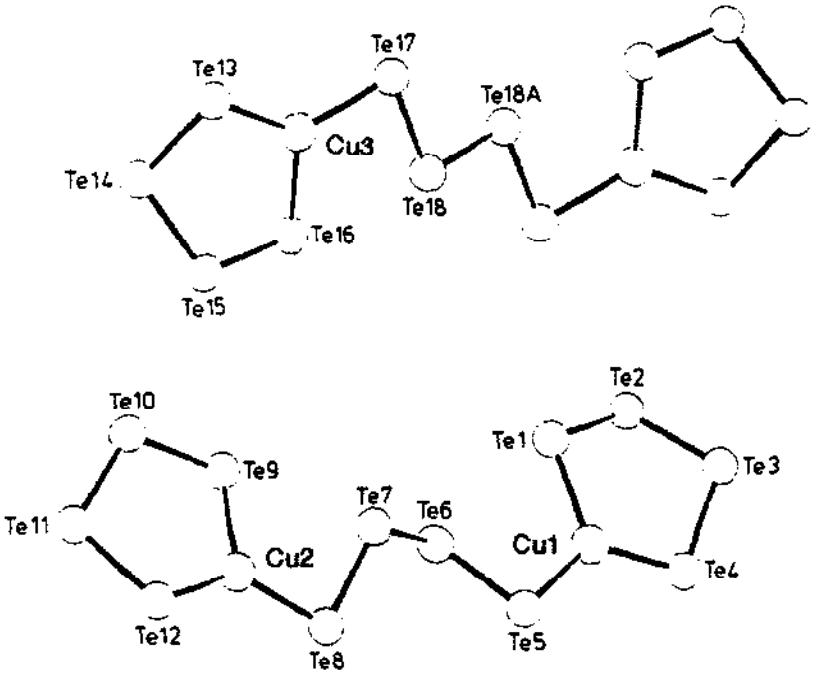

Fig. 36. The structures of two crystallographically independent $[Cu_2(Te_4)_3]^{4-}$ anions.

Copper atoms have a distorted tetrahedral coordination. The Cu–Te bond distances range from 2.578(2) to 2.725(3) Å.

As a consequence of the polymerization mode of the $CuTe_4$ ring, the layers possess large holes made of 14-membered rings (see Fig. 38) with dimensions of

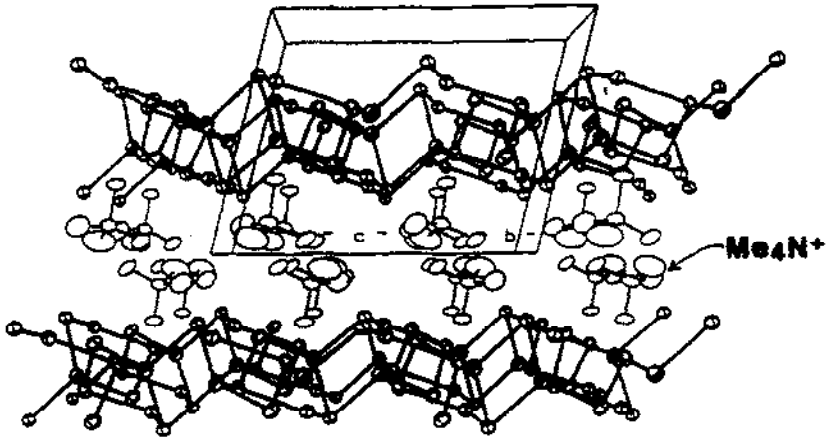

Fig. 37. The two-dimensional structure of $(Me_4N)[Cu(Te_4)]$.

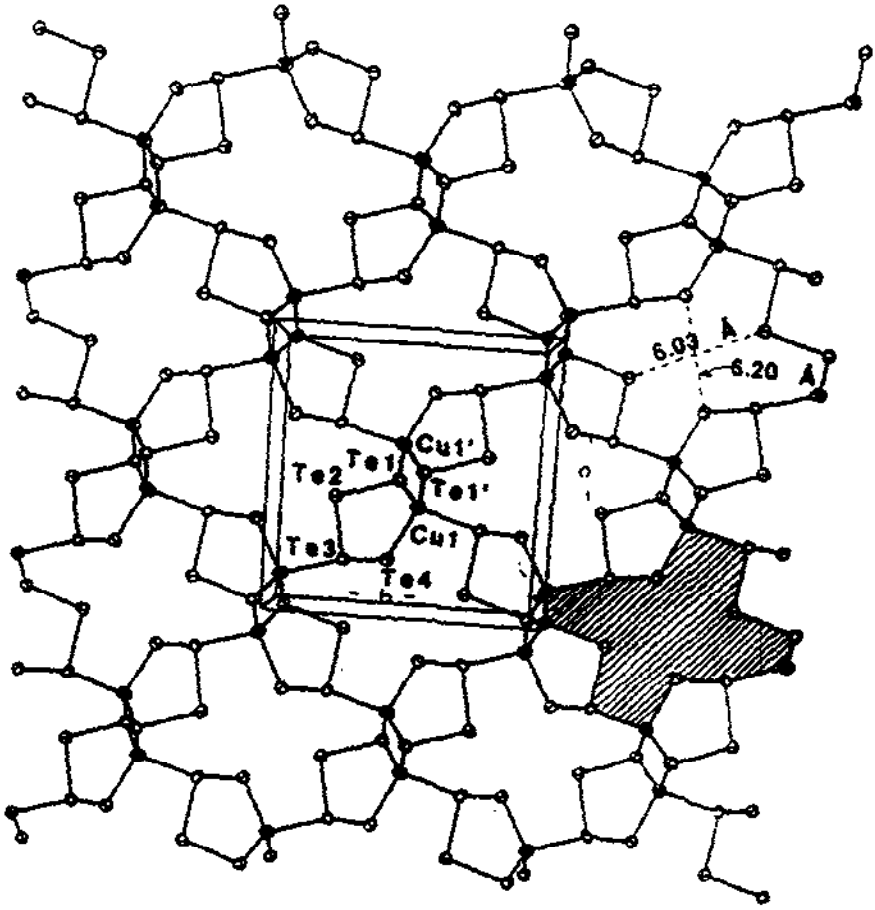

Fig. 38. A view of one $[Cu(Te_4)]^-$ layer.

6.034(2) × 6.195(3) Å. The conformation of this ring is puckered with the four Te atoms (two Te(4) and two Te(2)) pointed inwards defining a square planar site. The Me_4N^+ cations assemble as a double layer between the $[CuTe_4]^-$ layers (see Fig. 37), raising the possibility for ion-exchange studies with other cations. $(Me_4N)[CuTe_4]$ represents a new addition to the already known AMQ_x family (A = Ph_4P, Me_4N, K, Rb, Cs; M = Cu^+, Ag^+, Au^+; Q = S, Se, Te) all of which feature low-dimensional structures.

$(Me_4N)[Cu(Te_4)]$ is a diamagnetic semiconductor with a room temperature electrical conductivity 10^{-3} S/cm. This material starts to strongly absorb light in the near-infrared region, as shown in the optical spectrum in Fig. 39, suggesting a band gap (determined from diffuse reflectance measurements) of 0.82 eV.

The chemistry of silver polyselenides has proven to be equally versatile since several compositionally and structurally different species are readily isolable from a common reaction solution by using different counterions, as shown in eqn. (1) [107]:

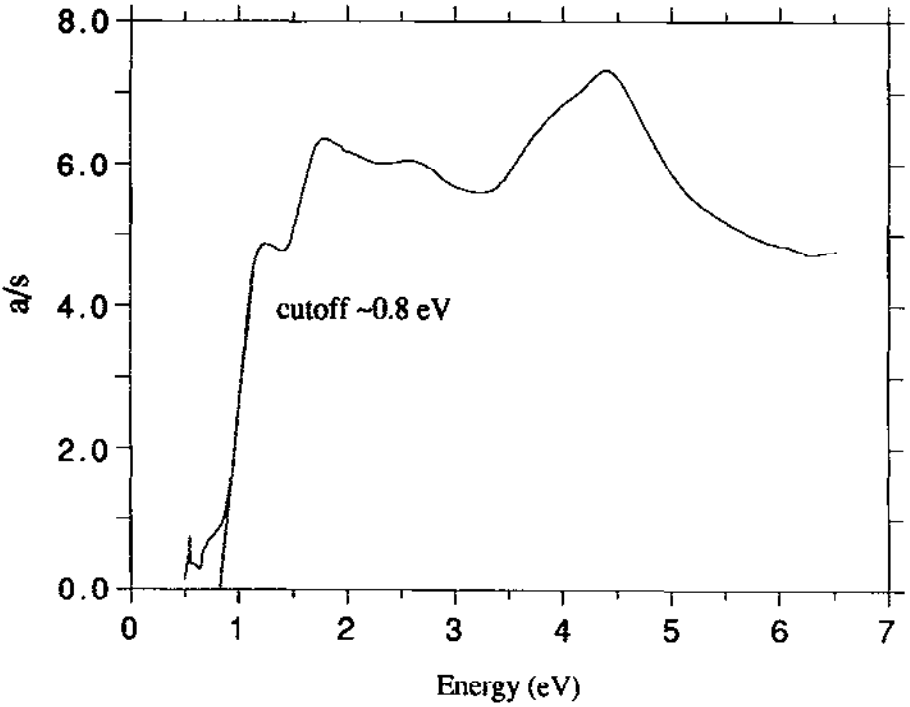

Fig. 39. Solid-state optical absorption spectrum of $(Me_4N)[Cu(Te_4)]$.

$$AgNO_3 + Na_2Se_5 + \underset{(\text{or } Ph_4PCl)}{R_4NCl} \rightarrow \underset{(\text{or } [(Ph_4P)_xAg_y(Se_n)_z])}{[(R_4N)_xAg_y(Se_n)_z]} + NaCl + NaNO_3 \quad (1)$$

The $[(Ph_4P)Ag(Se_4)]_n$ (**60**), $[(Et_4N)Ag(Se_4)]_4$ (**61**) and $[(Me_4N)Ag(Se_5)]_n$ (**62**) belong to the general family $[Ag(Se_x)]_n^{n-}$. However, **60** and **62** have polymeric structures while **61** is a molecular cluster. Figure 40 shows three different views of an individual $[Ag(Se_4)]_n^{n-}$ chain in **60** [38a,107]. The one-dimensional chain is generated through the bridging between a terminal selenium atom and the silver atom in two neighboring $AgSe_4$ rings. The coordination geometry of the silver atom is trigonal planar. The four-membered $AgSe_4$ ring has an envelope conformation. The average Ag–Se bond distance is 2.59(4) Å. The structure of the $[Ag(Se_5)]_n^{n-}$ in **62** differs from that of $[Ag(Se_4)]_n^{n-}$ in two ways as can be seen in Fig. 41. First, in **62**, both terminal selenium atoms from the $AgSe_4$ ring are engaged in bridging, one directly bound to a neighboring silver atom and the other to an extra selenium atom which is subsequently coordinated to another silver atom as shown below.

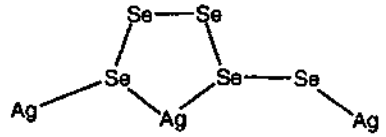

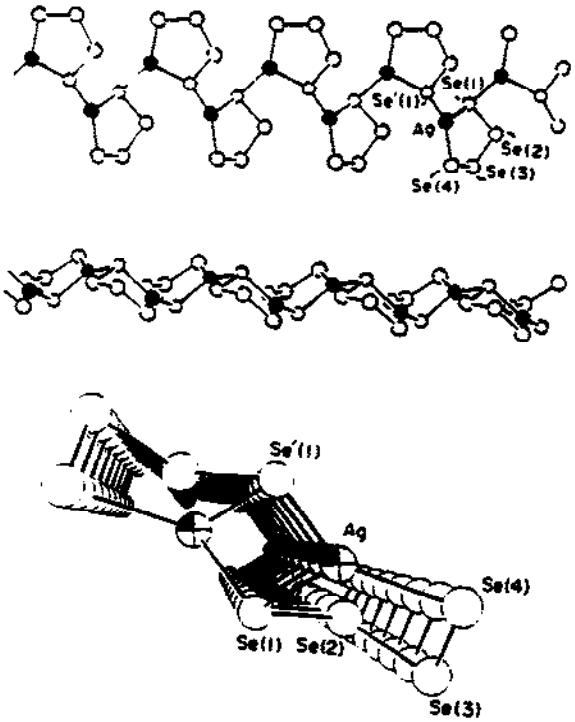

Fig. 40. Three different views of the one-dimensional $[Ag(Se_4)]_n^{n-}$ chain.

Therefore, the molecule contains Se_5^{2-} instead of Se_4^{2-}, although the $AgSe_4$ ring is easily recognizable; Second, the silver atom in **62** assumes tetrahedral geometry.

The structure of the $[Ag(Se_4)]_4^{4-}$ tetrameric cluster in **61** can be regarded as assembled by four $AgSe_4$ rings (Fig. 42). Four silver atoms are symmetrically disposed around a crystallographic inversion center, forming a planar rhombus. They are then "glued" together via two different types of bridging terminal selenium atoms, i.e. two Se_4^{2-} ligands each have one terminal selenium atom being μ_2-type, the other two Se_4^{2-} ligands

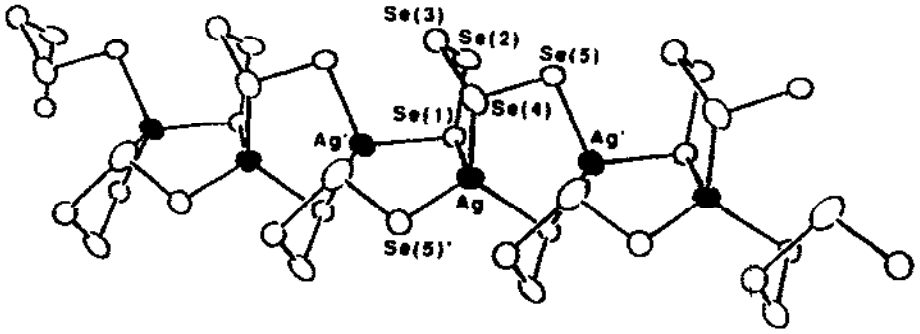

Fig. 41. The structure of the one-dimensional $[Ag(Se_5)]_n^{n-}$ chain.

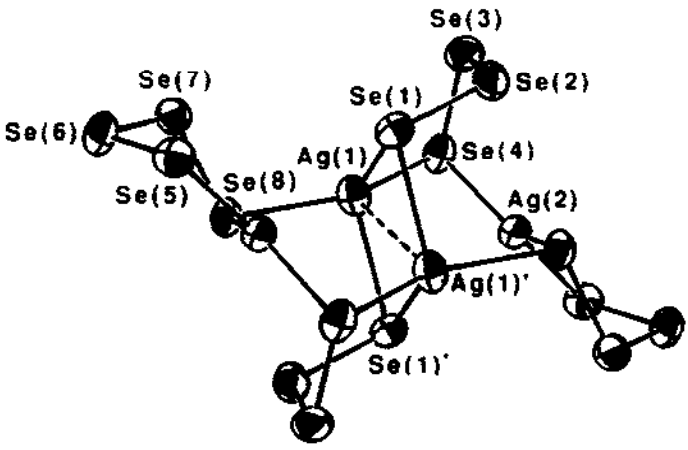

Fig. 42. The structure of $[AgSe_4]_4^{4-}$.

have all the terminal selenium atoms of μ_2-type. The silver atoms are found to have two different coordination spheres, distorted tetrahedral (Ag(1) and Ag(1)') and trigonal planar (Ag(2) and Ag(2)'). Both twisted-boat (Ag(1)-containing $AgSe_4$ ring) and envelope (Ag(2)-containing $AgSe_4$ ring) conformations are found for the $AgSe_4$ rings.

When the counterion is changed to Pr_4N^+, a different composition will be adopted by the system to yield $(Pr_4N)_2[Ag_4(Se_4)_3]$ (**63**). The structure of $[Ag_4(Se_4)_3]^{2-}$ is analogous to the aforementioned trinuclear copper polyselenide cluster, $(Ph_4P)_2[Cu_4(Se_4)_{2.4}(Se_5)_{0.6}]$ (**57**) (see Fig. 35). Its Ph_4P^+ salt is also known and found to have disorder containing either Se_4^{2-} or Se_5^{2-} in the molecule [104]. The actual composition was found to be $(Ph_4P)_2[Ag_4(Se_4)_{2.1}(Se_5)_{0.9}]$ (**64**) as derived from the X-ray crystallographic results [104]. Unlike the anion in **64**, no disorder is found for the Se_4^{2-} ligands in **63**.

The first silver polytelluride compound was $(Ph_4P)_4[Ag_2(Te_4)_3]$ (**65**), prepared from the reaction of $AgNO_3$ with K_2Te_3 in the presence of Ph_4PBr in DMF [105]. It is isostructural to $(Ph_4P)_4[Cu_2(Te_4)_3]$ (**58**). The structure of the $[Ag_2(Te_4)_3]^{4-}$ anion is similar to the copper analog and warrants no further comments. Recently, we have isolated a new silver-polytelluride $(Me_4N)[Ag(Te_4)]$ (**66**) which is isomorphous to the layered polymeric $(Me_4N)[Cu(Te_4)]$. $(Me_4N)[Ag(Te_4)]$ is also a diamagnetic semiconductor with a band gap (determined from optical measurements) of 0.8 eV.

Interestingly, further structural diversity is encountered in the gold polyselenide system. It is largely due to a vacillating redox chemistry between Au^{n+} (n = 1,3) and Se_x^{2-}. In DMF solution, the reaction of $AuCl_3$ with Na_2Se_5 resulted in the isolation of α-$(Ph_4P)_2[Se(Se_5)_2]$ (**67**), an oxidation product of Se_5^{2-} by Au^{3+} [108]. The existence of this peculiar molecule had been mentioned before in a review article [109], and its structure is discussed later along with those in the $[A(Q_5)_2]^{2-}$ (A = Te, Q = S, Se or A = Se, Q = Se) family. The above redox process is avoided if AuCN is used as the starting material. Surprisingly, a reverse redox reaction occurs in this case, that is, Au^+ is oxidized by the

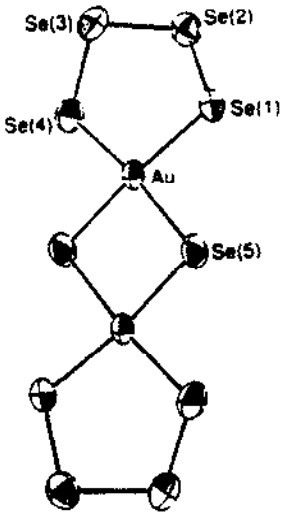

Fig. 43. The structure of $[Au_2Se_2(Se_4)_2]^{2-}$.

Se_5^{2-} to Au^{3+}, yielding the dimeric complex $(PPN)_2[Au_2Se_2(Se_4)_2]$ (**68**) [108]. This compound contains two square-planar (d^8 configuration) Au^{3+} atoms bonded by two μ_2-Se^{2-} and two bidentate chelating Se_4^{2-} ligands, shown in Fig. 43. The four-membered $[Au_2Se_2]^{2+}$ core is perfectly planar because this molecule is situated on a crystallographic inversion center (at the midpoint of the Au···Au vector). The Au···Au distance of 3.660(1) Å in the structure represents a non-interacting situation of two gold atoms in the molecule. The five-membered $AuSe_4$ ring has a twist-boat conformation. The Au–Se bond distances are in the range of 2.444(2) to 2.461(2) Å. The formation of **68** was speculated through an internal two-electron transfer from the Au^+ to the terminal Se–Se bond of the Se_5^{2-} ligand. Scheme 9 illustrates this process. Although the Au^+ intermediate, $[Au_2(Se_5)_2]^{2-}$, has not been isolated or detected, such a complex is structurally similar to $[Au_2(S_4)_2]^{2-}$ (**69**).

In a further attempt at stabilizing the gold(I) polyselenide compounds, shorter polyselenide Se_x^{2-} ($x = 2$–4) ligands were used [110]. Three new compounds containing Au^+ were consequently obtained. The $(Ph_4P)_2[Au_2(Se_2)(Se_3)]$ (**70**) and $(PPN)_2[Au_2(Se_2)(Se_3)]$ (**71**) were synthesized in a similar manner as above using Na_2Se_2 or Na_2Se_3 while

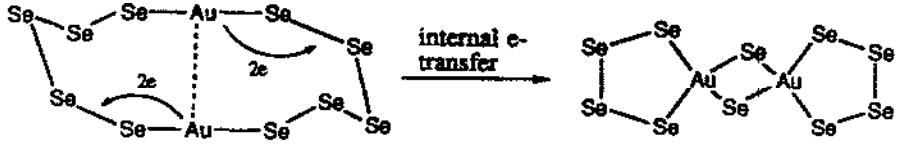

Scheme 9. Transformation from $[Au_2(Se_5)_2]^{2-}$ to $[Au_2Se_2(Se_4)_2]^{2-}$ via an internal electron transfer process.

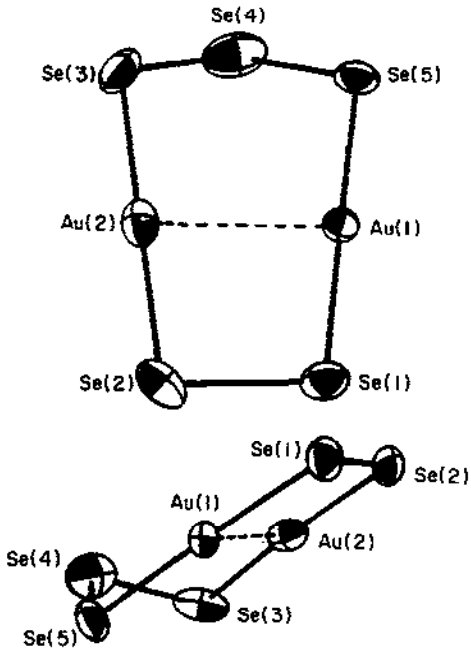

Fig. 44. Two views of the $[Au_2(Se_2)(Se_3)]^{2-}$ anion.

$(Ph_4P)_2[Au_2(Se_2)(Se_4)]$ (**72**) was obtained using Na_2Se_4. Compounds **70** and **71** contain the same anion $[Au_2(Se_2)(Se_3)]^{2-}$ whose structure is represented in Fig. 44 by the crystallographically refined anion in **70**. This envelope-shaped seven-membered ring is made up of two linearly coordinated Au^+ atoms bridged by a Se_2^{2-} and a Se_3^{2-} ligand. It has C_2 molecular symmetry. Two Au^+ atoms show d^{10}–d^{10} interaction at 3.004(2) Å. The average Au–Se bond distance is 2.397(5) Å. The $[Au_2(Se_2)(Se_4)]^{2-}$ anion in **72** is structurally similar to $[Au_2(Se_2)(Se_3)]^{2-}$, as shown in Fig. 45. It has C_2 molecular symmetry with the twofold axis running across the center of the Au···Au and Se(1)–Se(1) vectors. The Au–Se bonds to Se_2^{2-} are long at 2.433(5) Å, while those to Se_4^{2-} are short at 2.355(5) Å. The Au···Au separation is also longer at 3.132(3) Å, presumably due to the presence of the Se_4^{2-} ligand.

The isolation of $[Se_{11}]^{2-}$ and the Au^+ and Au^{3+} complexes suggests that the Au^+ versus Au^{3+} interplay is largely influenced by the size of the Se_x^{2-} ligands. This is an exception to a wide perception in this field that ligand preference of the metal ions are more important in determining structure than the sizes of the Se_x^{2-} ligands used.

The only known polytelluride of gold is the planar symmetric $[Au_2(Te_2)_2]^{2-}$ ring complex. This anion can be crystallized as $(PPN)_2[Au_2(Te_2)_2]$ (**73**) [111] and $(Ph_4P)_2[Au_2(Te_2)_2]$ (**74**) [112]. Figure 46 shows the structure of this anion found in **74**. The molecule is situated on a crystallographic inversion center. The Au···Au distance is 2.905(2) Å. The selenium analog of $[Au_2(Te_2)_2]^{2-}$ cannot be made even if Na_2Se_2 is used

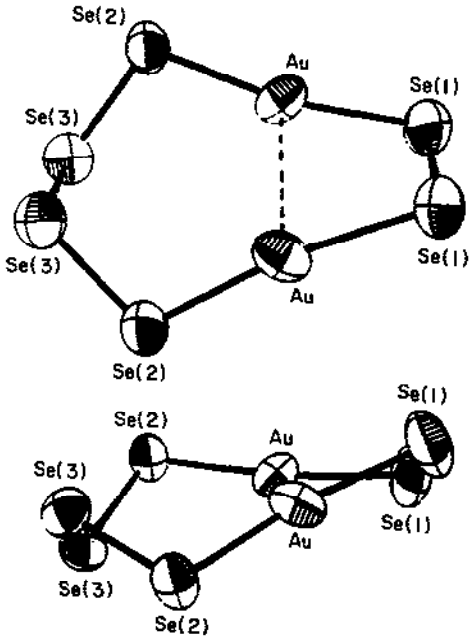

Fig. 45. Two views of the $[Au_2(Se_2)(Se_4)]^{2-}$ anion.

as the starting material. This is because of the inability of the Se_2^{2-} unit (~2.4 Å) to accommodate two gold atoms 2.9–3.0 Å apart. In other words, such a molecule would force the gold atoms to severely deviate from linear coordination.

(k) The chemistry of Group 12 elements (Zn, Cd and Hg)

The predominant structure for the divalent metal ions in this group is once again the tetrahedral molecule with two bidentate Q_4^{2-} ligands. The α-$(Ph_4P)_2[M(Se_4)_2]$ (i.e. the monoclinic phase) is known for M = Zn (**75**) [92a] and Cd (**76**) [92a], and $(Ph_4P)_2[Zn(Se_4)_2]$ is also found in triclinic form (**77**) (i.e. the β-form) [113]. Interestingly,

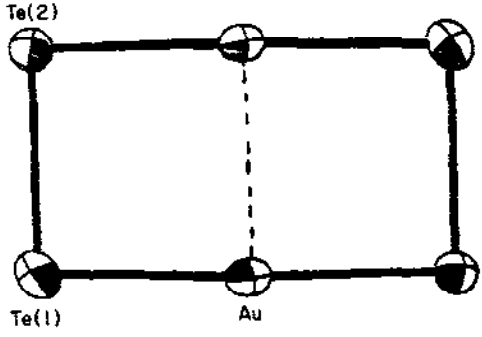

Fig. 46. The structure of $[Au_2(Te_2)_2]^{2-}$ found in $(Ph_4P)_2[Au_2(Te_2)_2]$.

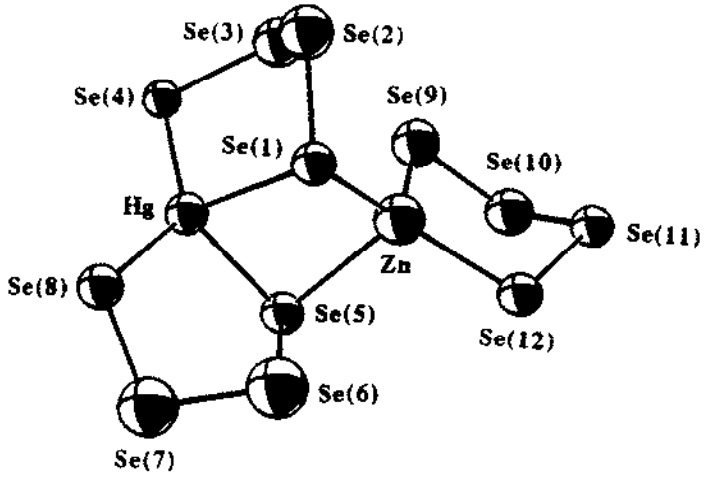

Fig. 47. The structure of $[Hg(Se_4)_2Zn(Se_4)]^{2-}$.

$(Ph_4P)_2[Hg(Se_4)_2]$ also forms two crystal modifications, but neither is isostructural to the two known $(Ph_4P)_2[M(Se_4)_2]$ phases (i.e. α- or β-form). The α-$(Ph_4P)_2[Hg(Se_4)_2]$ **(78)** [92a] and β-$(Ph_4P)_2[Hg(Se_4)_2]$ **(79)** [114] both crystallize in the same space group ($P2_1/c$, No. 14) with different unit cells. Two structurally similar, but conformationally different spirocycles of the $[Hg(Se_4)_2]^{2-}$ occur in the α-form while the β-form contains only one $[Hg(Se_4)_2]^{2-}$ anion in the asymmetric unit.

The easy access to these metal octaselenides are attested by the repeated X-ray structure determination of the same anions with various counterions by several research groups. The following is a collection of those reported: $[Na(15\text{-crown-}5)]_2[M(Se_4)_2]$ (M = Zn, Cd or Hg) [115], $(Ph_4P)_6[M(Se_4)_2]_2[WSe_4]\cdot DMF$ (M = Zn and Hg; co-crystallized with WSe_4^{2-}) [116], $[Li_3(12\text{-crown-}4)(O_2CCH_3)][Cd(Se_4)_2]$ [117], $\{[K(18\text{-crown-}6)]_2[Hg(Se_4)_2]\}_2$ [117] (a dimer formed through K···Se interactions in the crystal lattice), $[Ba(18\text{-crown-}6)(DMF)_4][Cd(Se_4)_2]$ [118].

A heteronuclear compound containing two different metal atoms from this same group has been synthesized. The $(Et_4N)_2[Hg(Se_4)_2Zn(Se_4)]$ **(80)** [119], obtained from the reaction of $[Hg(Se_4)_2]^{2-}$ with $ZnCl_2$ in DMF, consists of the $[Hg(Se_4)_2Zn(Se_4)]^{2-}$ anion formed by the chelating of the $[Hg(Se_4)_2]^{2-}$ molecule, via its two terminal selenium atoms, to a $ZnSe_4$ ring, as shown in Fig. 47. A limited postional disorder exists between Zn and Hg. Interestingly, this compound can give rise to a coordination isomer, $(Et_4N)_2[Zn(Se_4)_2$ $Hg(Se_4)]$ **(81)**, i.e. by switching the positions of Hg and Zn. However, the latter has not been prepared thus far.

Isolation of new complexes other than the octaselenides in this group is also achievable by changing the reaction conditions. For instance, $[Zn(Se_4)(Se_6)]^{2-}$ **(82)** [120] is obtained by using [Rb(18-crown-6)]+ as the counterion. The zinc atom is now chelated by Se_4^{2-} and Se_6^{2-} ligands. In addition, there is a unique interaction between the Rb^+ ions and

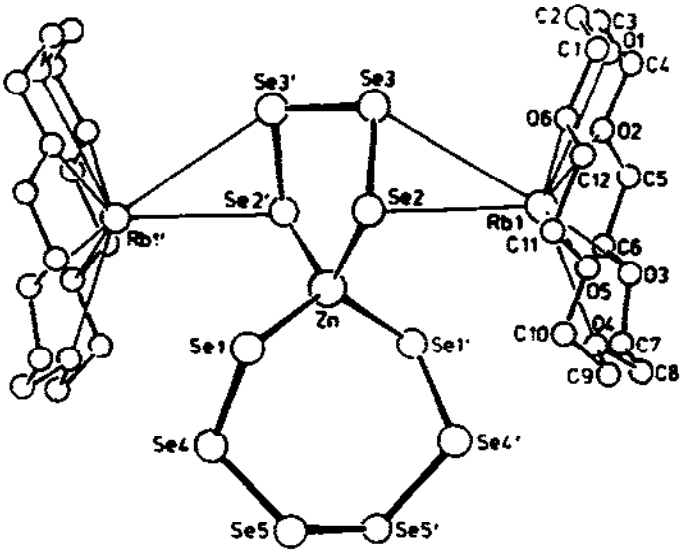

Fig. 48. The structure of $[Rb(18\text{-crown-6})]_2[Zn(Se_4)(Se_6)]$, showing the interaction between Rb^+ ions and Se_4^{2-} ligand.

the selenium atoms of the Se_4^{2-} ligand, as shown in Fig. 48. The $[Hg_2(Se_4)_3]^{2-}$ (**83**) was crystallized with two different counterions Ph_4P^+ and $[Cs(18\text{-crown-6})]^+$ [114]. The $[Hg_2(Se_4)_3]^{2-}$ anion is the homonuclear analog of $[Hg(Se_4)_2Zn(Se_4)]^{2-}$. Figure 49 shows the structure of the $[Hg_2(Se_4)_3]^{2-}$ anion. In addition, there are also extensive interactions between the Cs^+ ions and the Se_4^{2-} ligands in the crystal lattice as shown in Fig. 50.

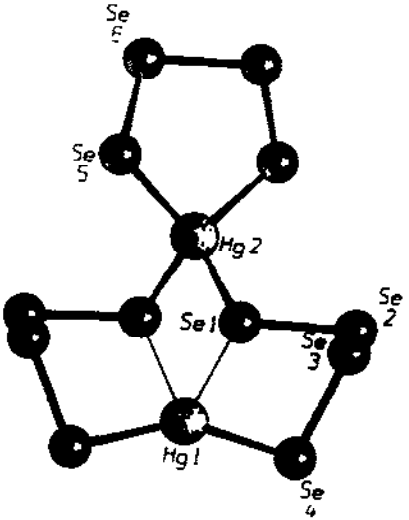

Fig. 49. The structure of the $[Hg_2(Se_4)_3]^{2-}$ anion.

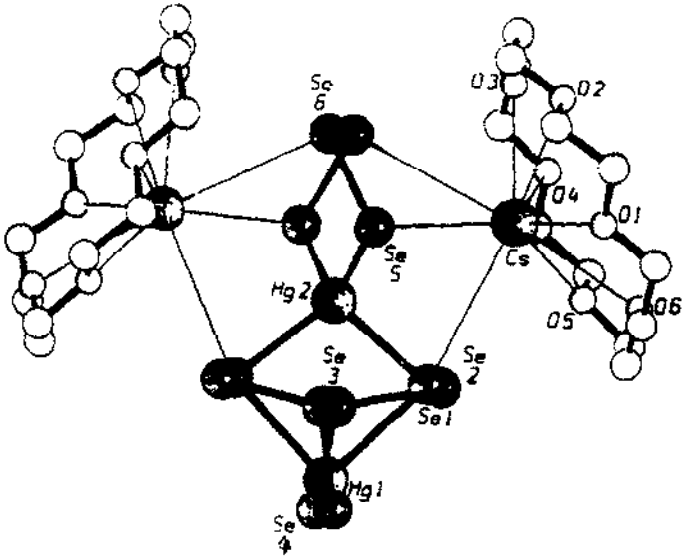

Fig. 50. The interactions between Cs^+ ions and the Se_4^{2-} ligands in $[Cs(18\text{-crown-6})]_2[Hg_2(Se_4)_3]$ crystal lattice.

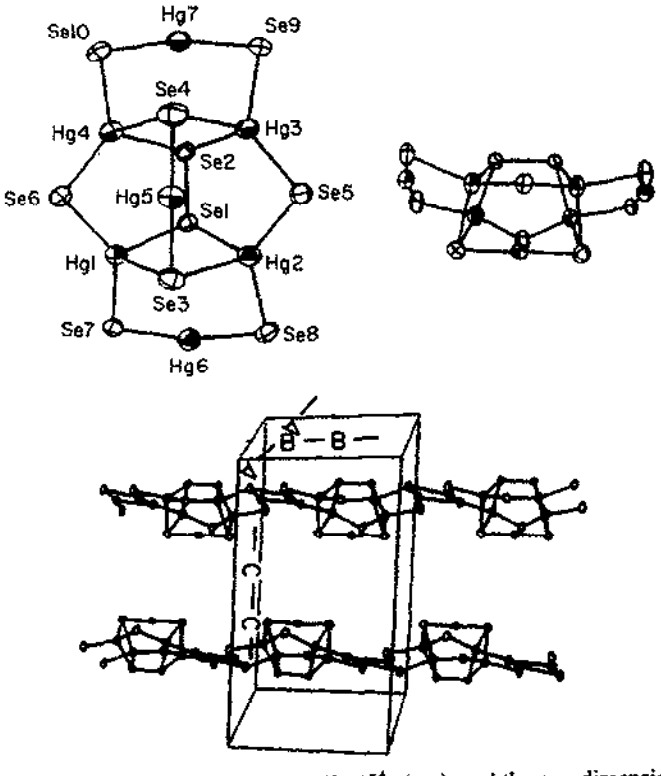

Fig. 51. Two views of $[Hg_7(Sc)_8(Se_2)]^{4-}$ (top), and the one-dimensional connectivity of the clusters (bottom).

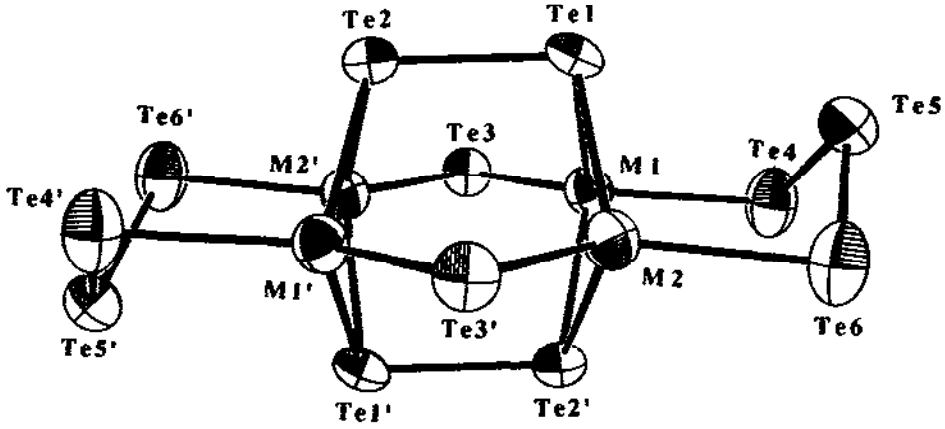

Fig. 52. The structure of $[M_4(Te)_2(Te_2)_2(Te_3)_2]^{4-}$ (M = Cd, Hg).

If shorter polyselenide ligands, such as Na_2Se_2, are reacted with $HgCl_2$, a multinuclear cluster, $(Et_4N)_4[Hg_7(Se)_8(Se_2)]$ (**84**) is produced [121]. As shown in Fig. 51, the $[Hg_7(Se)_8(Se_2)]^{4-}$ anion in **84** can be best described as "a basket with two handles". It contains four tetrahedral and three linear mercury atoms held together by a μ_4-Se_2^{2-} and eight μ_2- or μ_3-Se^{2-} ligand. The weak interactions of Hg···Se, at 3.256(5) and 3.235(5) Å, between the clusters results in a linear chain of clusters running parallel to the crystallographic (1 1 0) direction. The Hg–Se bond distances around the tetrahedral mercury atoms ranges from 2.508(6) to 3.101(7) Å, while those around the linear mercury atoms are between 2.399(5) and 2.452(5) Å.

By treating the ethylenediamine extract of the ternary alloy $K_2Hg_2Te_3$ with a methanolic solution of Bu_4NBr or Ph_4PBr, two novel mercury polytelluride compounds, $(Bu_4N)_4[Hg_4(Te)_2(Te_2)_2(Te_3)_2]$ (**8**) [35] and $(Ph_4P)_2[Hg_2(Te)(Te_2)_2]$ (**9**) [35], are obtained. Figure 52 shows the structure of the $[Hg_4(Te)_2(Te_2)_2(Te_3)_2]^{4-}$ anion. The structural similarity between the current cluster and $[Hg_7(Se)_8(Se_2)]^{4-}$ is apparent. A comparison of the two structures is given in Fig. 53. Conceptually, the structure of $[Hg_7(Se)_8(Se_2)]^{4-}$ can be derived by replacing the Te_3^{2-} handles with two linear Se–Hg–Se units and one μ_4-Te_2^{2-} unit with another linear Se–Hg–Se unit. The Hg–Te bond distances are split into two groups: the average distance involving two coordinate tellurium atoms is 2.737 Å,

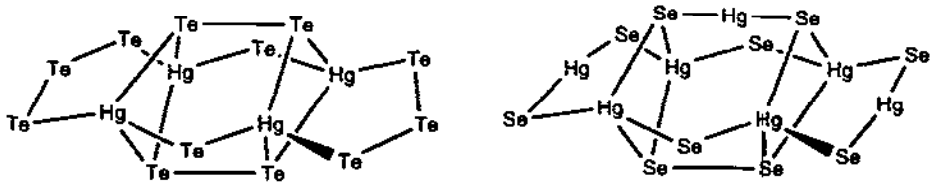

Fig. 53. Comparison between the $[Hg_4(Te)_2(Te_2)_2(Te_3)_2]^{4-}$ and $[Hg_7(Se)_8(Se_2)]^{4-}$.

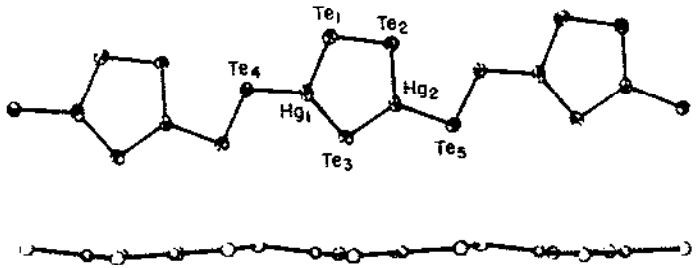

Fig. 54. Two views of the $[Hg_2(Te)(Te_2)_2]^{2-}$ chain.

while that involving three coordinate tellurium atoms is 2.954 Å. Recently, we have prepared the cadmium analog of this polytelluride cluster, $(Et_4N)_4[Cd_4(Te)_2(Te_2)_2(Te_3)_2]$ (**85**) [122]. The $[Hg_2(Te)(Te_2)_2]^{2-}$ anion in **9** is a one-dimensional polymer, consisting of Hg_2Te_3 five-membered rings bridged by Te_2^{2-} units (Fig. 54, top). This one-dimensional chain is essentially planar, featuring trigonal planar geometry around the two mercury atoms (Fig. 54, bottom). The average Hg–Te bond distance is 2.71 Å.

In the presence of (15-crown-5), zinc or mercury acetate reacts with K_2Te_3 in DMF to form $[K(15\text{-crown-}5)_2]_2[MTe_7]$ (M = Zn, Hg) (**86,87**) at 0°C (M = Zn) or –55°C (M = Hg) [123]. X-Ray diffraction studies show that both compounds have two-

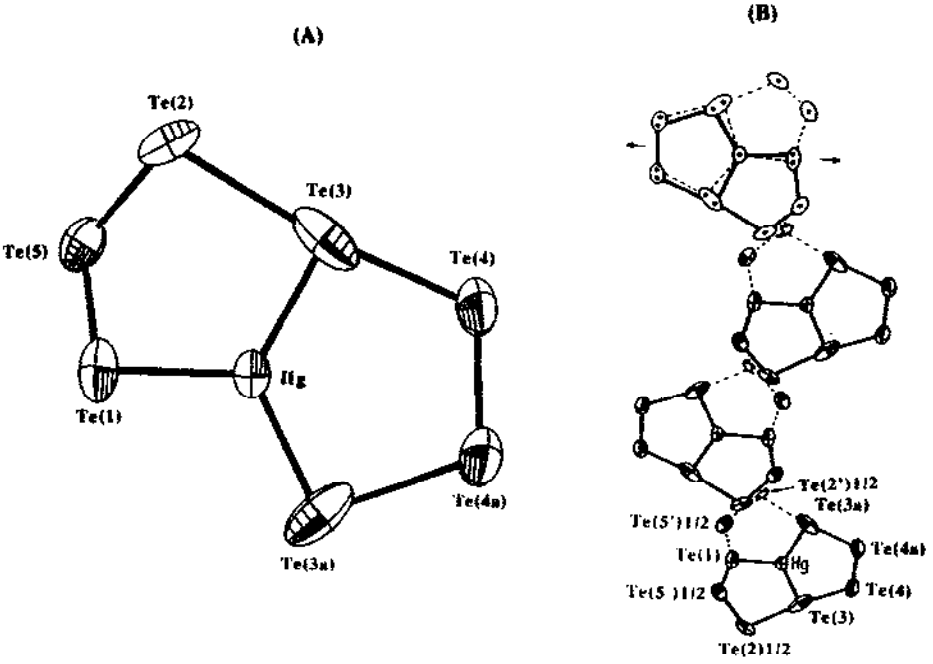

Fig. 55. The structure of the unusual $[HgTe_7]^{2-}$ anion.

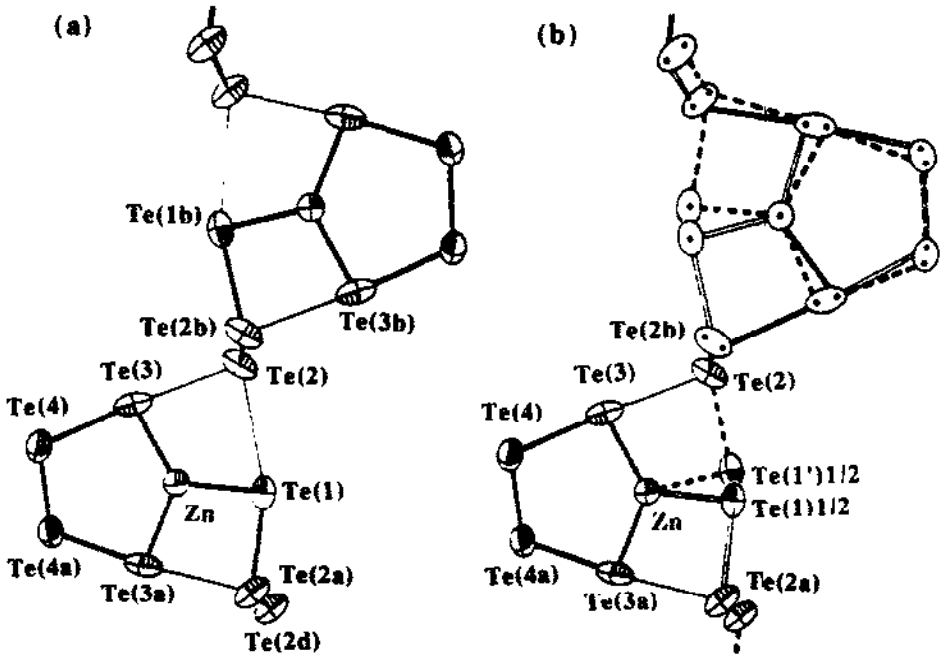

Fig. 56. The structure of the $[ZnTe_7]^{2-}$ anion.

dimensional disorder. Although the two compounds have similar unit cell parameters, their molecular structures are different. $[HgTe_7]^{2-}$ is very unusual and contains formally Te_4^{2-} and a Te_3^{2-} ligands. The Hg^{2+} center is trigonal planar and is coordinated by one Te atom of a Te_3^{2-} ligand and chelated by another Te_4^{2-} ligand, as shown in Fig. 55(A). Figure 55(B) shows how these anions are arranged in the crystal lattice and the orientational disorder. The other terminal Te atom of the Te_3^{2-} fragment, is interacting with a Te atom from Te_4^{2-} via a close Te---Te contact of 3.258 Å. This novel bonding arrangement results in the new Te_7^{4-} ligand. The Te---Te interactions between atoms of different ligands are reminiscent of similar interactions described above in the Mo/Se_x^{2-} and Nb/Te_x^{2-} systems. It is noteworthy that two of the Te–Te bond distances, i.e. Te(1)–Te(5) = 2.588(8) Å and Te(2)–Te(5) = 2.657(9) Å, are unusually short. The $[ZnTe_7]^{2-}$ anion can be viewed as a Zn^{2+} bonded by a bidentate Te_4^{2-} ligand and an η^1-type Te_3^{2-} ligand, producing a rare trigonal planar geometry for this ion. Figure 56 shows the arrangement of these anions in the lattice via Te···Te interactions and the disorder of the Te_3^{2-} fragment.

(l) The chemistry of Group 13 elements (Ga, In and Tl)

The scarcity of polychalcogenide complexes with Group 13 elements [27,28,39–41, 124], fueled with the search for soluble precursors to the semiconducting compounds In_2Se_3, InSe, TlSe and $CuInSe_2$, prompted a systematic investigation in our laboratory

into the synthesis of new soluble polychalcogenide complexes. In addition to the conventional solution method, exotic approaches such as hydrothermal techniques [79], and molten salt methods, using the polychalcogenides of organic cations (e.g. $(Ph_4P)_2Se_5$) as fluxes, have been introduced for the preparation of new compounds [58]. These studies have not only benefited the chemistry of heavy polychalcogenides with Group 13, but also expanded significantly the field of polysulfides because several new polysulfide complexes of this group have also been obtained. They are $[In_2(S_4)_2(S_6)_2(S_7)]^{4-}$ [125], $[In_2S(S_5)(S_4)_2]^{2-}$ [125], $[In_2S(S_5)(S_4)(S_6)]^{2-}$ [125], $[In(S_4)(S_6)X]^{2-}$ (X = Cl and Br) [125,126] and $[Tl_2(S_4)_2]^{2-}$ [125].

The first reported polyselenide complex was $(Ph_4P)_4[In_2(Se_4)_4(Se_5)]$ (**88**) [127]. This selenium-rich dimer is prepared by reacting $InCl_3$ with Na_2Se_5 in DMF in the presence of Ph_4PCl. The anion $[In_2(Se_4)_4(Se_5)]^{4-}$ consists of two $[In(Se_4)_2]^-$ spirocyclic rings bridged by a Se_5^{2-} chain, as shown in Fig. 57. Each indium atom is chelated by two Se_4^{2-} ligands and bound to a terminal selenium atom of the Se_5^{2-} chain, resulting in an uncom-

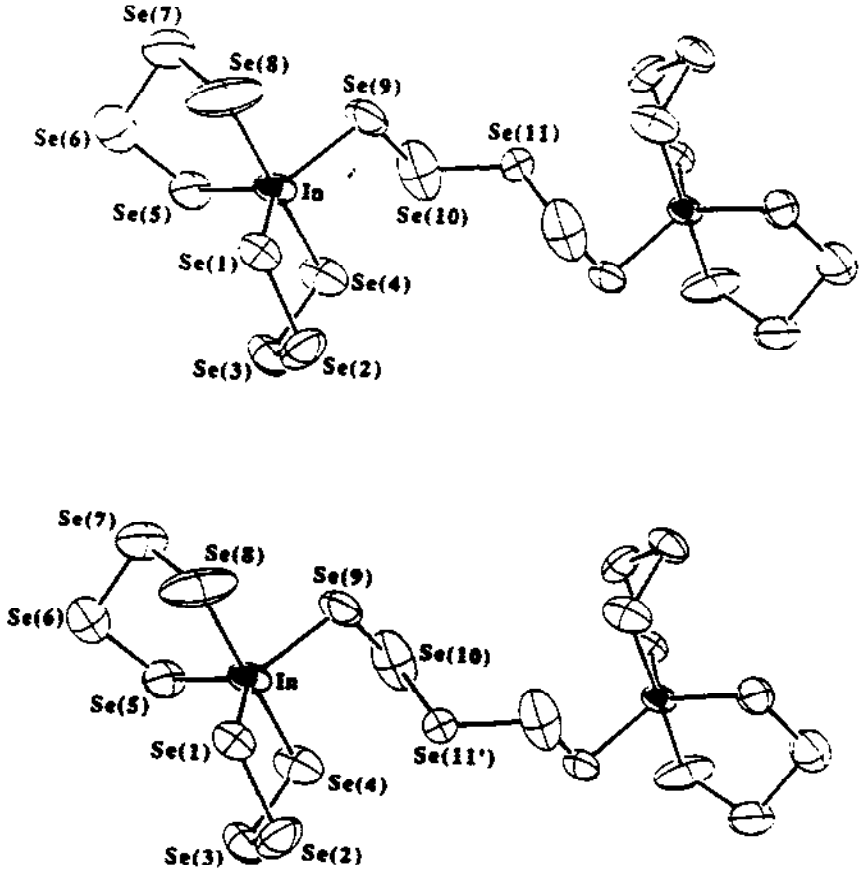

Fig. 57. Two different conformations of the $[In_2(Se_4)_4(Se_5)]^{4-}$ in the crystal lattice.

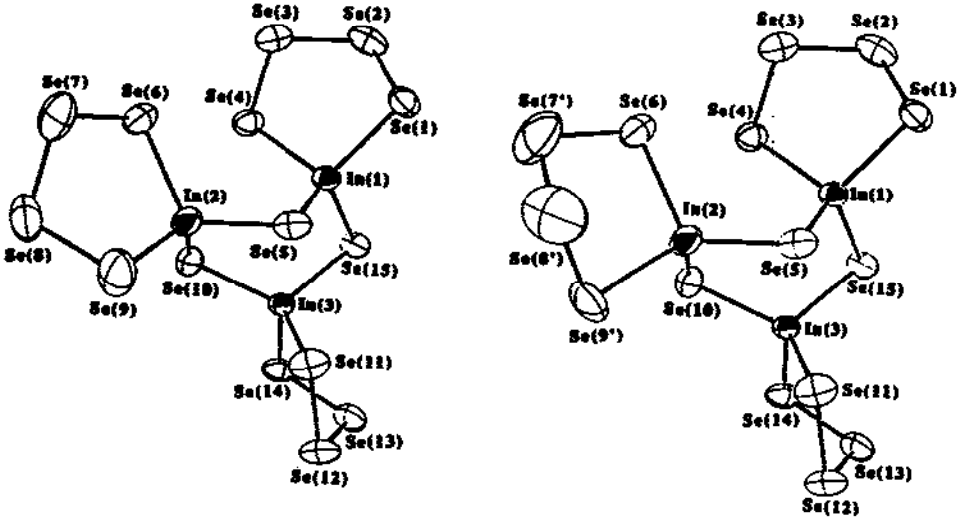

Fig. 58. Two different conformations of the $[In_3Se_3(Se_4)_3]^{3-}$ resulting from disorder of the Se_4^{2-} in In(2).

mon trigonal-bipyramidal geometry for the metal centers. The terminal selenium atom from the Se_5^{2-} chain is found to occupy one of the equatorial positions. Such a coordination geometry is uncommon in indium chalcogenide chemistry. All $InSe_4$ rings adopt an envelope conformation. Despite the lack of centrosymmetry in this molecule, there is an inversion center located half way between the In···In vector, causing a positional disorder in the Se_5^{2-} chain.

Often the formation and crystallization of metal polychalcogenide complexes can be greatly influenced by the nature of the counterions (vide supra). For some systems, compositionally and structurally different compounds were isolated from the same reaction just by the selection of different counterions [35,107,128,129]. This was also probed for the In^{3+}/Se_x^{2-} system by using various organic counterions to crystallize the complexes but no apparent dependence on counterion was found, as evidenced by the isolation of the same complex with two other cations Pr_4N^+ and Et_4N^+. The structures of $(Pr_4N)_4[In_2(Se_4)_4(Se_5)]$ (**89**) and $(Et_4N)_4[In_2(Se_4)_4(Se_5)]$ (**90**) were established by the X-ray single-crystal analysis [130]. The anions in **89** and **90** were found to be identical (within experimental error) to that in **88**. However, when the above reaction was carried out in CH_3CN solution in the presence of Et_4NBr a different compound, $(Et_4N)_3[In_3Se_3(Se_4)_3]$ (**91**), was obtained [130]. The molecule can be viewed as being formed by three $[In(Se_4)]^+$ rings connected together through three μ_2-Se^{2-} ligands. It therefore contains a six-membered In_3Se_3 ring with a puckered conformation. Three $InSe_4$ rings adopt two different conformations. The one containing In(1) is like a twisted boat, and the others have an envelope conformation. The Se_4^{2-} ligand chelating to In(2) has a positional disorder on two selenium atoms, leading to two different conformations of this $InSe_4$ ring as shown by the two ORTEP presentations in Fig. 58. All indium atoms are found to be in a tetrahedral environment.

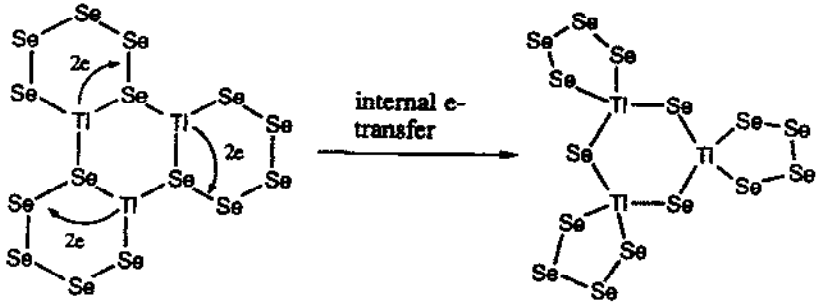

Scheme 10. Transformation from $[Tl_3(Se_5)_3]^{3-}$ to $[Tl_3Se_3(Se_4)_3]^{3-}$ via an internal electron transfer process.

Thallium(III) forms an analog to $(Et_4N)_3[In_3Se_3(Se_4)_3]$ (**91**) [131]. The structure of $(Et_4N)_3[Tl_3Se_3(Se_4)_3]$ (**92**) is identical to **91**, and shows no disorder in any of its $TlSe_4$ rings. Since the synthesis of **92** is accomplished by reacting TlCl with Na_2Se_5, the formation of this Tl^{III} compound is thought to occur through an internal two-electron transfer from the Tl^+ to the terminal Se–Se bond of the Se_5^{2-} ligand involving a precursor complex of Tl^I, $[Tl_3(Se_5)_3]_3^{3-}$ (**93**). This is similar to what has been suggested in the Au^+/Se_5^{2-} system (vide supra), as shown in Scheme 10.

Since the use of different solvents (i.e. DMF or CH_3CN) gives different complexes, the structural dependence on solvent was further probed using water. In order to overcome the solubility problem of the starting materials as well as the products (i.e. quaternary phosphonium or ammonium salts) in water at room temperature and pressure, the hydrothermal technique was applied. Several new compounds have been prepared [131]. The structures of these compounds are assembled with the proper number of $[M(Se_n)]^+$ units and an equal number of monoselenide ligands. For example, the simplest combination of these two ingredients leads to a dimer, $[In_2Se_2(Se_4)_2]^{2-}$, shown in Fig. 59. It crystallizes with either Pr_4N^+ or PPN^+, giving $(Pr_4N)_2[In_2Se_2(Se_4)_2]$ (**94**) and $(PPN)_2[In_2Se_2(Se_4)_2]$ (**95**). Both anions have essentially the same structure, featuring tetrahedrally-coordinated In^{3+} chelated by Se_4^{2-} ligands as well as two bridging Se^{2-} ligands. However, Ga^{3+} adopted Se_5^{2-} ligands forming $(Ph_4P)_2[Ga_2Se_2(Se_5)_2]$ (**96**) (see Fig. 60)

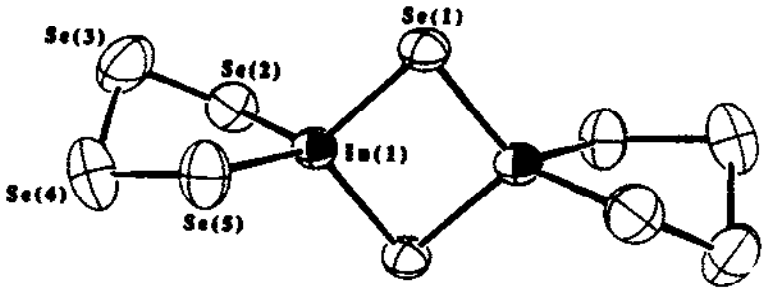

Fig. 59. The structure of $[In_2Se_2(Se_4)_2]^{2-}$ in $(Pr_4N)_2[In_2Se_2(Se_4)_2]$.

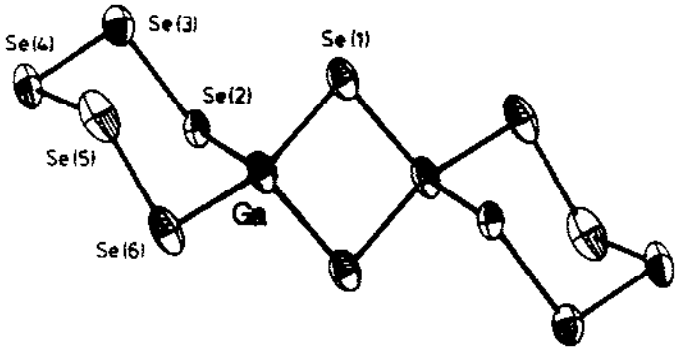

Fig. 60. The structure of $[GaSe_2(Se_5)_2]^{2-}$.

[132]. $(Ph_4P)_2[Ga_2Se_2(Se_5)_2]$ is isomorphous to $(Ph_4P)_2[Fe_2Q_2(Q_5)_2]$ (Q = S or Se). It should be noted that the gallium dimer was prepared by the reaction of $GaCl_3$ with Na_2Se_5 in DMF in the presence of Ph_4PCl. Interestingly, $(Et_4N)_5[NaIn_6Se_6(Se_4)_6]$ (97) [131] contains a much larger ring. This time, the number of the structural units is sextupled, giving another homologue of the $[InSe_n(Se_x)_n]^{n-}$ family. The molecule contains a large puckered In_6Se_6 ring which creates a pocket with an octahedral environment, as shown in Fig. 61. A Na^+ ion is found to be encapsulated in this cavity. In view of its structural analogy to crown ethers, this compound may be seen as an inorganic crown ether.

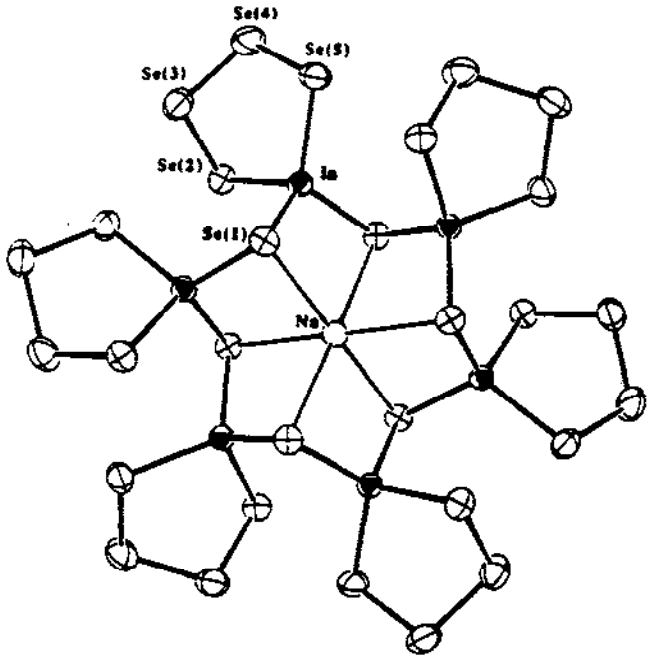

Fig. 61. The structure of $[NaIn_6Se_6(Se_4)_6]^{5-}$.

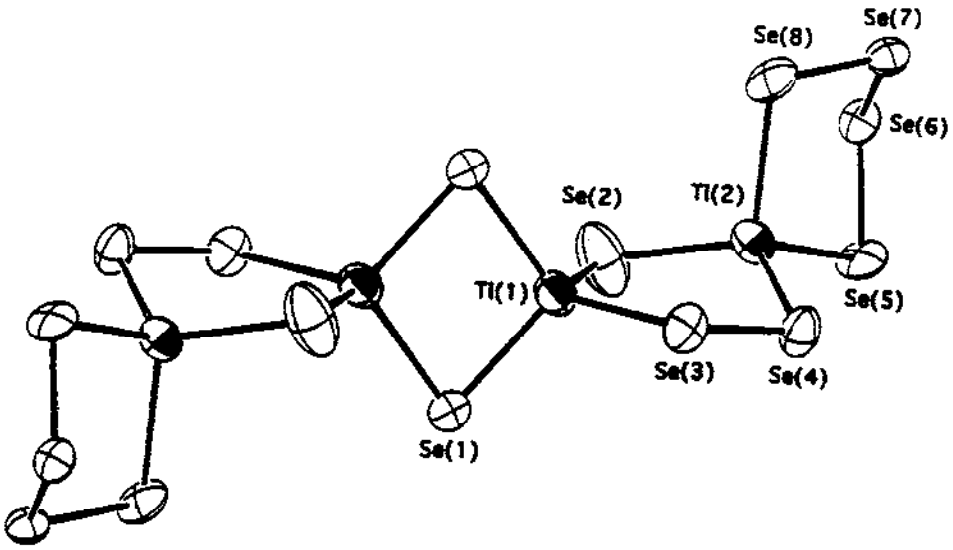

Fig. 62. The structure of $[Tl_4Se_4(Se_2)_2(Se_4)_2]^{4-}$.

When the hydrothermal technique is applied to the Tl/Se_x^{2-} system, a novel tetramer is obtained. $(Ph_4P)_4[Tl_4Se_4(Se_2)_2(Se_4)_2]$ (**98**) is prepared in a sealed Pyrex tube by the reaction of TlCl, K_2Se_4 and Ph_4PCl in a 1:1:1 molar ratio at 100°C for 1 day [133]. The structure of the $[Tl_4Se_4(Se_2)_2(Se_4)_2]^{4-}$ anion is shown in Fig. 62. The molecule consists of four, almost linearly arranged, tetrahedral Tl^{3+} centers which are upheld by two chelating Se_4^{2-}, two bridging Se_2^{2-} and four bridging Se^{2-} ligands. The Tl(1)–Tl(1)–Tl(2) angle is 164.7°. $[Tl_4Se_4(Se_2)_2(Se_4)_2]^{4-}$ is situated on an inversion center. The Tl(1)–Tl(1) distance is 3.583(6) Å, and the Tl(1)–Tl(2) distance is 3.834(4) Å. Each five-membered $TlSe_4$ ring has an intermediate conformation between envelope and half-chair. The Tl–Se bond distances range from 2.584(7) to 2.802(8) Å with an average of 2.665 Å.

Further exploration of the solvent dependence came across the use of $(Ph_4P)_2Se_5$ as the reaction medium as well as reagent [58]. The reaction of Ga, In or Tl with $(Ph_4P)_2Se_5$ in the presence of elemental selenium in a sealed Pyrex tube at 200°C yielded three isotypic compounds, $(Ph_4P)[Ga(Se_6)_2]$ (**99**), $(Ph_4P)[In(Se_6)_2]$ (**100**) and $(Ph_4P)[Tl(Se_6)_2]$ (**101**), respectively [134]. The $[M(Se_6)_2]^-$ (M = Ga, In or Tl) anions form an unprecedented two-dimensional framework with large channels filled with Ph_4P^+ cations, as shown in Fig. 63. Figures 64 and 65 show two different views of this layered framework. The structure contains tetrahedral M^{3+} centers each bridged by four Se_6^{2-} chains. The layers thus formed stack perfectly one on top of the other, giving rise to the large one-dimensional channels parallel to the *c*-axis. The Ph_4P^+ cations are situated in the layers, presumably acting as templates. To date, no aluminum polychalcogenide complex has been reported. Generally, polychalcogenide compounds are thermally unstable and

decompose upon melting. However, $(Ph_4P)[In(Se_6)_2]$ is remarkably stable up to 350°C and it melts at 242°C without decomposition. On cooling, a glassy state is formed which, upon subsequent reheating, recrystallizes at 160°C. This unusual melt-glass-crystallization property suggests that $(Ph_4P)[In(Se_6)_2]$ could have potential applications as energy storage as well as optical information storage material. Figure 66 shows the optical spectrum of $(Ph_4P)[In(Se_6)_2]$ which features an optical band gap of 1.42 eV.

(m) The chemistry of Group 14 elements (Sn and Pb)

Thus far, only two molecular polyselenide compounds are known for this group. Tin and lead each form a complex with polyselenides. $(Ph_4P)_2[Sn(Se_4)_3]$ **(102)** has been prepared by reacting either $SnCl_4$ or $SnCl_2 \cdot 2H_2O$ with Na_2Se_5 in DMF [135]. The structure consists of a central Sn^{4+} ion chelated by three Se_4^{2-} ligands, as shown in Fig. 67. This is very similar to the structure of $[Pt(Se_4)_3]^{2-}$ (vide supra). The coordination geometry for the Sn^{4+} is octahedral approaching D_3 symmetry, with an average Sn–Se bond dis-

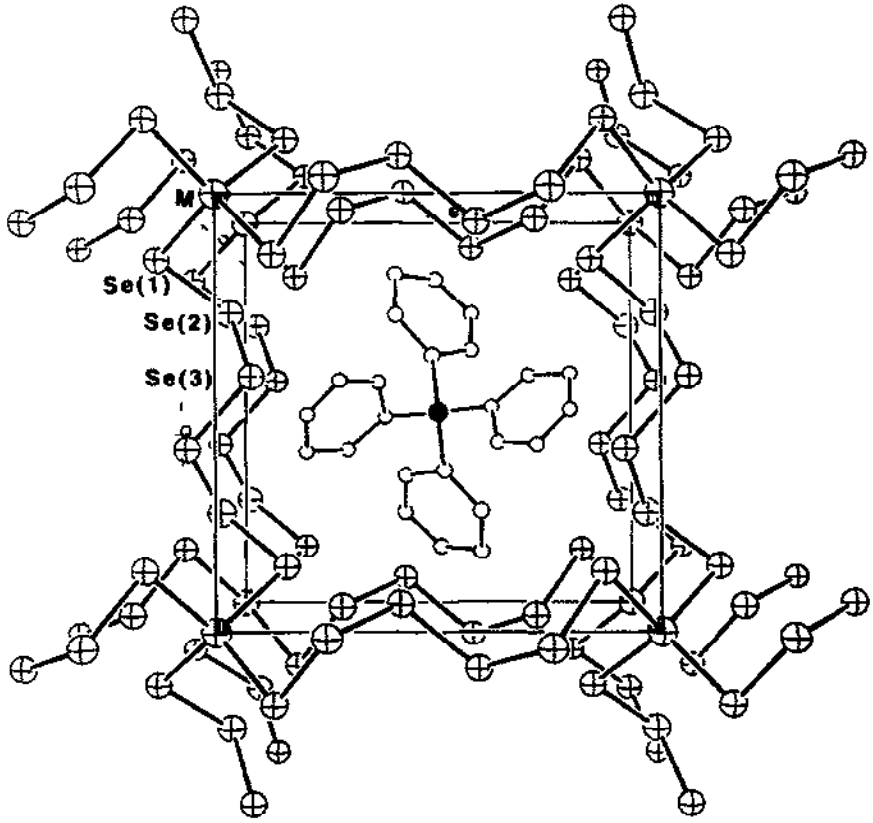

Fig. 63. A single unit cell of the $(Ph_4P)[M(Se_6)_2]$.

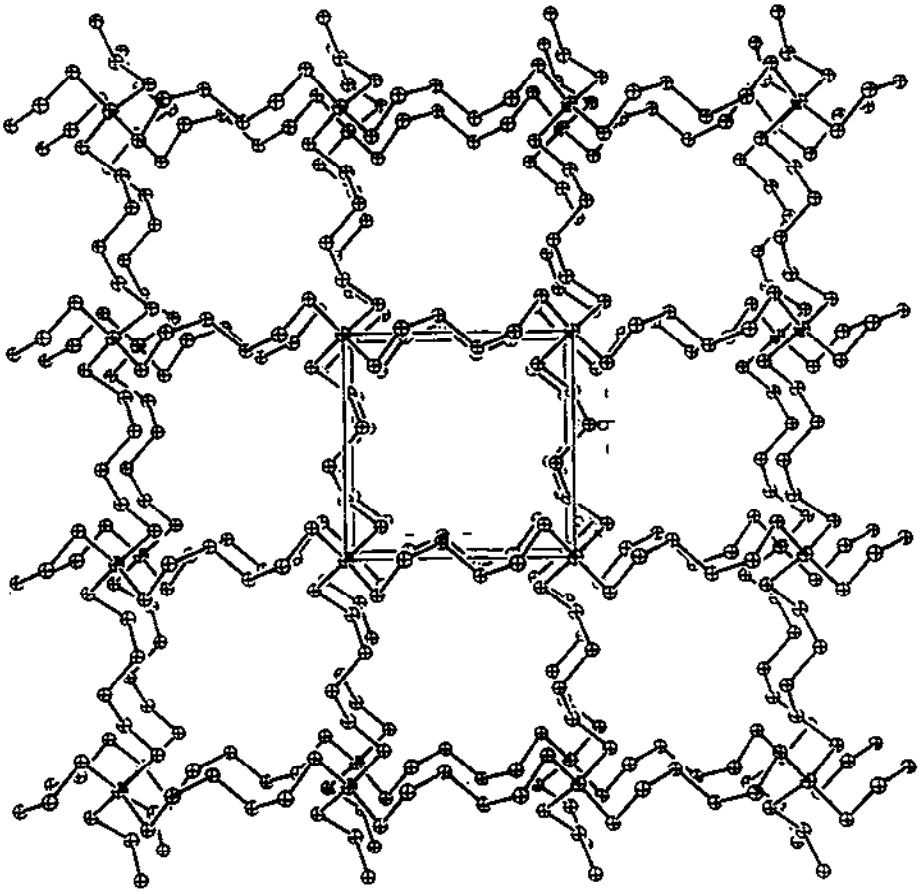

Fig. 64. The structure of $[M(Se_6)_2]_n^{n-}$ layers along the crystallographic *ab* plane with the Ph_4P^+ cations omitted.

tance of 2.709(13) Å, and a Se–Sn–Se angle of roughly 90°. Both envelope (i.e. SnSe(1)Se(2)Se(3)Se(4)) and puckered (i.e. SnSe(5)Se(6)Se(7)Se(8) and SnSe(9)Se(10) Se(11)Se(12)) conformations are adopted by the $SnSe_4$ rings. It should be noted that this complex can also give rise to optical isomerism, and the isolated product is a racemic mixture [83].

The reaction of $PbCl_2$, Na metal and elemental selenium in DMF in the presence of Ph_4PBr gave $(Ph_4P)_2[Pb(Se_4)_2]$ (**103**) [92a]. Figure 68 shows the odd-shaped structure of the $[Pb(Se_4)_2]^{2-}$ anion. The metal center is chelated by two Se_4^{2-} ligands with an irregular geometry. This is because the lone electron pair of the Pb^{2+} ion occupies one of the equatorial positions of what can be described overall as the trigonal bipyramidal shape, as predicted by the valence shell electron pair repulsion (VSEPR) model.

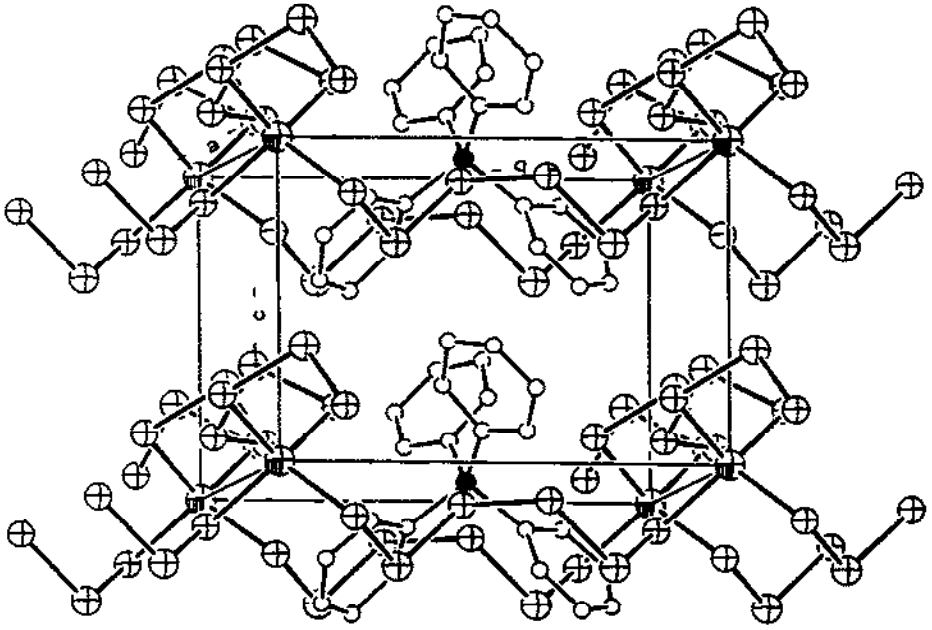

Fig. 65. A different view of the $(Ph_4P)[M(Se_6)_2]$ layers.

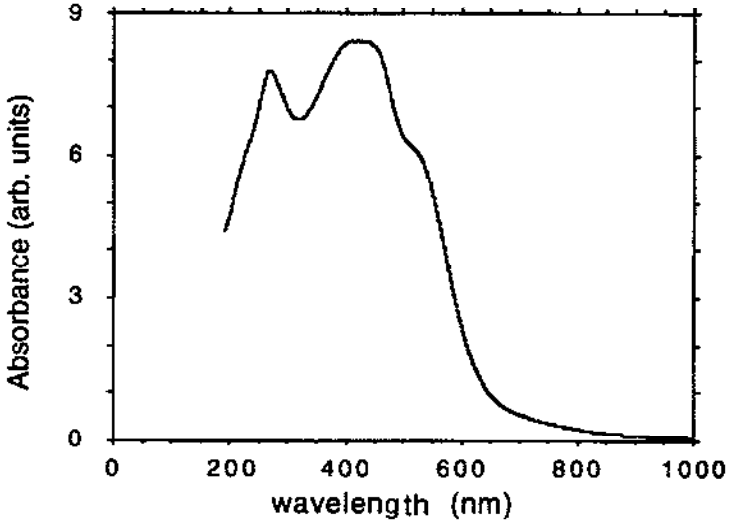

Fig. 66. Optical absorption spectrum of solid $(Ph_4P)[In(Se_6)_2]$.

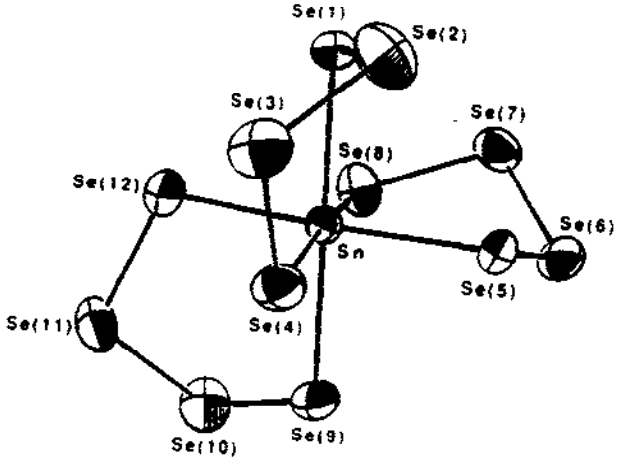

Fig. 67. The structure of $[Sn(Se_4)_3]^{2-}$.

(n) The chemistry of Group 15 elements (As, Sb and Bi)

A number of soluble heteroatomic polyanionic clusters of the type $[As_xQ_y]^{n-}$ (Q = S, Se or Te) have been synthesized and structurally characterized. These include $[AsSe_4]_3$ [136a], $[As_2Q_6]^{2-}$ (Q = Se or Te) [136b–d], $[As_3Se_6]^{3-}$ [136e], $[As_4Q_6]^{2-}$ (Q = S, Se) [136c,f], $[As_7Se_4]^-$ [136g] and $[As_{10}Q_3]^{2-}$ (Q = Se, Te) [136h,i]. However, only $[As_2Q_6]^{2-}$ contains Q–Q bonds (see Fig. 69). It consists of a six-membered As_2Q_4 ring in a chair formation. Two extra chalcogen atoms each complete the trigonal pyramidal coordination of the arsenic atom.

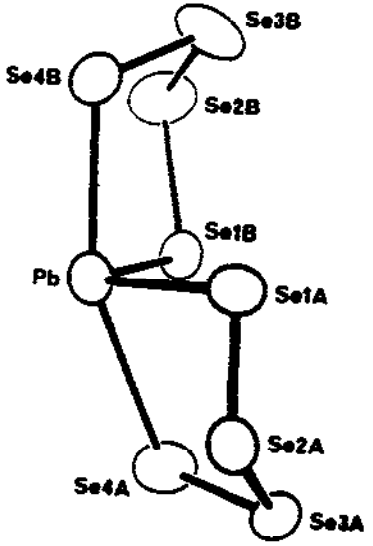

Fig. 68. The structure of $[Pb(Se_4)_2]^{2-}$.

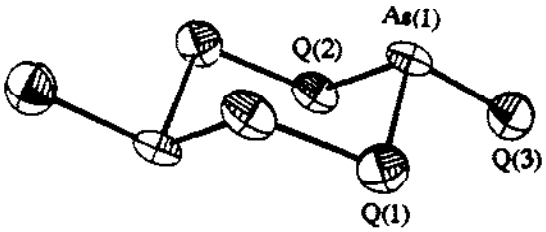

Fig. 69. The structure of $[As_2Q_6]^{2-}$ (Q = Se, Te).

(o) The chemistry of Group 16 elements (Se and Te)

In general, the polychalcogenide ligands exist as open chains in solutions and helical structures in the solid state. However, under the conditions of oxidation-reduction, an oxidized chalcogen atom (in the +2 or +4 oxidation state) itself can be chelated by polychalcogenide ligands to form a closed cyclic structure, acting as the central metal. In a structural sense, these mixed-valence polychalcogenides are no different from the metal complexes described in this review, and thus, they warrant a separate treatment from the open-chain anions.

In the $[A(Q_5)_2]^{2-}$ (when A = Se, Q = Se and A = Te, Q = S or Se) family of the homo- and heteropolychalcogenides, either a selenium or a tellurium atom acts like a "metal", being in the formal oxidation state 2+, and chelated by two Se_5^{2-} or S_5^{2-} ligands. The molecules are spirocyclic, and reminiscent of $[M(Q_4)_2]^{2-}$ (M = Ni, Pd; Q = S, Se and Te). Thus far, the structurally characterized ones include $(Ph_4P)_2[Se(Se_5)_2]$ (**67**) (two crystal modifications) [108,109,137,138], $(Ph_4P)_2[Te(S_5)_2]$ (**104**) [137], [K(222-crypt)]$_2$[$Te(Se_5)_2$] (**105**) [139] and [Ba(222-crypt)(en)][$Te(Se_5)_2$]·0.5en (**106**) [139]. Figure 70 shows the structures of $[Se(Se_5)_2]^{2-}$ (in β-form) and $[Te(S_5)_2]^{2-}$. Figure 71 shows the structure of $[Te(Se_5)_2]^{2-}$ in **105** and **106**. The X-ray single-crystal structure studies on these compounds reveal that the central atoms have the expected square-planar geometry. The bond distances of the central atom to the four chelating atoms are significantly longer than the sum of the corresponding covalent radii, suggesting a strong ionic character for these bonds.

In order to put the above description of mixed-valence polychalcogenides in perspective, two more related free polyselenides are worthy of discussion here. The $(PPN)_2[Se_{10}]\cdot DMF$ (**107**) [140] and $[Sr(15\text{-crown-}5)_2][Se_9]$ (**108**) [18], crystallized from a DMF solution of polyselenides with PPN^+ or Sr^{2+} respectively in the presence of the crown ether, represent two incredible examples of how large polyselenide ligands stabilize themselves in the absence of metal ions. The $[Se_{10}]^{2-}$ anion forms a decalin-like molecule, i.e. it consists of two fused six-membered Se_6 rings as shown in Fig. 72. The molecule is situated on a crystallographic C_2 axis (perpendicular to Se1–Se', Se3–Se3' and Se5–Se5' vectors), and both individual rings have chair conformation. The reason for this is electronic. First, two selenium atoms in the central Se–Se unit have a distorted trigonal-bipyramidal geometry, and are linked together through one of the equatorial positions of each atom. The Se–Se bond distance of 2.460(2) Å in the central Se_2 unit is slightly

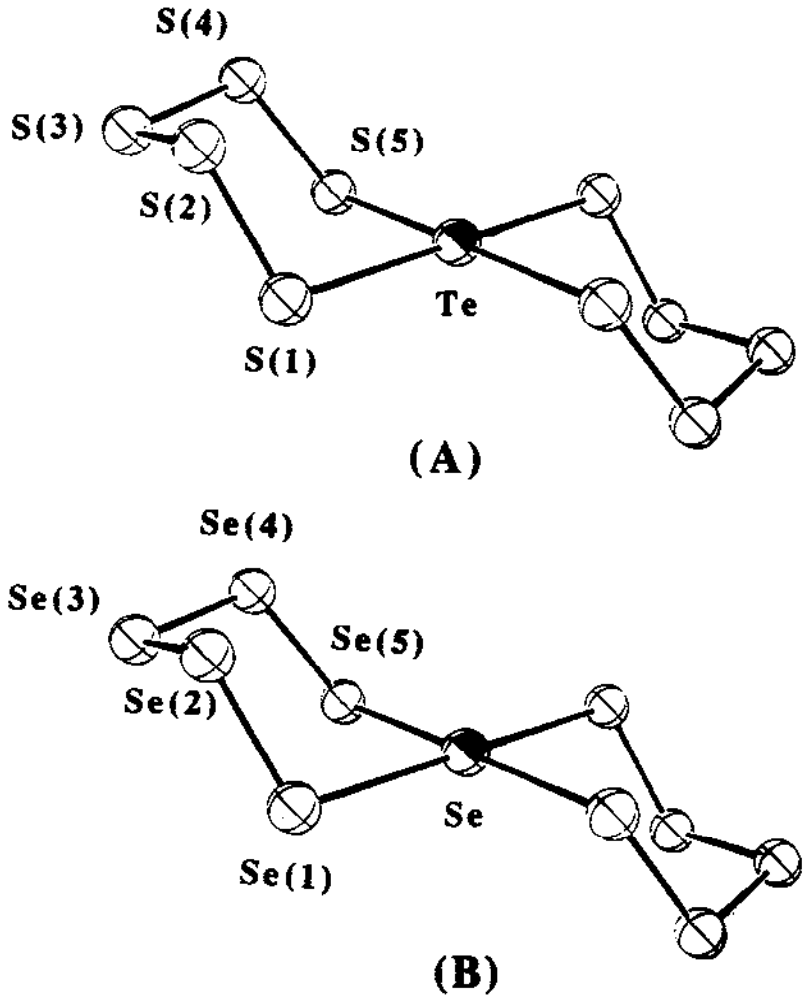

Fig. 70. The structures of $[Se(Se_5)_2]^{2-}$ and $[Te(S_5)_2]^{2-}$.

longer than typical Se–Se distances in most unbranched Se_x^{2-} chains (e.g. Se–Se 2.38(5) Å in Na_2Se_2). Secondly, Se(3) forms two long bonds with Se(2) and Se(4) at 2.759(3) and 2.572(3) Å. Therefore, the molecule might be conveniently described as a $\{Se_2\}^{2+}$ unit chelated by two Se_4^{2-} ligands with bonds having ionic character.

In a large polyselenide system such as $[Se_{10}]^{2-}$, the catenation ability of selenium may not allow the anion to maintain an unbranched helical chain structure in the solid state. A more stable system is achieved through internal electron transfer. This is also found to be operative in the $[Se_9]^{2-}$ system. Figure 73 shows the structure of the $[Se_9]^{2-}$ anion in **109** [18]. Instead of being a zigzag chain, this molecule is somewhat related to $[Se_{10}]^{2-}$. Topologically, $[Se_9]^{2-}$ can be viewed as formed through the $[Se_{10}]^{2-}$ by removing

a terminal selenium atom from one of the Se_4^{2-} ligands. The remaining Se_6 ring still has the chair conformation as shown in Fig. 73. Although the bond distance of the "central" Se_2 unit, i.e. Se(5)–Se(6) at 2.473 Å, is comparable to that in $[Se_{10}]^{2-}$, the normal bond distance of Se4–SeS at 2.341(4) Å, as well as the weak interaction between Se(1) and Se(6) (i.e. 2.953(4)Å) gives the molecule certain characteristics of the open chain structure. This clearly indicates a transition state of the molecule from abandoning the unbranched helical chain structure by seeking a similar electronic configuration to that in $[Se_{10}]^{2-}$ or $[Se_{11}]^{2-}$.

Another mixed-valence polyselenide, $Cs_4[Se(Se_5)_3]$ (**110**), is prepared by the methanothermal reaction of Cs_2CO_3 with elemental selenium at 160°C [141]. The $[Se(Se_5)_3]^-$ anion contains a square-planar Se^{2+} center coordinated by three Se_5^{2-} chains, of which one chelates while the other two act as monodentate ligands, resulting in a structure of a six-membered ring on one side with two Se_5^{2-} "tails" dangling on the other (see Fig. 74). As in $[Se(Se_5)_2]^{2-}$, $[Se(Se_5)_3]^{4-}$ shows four long Se–Se bond distances around the Se^{2+} atom.

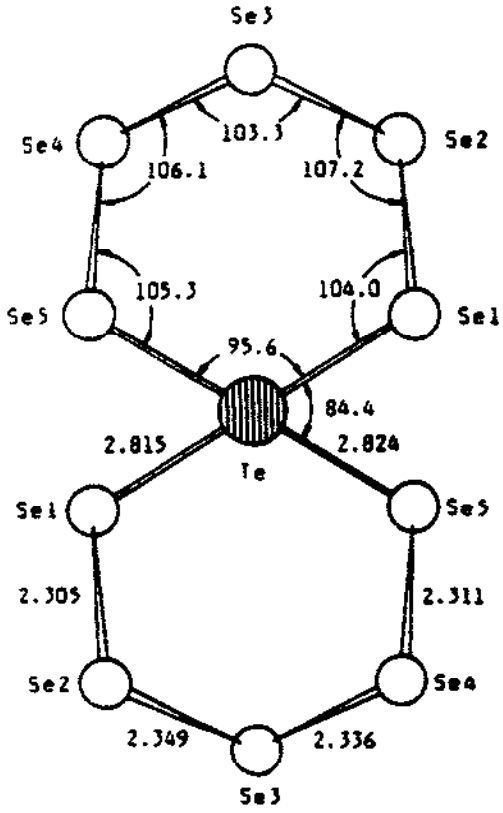

Fig. 71. The structure of $[Te(Se_5)_2]^{2-}$ anion in $[K(222\text{-crypt})]_2[Te(Se_5)_2]$ and [Ba(222-crypt)(en)][$Te(Se_5)_2$]·0.5en].

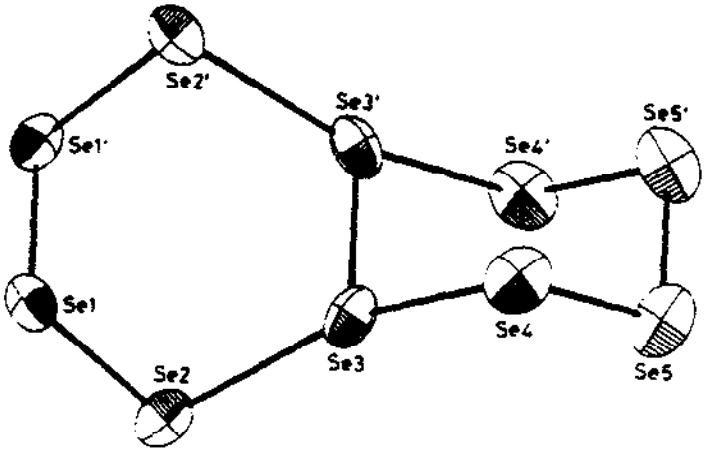

Fig. 72. The decalin-like structure of $[Se_{10}]^{2-}$.

(ii) Organometallic compounds of metal/polychalcogenides

(a) The chemistry of Group 4 elements (Ti, Zr and Hf)

The polychalcogenide chemistry of this group is exclusively dominated by compounds containing cyclopentadienyl ligands. All three metals in this group form bis(η^5-cyclopentadienyl)(pentaselenido)metal complexes (η^5-Cp)$_2$M(Se$_5$), M = Ti (**111**) [142,143], Zr (**112**) [143] and Hf (**113**) [143]. These compounds can be readily prepared by the metathetical reaction of Cp_2MCl_2 with alkali polychalcogenides (e.g. Li_2Se_5 or Na_2Se_5)[142,143]. This method was used first in the late 1960s for the synthesis of the ti-

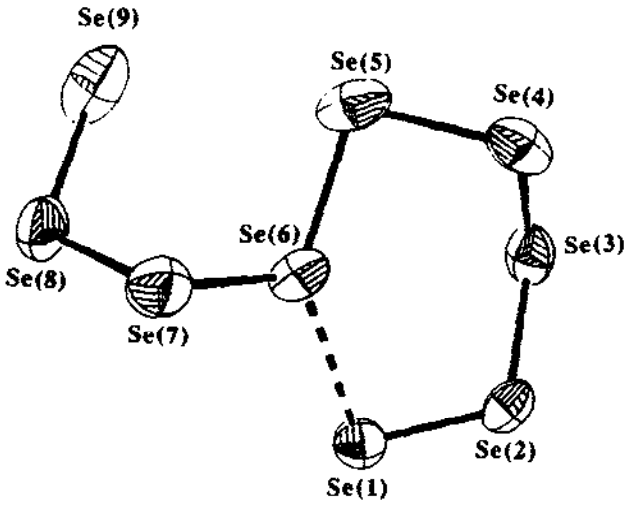

Fig. 73. The structure of $[Se_9]^{2-}$.

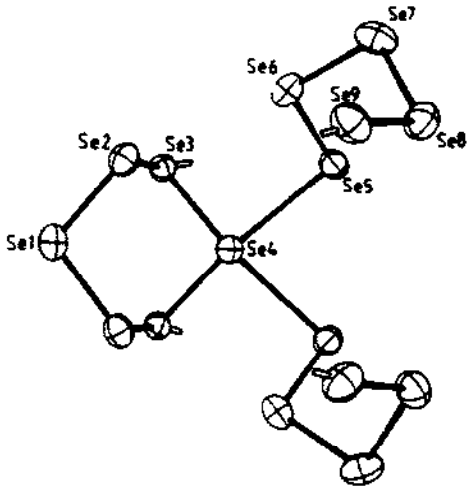

Fig. 74. The structure of $[Se(Se_5)_3]^{4-}$.

tanium complex, for which a correct structure was proposed based on spectroscopic and elemental analytical data [31]. Figure 75 shows the structure of these complexes. The six-membered MSe_5 ring has a chair conformation. The metal center is essentially in a tetrahedral environment, i.e. in addition to two M–Se bonds two other vertices are pointed to the centroids of two Cp rings. When Cp_2TiCl_2 reacts with a THF solution of a mixture of lithium polyselenide and lithium polysulfide at different molar ratios, a series of mixed selenide-sulfides, $[(\eta^5\text{-Cp})_2TiSe_xS_{5-x}]$ can been obtained [144]. This class of compounds has the same structure as the $(\eta^5\text{-Cp})_2M(Se_5)$ as shown by the X-ray structure determination on one specific crystal. The MQ_5 ring is disordered with all positions partially occupied by both sulfur and selenium [144]. It is interesting to note that Group 4 metals also

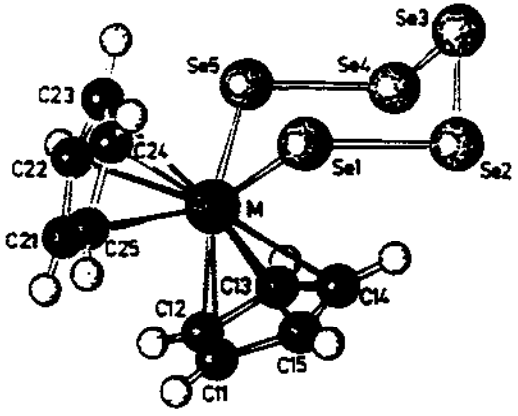

Fig. 75. The structure of $(\eta^5\text{-Cp})_2M(Se_5)$ (M = Ti, Zr or Hf).

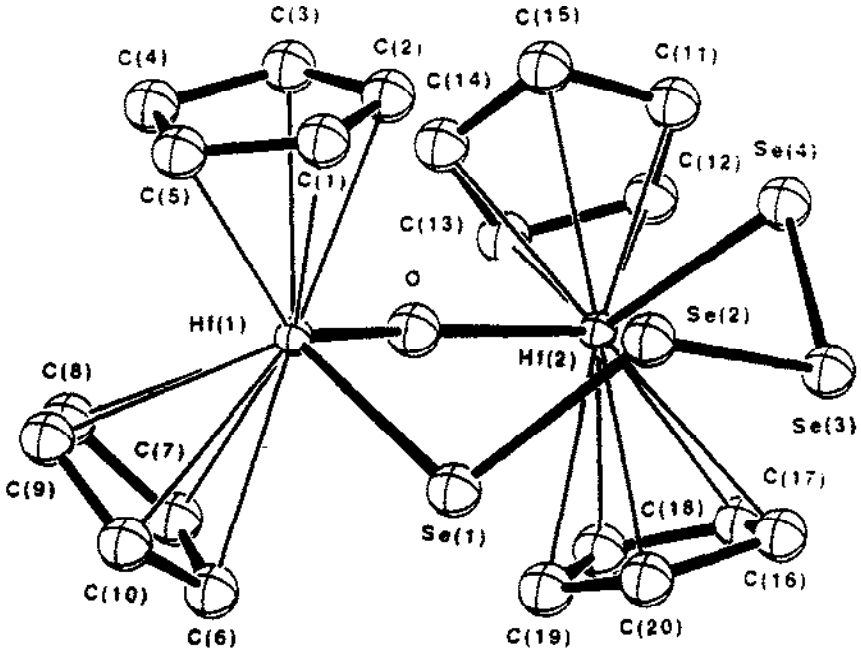

Fig. 76. The structure of $[(\eta^5\text{-}Cp_2Hf)_2(\mu_2\text{-}O)(\mu_2\text{-}Se_4)]$.

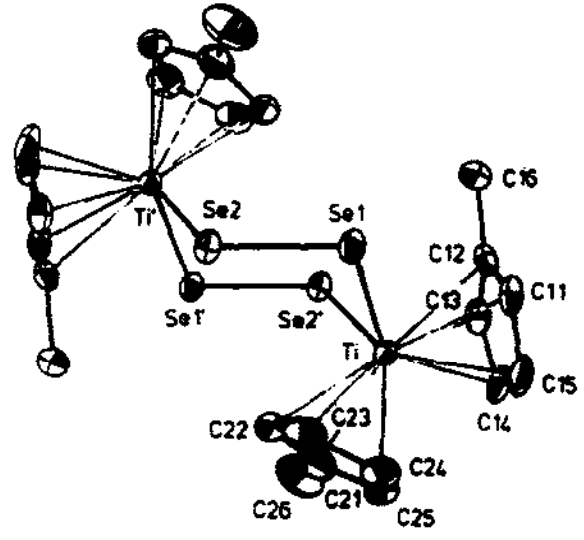

Fig. 77. The structure of $[(\eta^5\text{-}MeCp)_2Ti]_2(\mu_2\text{-}Se_2)_2]$.

have known polysulfide analogs [45]. However, no polytelluride analogs have been reported.

When exposed to air, $(\eta^5\text{-Cp})_2\text{Hf}(\text{Se}_5)$ was found to transform to a μ_2-O bridged dimer, $[(\eta^5\text{-Cp}_2\text{Hf})_2(\mu_2\text{-O})(\mu_2\text{-Se}_4)]$ **(114)** [143]. The structure of this complex, as shown in Fig. 76, contains an unusual seven-membered Hf_2OSe_4 ring. On the other hand, $(\eta^5\text{-RCp})_2\text{Ti}(\text{Se}_5)$ (R = H, Me or ^{i}Pr) reacts with selenium abstracting reagents such as Ph_3P or Bu_3P, to condense to a symmetric dimer $[\{(\eta^5\text{-RCp})_2\text{Ti}\}_2(\mu_2\text{-Se}_2)_2]$ **(115)** [145]. This compound is also accessible by the direct reaction between $(\text{RCp})_2\text{TiCl}_2$ and Li_2Se_2 [145]. In the structure of $[\{(\eta^5\text{-MeCp})_2\text{Ti}\}_2(\mu_2\text{-Se}_2)_2]$, shown in Fig. 77, the six-membered Ti_2Se_4 ring also adopts the chair conformation. The Ti–Se and Se–Se bond distances of 2.563(1) and 2.343(1) Å are comparable to those found in the monomer.

Reaction of CpTiCl_3 with $(\text{Me}_3\text{Si})_2\text{Se}$ in THF leads to the formation of a tetranuclear compound $[(\eta^5\text{-Cp})_4\text{Ti}_4(\mu_4\text{-O})(\mu_2\text{-Se})(\mu_3\text{-Se})_2(\mu_3\text{-Se}_2)_2]$ containing a diselenide unit **(116)** [146]. This cluster contains four titanium atoms arrayed in a tetrahedral fashion. An oxygen atom, probably originating from THF, is encapsulated in the center as shown in Fig. 78. The four tetrahedral faces are alternately capped by two $\mu_3\text{-Se}^{2-}$ and two $\mu_3\text{-Se}_2^{2-}$ ligands while an edge (Ti1–Ti4) is bridged by a $\mu_2\text{-Se}^{2-}$ ligand. All titanium atoms have distorted octahedral geometry.

(b) The chemistry of Group 5 elements (V, Nb and Ta)

Thus far, successful synthesis of heavy polychalcogenide-containing compounds has been limited to the vanadium system. The preferred motif found either in the polysul-

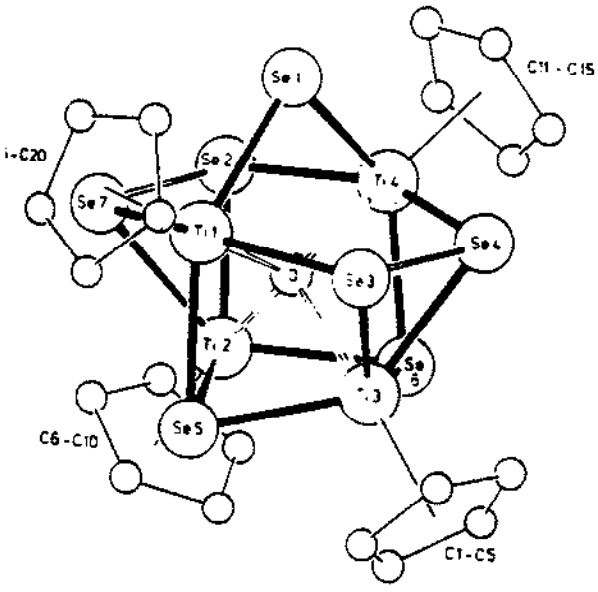

Fig. 78. The structure of $[\eta^5\text{-Cp}_4\text{Ti}_4(\mu_4\text{-O})(\mu_2\text{-Se})(\mu_3\text{-Se})_2(\mu_3\text{-Se}_2)_2]$.

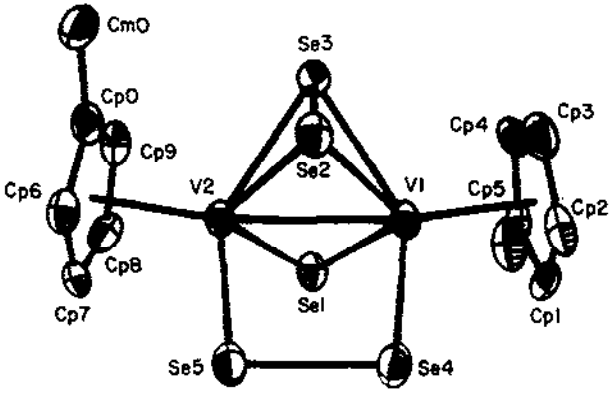

Fig. 79. The structure of $[\eta^5\text{-MeCp}_2\text{V}_2(\mu_2\text{-Se})(\mu_2\text{-Se}_2)(\mu_2\text{-}\eta^2\text{-Se}_2)]$.

fides or in the heavy polychalcogenides seems to be binuclear complexes containing metal–metal bonding.

Although the existence of a monomeric cyclopentadienyl pentachalcogenide complex of vanadium, $(\eta^5\text{-Cp})_2\text{V}(\text{Q}_5)$ (Q = S, Se), was reported as early as 1971 [32], their X-ray structure studies were never substantiated. Nevertheless, if the $(\eta^5\text{-MeCp})_2\text{V}(\text{Se}_5)$ (generated in situ from $(\text{MeCp})_2\text{VCl}_2$ and H_2Se) is allowed to thermolyze in THF, the diamagnetic compound $[(\eta^5\text{-MeCp})_2\text{V}_2(\mu_2\text{-Se})(\mu_2\text{-Se}_2)(\mu_2\text{-}\eta^2\text{-Se}_2)]$ (**117**) can be obtained [147]. A better method of making this compound is to react Cp_2VCl_2 with $(\text{SiMe}_3)_2\text{Se}$ [148]. Figure 79 shows the structure of the $[\eta^5\text{-MeCp}_2\text{V}_2(\mu_2\text{-Se})(\mu_2\text{-Se}_2)(\mu_2\text{-}\eta^2\text{-Se}_2)]$. Unlike the dimers in Group 4, the V–V distance of 2.779(4) Å in **117** indicates a metal–metal bond.

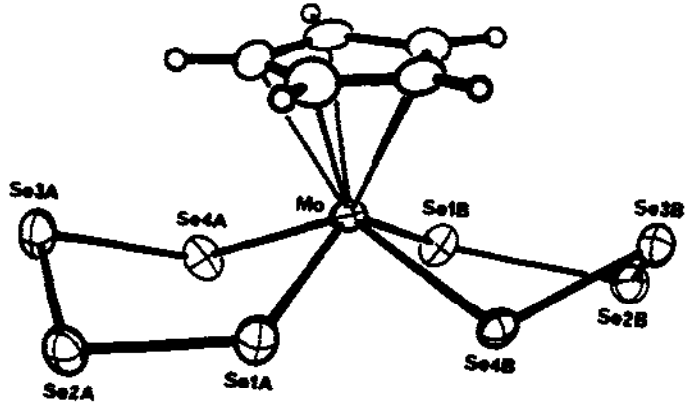

Fig. 80. The structure of the $[(\eta^5\text{-Cp})\text{Mo}(\text{Se}_4)_2]^-$ anion.

(c) The chemistry of Group 6 elements (Cr, Mo and W)

Similar to the homoleptic compounds of this group, these three elements demonstrate rich organometallic/polychalcogenide chemistry. The compounds $(\eta^5\text{-Cp})_2M(Se_4)$ (M = Mo, W) (**5,6**) form upon the reaction of $CpMCl_2$ with an ethanolic solution of Na_2Se_5 [33]. Their identities were deduced from elemental analyses and molecular weights, determined cryoscopically. However, a cyclopentadienyl complex of molybdenum containing Se_4^{2-} ligands has recently been prepared and structurally characterized. The $(Ph_4P)[(\eta^5\text{-Cp})Mo(Se_4)_2]$ (**118**) was obtained by the reaction of $[Cp_2Mo(CO)_3]_2$, Na, Se and Ph_4PBr at 60°C in DMF [135b]. The structure of the $[(\eta^5\text{-Cp})Mo(Se_4)_2]^-$ anion is shown in Fig. 80. If the Cp group is viewed as occupying one coordination site, this structure is similar to that of $[MoX(Q_4)_2]^{2-}$ (X = O, S, Se; Q = S, Se, Te) anions. The average Mo–Se bond distance is 2.50 Å, and the Se–Se distances range from 2.343 to 2.419 Å.

When $[Cp_2Mo(CO)_3]_2$ is allowed to react with tetraethylammonium polyselenide at room temperature in ethanol, $(Et_4N)[(\eta^5\text{-Cp})Mo(Se_2)(CO)_2]$ (**119**) can be obtained [149]. In the structure, the molybdenum atom is surrounded by a η^5-Cp ring, two *cis*-CO groups and the side-on $\eta^2\text{-}Se_2^{2-}$ ligand as shown in Fig. 81. The Mo–Se bond distances are 2.596(1) and 2.598(1) Å, while the Se–Se distance is 2.310(2) Å. This Mo^{2+} compound is the precursor to the $[(\eta^5\text{-Cp})Mo(Se_4)_2]^-$ in which the formal oxidation state of Mo is 4+. Reaction of the $[(\eta^5Cp)Mo(Q_2)(CO)_2]$ (Q = S, Se) with elemental selenium leads to the completely decarbonylated compound $[(\eta^5\text{-Cp})Mo(Q_4)_2]^-$ [41,150]. By analogy, when $[Cp_2Cr(CO)_3]_2$ reacts with elemental selenium, one of the products isolated is $[(\eta^5\text{-Cp})_2Cr_2(Se_2)(CO)_4]$ (**120**) [151]. As shown in Fig. 82, the structure of **120** contains the similar $[(\eta^5\text{-Cp})M(Se_2)(CO)_2]$ fragment to the molybdenum monomer. The diselenide ligand, having a short bond of 2.277 Å, has some multiple bond character, and is now a $\mu\text{-}\eta^2,\eta^2$-type ligand. Interestingly, an asymmetric dimer $[(\eta^5\text{-Cp}^*)_2Cr_2(Se_2)(CO)_5]$ (**121**) is also known to form [152]. It contains one more CO group than **120**. The diselenide ligand in this asymmetric dimer was speculated to adopt the $\mu\text{-}\eta^1,\eta^2$ bonding mode as shown in Scheme 11.

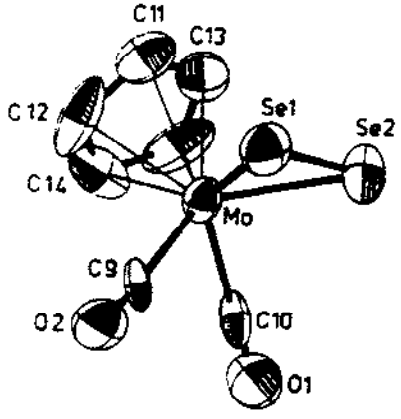

Fig. 81. The structure of the $[(\eta^5\text{-Cp})Mo(Se_2)(CO)_2]^-$ anion.

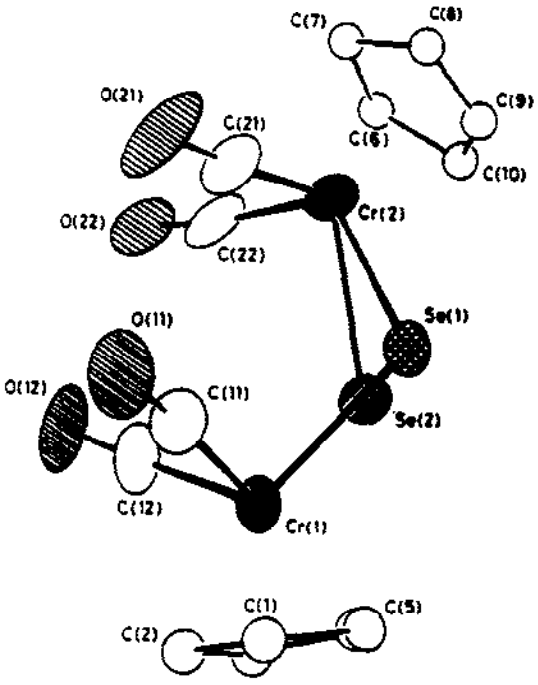

Fig. 82. The structure of $[(\eta^5\text{-Cp})_2Cr_2(Se_2)(CO)_4]$.

Kolis and co-workers have found that reactions between metal carbonyls and alkali polychalcogenides K_2Q_n (A = alkali metal; Q = S, Se or Te; $n = 2$–6) provide a convenient route, via either simple substitution of CO or oxidative decarbonylation, for introducing polychalcogenide ligands into metal centers. For instance, the reaction of $M(CO)_6$ (M = Cr, Mo, W) with an equimolar amount of K_2Te_4 in DMF gave the simple CO-substitution products, $[M(Te_4)(CO)_4]^{2-}$ [153]. $(Ph_4P)_2[Cr(Te_4)(CO)_4]$ (**122**) and $(Ph_4P)_2[W(Te_4)(CO)_4]$ (**123**) are isostructural to each other. The anions contain a metal octahedrally surrounded by a chelating Te_4^{2-} ligand and four CO groups, as shown in Fig. 83. The five-membered MTe_4 ring is found to adopt an envelope conformation. The average Cr–Te bond distance is 2.727 Å, while the average W–Te distance 2.838 Å. The reaction involving $Mo(CO)_6$ under the same conditions gave solutions with similar IR spec-

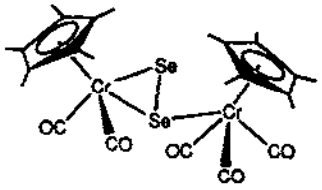

Scheme 11.

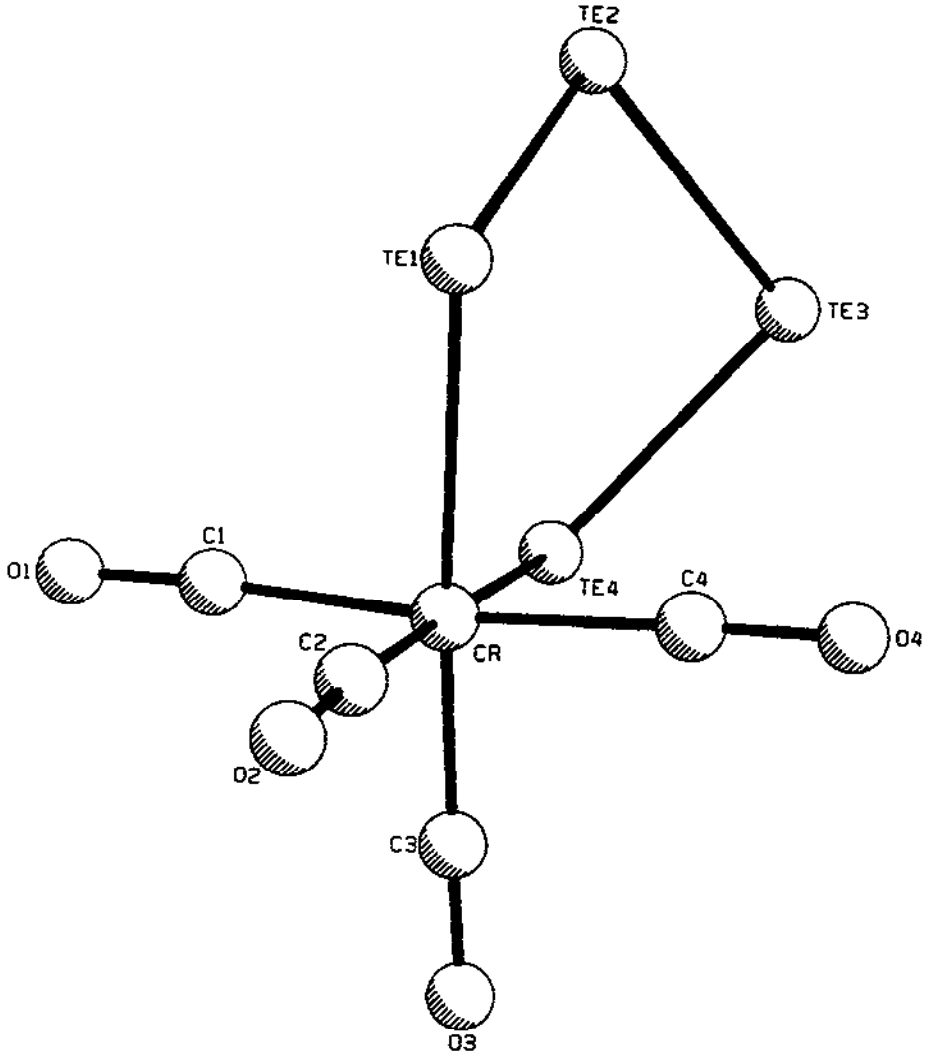

Fig. 83. The structure of $[M(Te_4)(CO)_4]^{2-}$ (M = Cr, W).

tra as the other metals, but isolation of the products resulted in oily solids [153]. On the other hand, the reactant stoichiometry, the length of polytelluride ligands used, and the reaction temperature in this system all have great influence on the final products. Thus, another two chromium carbonyl polytelluride clusters, $(Ph_4P)_2[Cr_4(Te_2)(CO)_{20}]$ **(124)** and $(Ph_4P)_2[Cr_4(Te_3)(CO)_{20}]$ **(125)**, can be obtained by reacting excess $Cr(CO)_6$ with K_2Te or K_2Te_3, respectively [154]. The structures of the $[Cr_4(Te_2)(CO)_{20}]^{2-}$ and $[Cr_4(Te_3)(CO)_{20}]^{2-}$ ions are very similar, containing a μ-η^2-Te_2^{2-} or μ-η^2-Te_3^{2-} ligand bonded to four $Cr(CO)_5$ fragments as shown in Fig. 84. The Cr–Te bond distances average

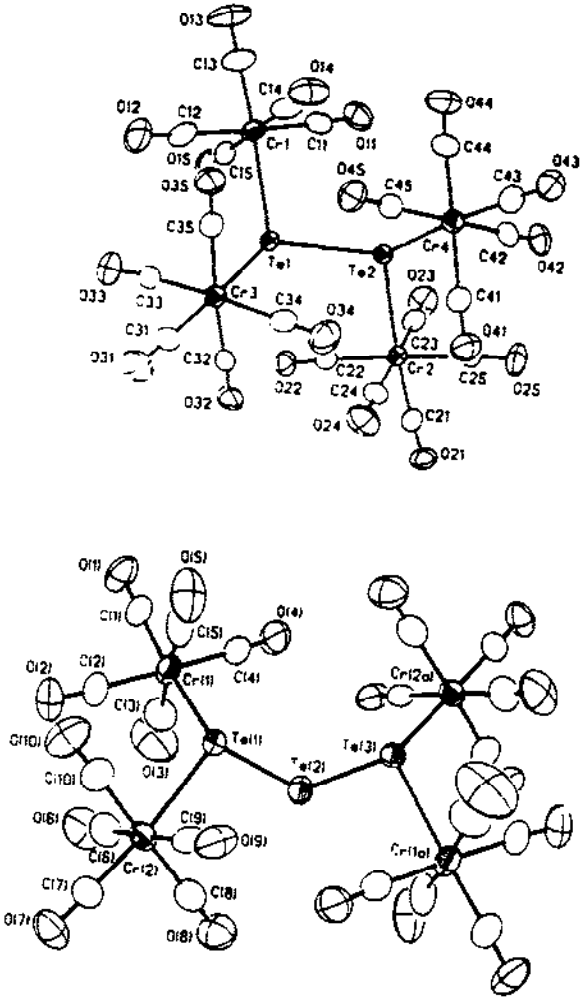

Fig. 84. The structures of $[Cr_4(Te_2)(CO)_{20}]^{2-}$ and $[Cr_4(Te_3)(CO)_{20}]^{2-}$.

2.749(2) Å in **124** and 2.76(1) in **125**, and the Te–Te distances are 2.784(2) Å in **124**, 2.734(1) and 2.738(1) Å in **125**.

The $[W_3(Te_2)(CO)_{15}]$ (**126**), obtained by HCl acidification of a mixture of $[\{(CO)_5W\}_3Sn]$ and Al_2Te_3, possesses an unusual Te_2^{2-} ligand [155]. It is first side-bonded to a $W(CO)_5$, then bridges another two $W(CO)_5$ fragments as shown in Scheme 12. The two W–Te bond distances are W(1)–Te = 2.881(3) and W(2)–Te = 2.739(2) Å, while the Te–Te distance of 2.686(4) Å is extremely short implying a double bond character.

When threefold amount of $W(CO)_6$ was reacted with the $(Ph_4P)_2Te_4$ at 100°C in DMF, the novel oxidative decarbonylation product, $(Ph_4P)_2[W_6(Te_2)_4(CO)_{18}]\cdot CH_2Cl_2$

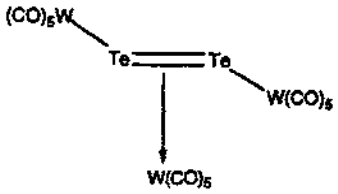

Scheme 12. The structure of [W3(Te2)(CO)15].

(127), was obtained [156]. Figure 85 shows the structure of the $[W_6(Te_2)_4(CO)_{18}]^{2-}$ cluster. First, two tellurium atoms in the central Te_2^{2-} unit are each side-bound to three metal atoms. The six tungsten atoms are in trigonal prismatic arrangement, allowing each two tungsten atoms to form a metal–metal bond. Thus, this W_3Te–TeW_3 fragment is similar to the CH_3CH_3 molecule in an eclipsed conformation. In addition, three μ_4-η^2-Te_2^{2-} ligands are distributed in the cluster periphery. The octahedral coordination of each tungsten is completed by three CO groups. If we ignore the CO groups, the cluster core looks like a "pinwheel" as shown Fig. 86. The W–Te bond distances range from 2.706 to 2.882 Å. The average Te–Te distance is 2.851(2) Å, and the average W–W distance 3.088(9) Å. Recently we have found that the molybdenum analog of this "pinwheel" cluster can be prepared hydrothermally in high yield. The reaction of $Mo(CO)_6$ with Na_2Te_2 in the presence of Ph_4PCl in H_2O in a sealed Pyrex tube at 110°C gave crystals of

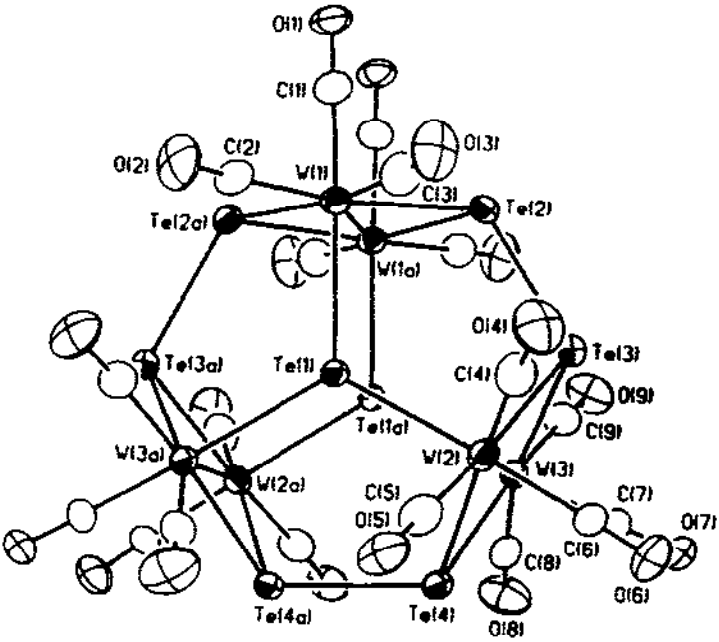

Fig. 85. The structure of $[W_6(Te_2)_4(CO)_{18}]^{2-}$.

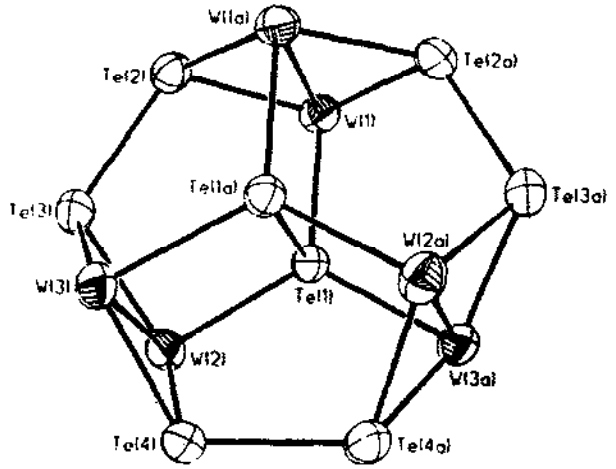

Fig. 86. Structure of the cluster $[W_6(Te_2)_4(CO)_{18}]^{2-}$ core with CO groups omitted.

$(Ph_4P)_2[Mo_6(Te_2)_4(CO)_{18}]$ (**128**) in 3 days. The $[Mo_6(Te_2)_4(CO)_{18}]^{2-}$ anion has essentially the same structure as that of the tungsten cluster, but the compound crystallizes in a different space group [157].

(d) The chemistry of Group 7 elements (Mn and Re)

Along with the neighboring elements in Group 6, these two metals are emerging as the active area of research.

The $[(\eta^5\text{-Cp}^*)Mn(Se_2)(CO)_2]$ (**129**), obtained from a reaction between $CpMn(CO)_3$ and elemental selenium, is isoelectronic to the $[(\eta^5\text{-Cp})Mo(Se_2)(CO)_2]^-$, and has a similar

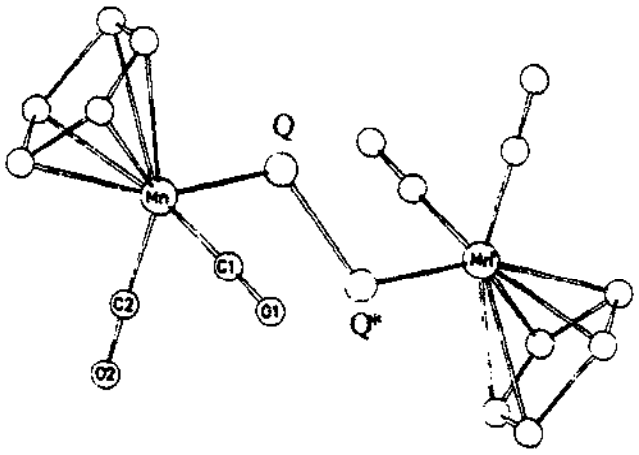

Fig. 87. The structure of $[(\eta^5\text{-Cp})_2Mn_2(Q_2)(CO)_4]$ (Q = S, Se).

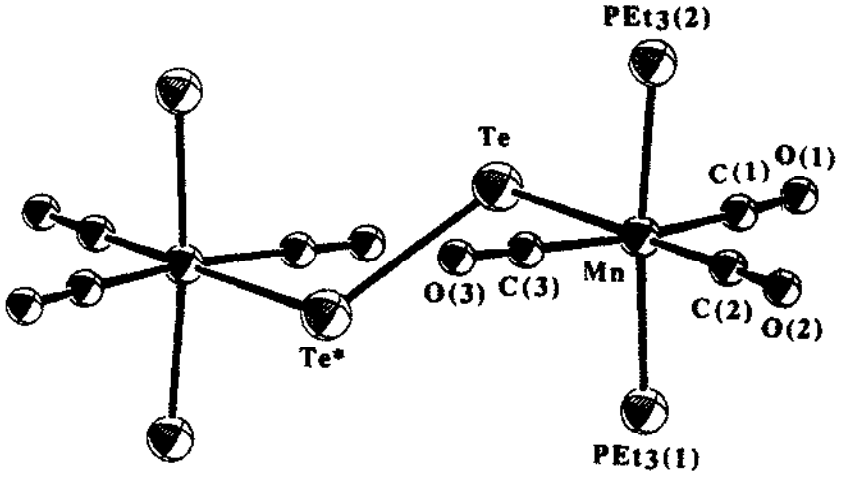

Fig. 88. The structure of $[(Et_3P)_4Mn_2(Te_2)(CO)_6]$.

molecular structure [158] (see Fig. 81). The Mn–Se bond distances average 2.463(4) Å, while the Se–Se distance of 2.263(8) Å also has some double bond character. The structure of another complex. $[(\eta^5\text{-}Cp)_2Mn_2(Se_2)(CO)_4]$ (**130**), formed from the reaction of $CpMn(CO)_2(THF)$ with COSe, was proposed to be the same with its sulfur analog $[(\eta^5\text{-}Cp)_2Mn_2(S_2)(CO)_4]$ (**131**) shown in Fig. 87 [159].

A manganese telluride compound, $[(Et_3P)_4Mn_2(Te_2)(CO)_6]$ (**132**), obtained by reacting $Mn_2(CO)_{10}$ with 2 equiv. of Et_3PTe in refluxing toluene, is also found to contain a *trans* μ_2-Te_2^{2-} ligand [160]. The molecule consists of two distorted octahedral Mn^+ centers bridged by the Te_2^{2-} unit in a *trans* fashion as shown in Fig. 88. Two phosphine ligands on each metal center are in *trans* positions. The Mn–Te distance is 2.718(1) Å, and the Te–Te distance is 2.763(1) Å. A rhenium telluride dimer with the same formula as **131** adopts a different structure, underscoring the significantly different intrinsic chemistry of tellurium. $[(\eta^5Cp^*)_2Re_2(Te_2)(CO)_4]$ (**133**) can be prepared by reaction of $CpRe(CO)_2(THF)$ with H_2Te (generated with Al_2Te_3/HCl), followed by 30 min of UV ir-

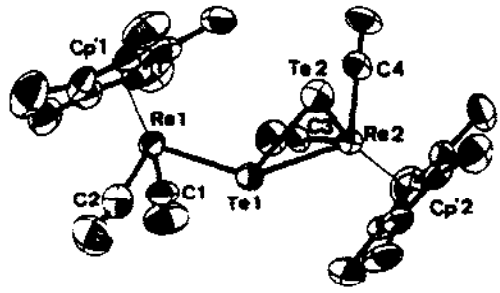

Fig. 89. The structure of $[(\eta^5\text{-}Cp)_2Re_2(Te_2)(CO)_4]$.

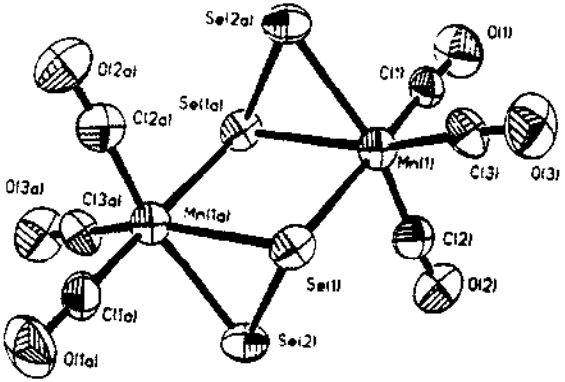

Fig. 90. The structure of $[Mn_2(Se_2)_2(CO)_6]^{2-}$.

radiation [161]. Figure 89 shows the structure of this compound. The main difference lies on the bonding mode of the ditelluride unit which is a μ-η^1,η^2-type ligand. The short bond distance of 2.632 Å for Re(1)–Te(1) was explained by invoking a Re–Te double bond. The distances of two tellurium atoms to Re(2) are 2.793(1) and 2.806(1) Å, and the Te–Te distance is 2.703(1) Å.

Two structurally related compounds can be obtained by the oxidative decarbonylation of $Mn_2(CO)_{10}$ with Se_x^{2-}. The $(Ph_4P)_2[Mn_2(Se_2)_2(CO)_6]\cdot Et_2O$ (**134**) is prepared by reacting $Mn_2(CO)_{10}$ with 1 equiv. of K_2Se_3 in DMF at room temperature, and $(Ph_4P)_2[Mn_2(Se_4)_2(CO)_6]$ (**135**) is produced under the same conditions using 2 equiv. of K_2Se_3 [84]. The centrosymmetric $[Mn_2(Se_2)_2(CO)_6]^{2-}$ dimer is formed from two $Mn(CO)_3$ fragments bridged by two Se_2^{2-} ligands as shown in Fig. 90. The coordination mode of the Se_2^{2-} ligands can be described as μ-η^1,η^2-type, i.e. the Se_2^{2-} is bonded to a manganese center in the side-on fashion, while one selenium atom bridges another manganese

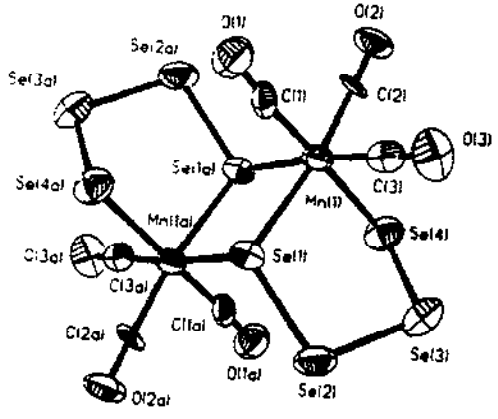

Fig. 91. The structure of $[Mn_2(Se_4)_2(CO)_6]^{2-}$.

center. The structure of the $[Mn_2(Se_4)_2(CO)_6]^{2-}$ anion is similar to that of the $[Mn_2(Se_2)_2(CO)_6]^{2-}$ as shown in Fig. 91. The molecule is centrosymmetric, and the MSe_4 ring adopts a puckered conformation. $(Ph_4P)_2[Mn_2(Se_4)_2(CO)_6]$ **(135)** can also be prepared by reacting $(Ph_4P)_2[Mn_2(Se_2)_2(CO)_6]$ with elemental selenium [84]. Heating of $[Mn_2(Se_4)_2(CO)_6]^{2-}$ at 90°C in DMF leads to complete decarbonylation of the metal center, producing $[Mn(Se_4)_2]^{2-}$ [84]. In fact, reaction of $Mn_2(CO)_{10}$ with K_2Se_3 in a 1:2 molar ratio in the presence of Ph_4PBr at 100°C in DMF constitutes another clean route to $(Ph_4P)_2[Mn(Se_4)_2]$ **(39)** [84]. Similar reaction between $Re_2(CO)_{10}$ and 2 equiv. of K_2Se_3 gave $(Ph_4P)_2[Re_2(Se_4)_2(CO)_6]$ **(136)**, an isostructural compound to **(135)** [162], whose structure is identical to the Mn analog (see Fig. 91).

Oxidative decarbonylation reactions of $Mn_2(CO)_{10}$ with Na_2Q_2 (Q = S, Se, Te) ligands in the sealed Pyrex tube under methanothermal conditions (i.e. 80°C) gave novel cluster compounds $(Ph_4P)_2[Mn_3(Q_2)_2(QCH_3)(CO)_9]$ **(137–139)** [163]. Although crystallized in different space groups, the anions of these three compounds have essentially the same structure. Figure 92 is an ORTEP representation of the $[Mn_3(Q_2)_2(QCH_3)(CO)_9]^{2-}$ (Q = S, Se or Te) anion. The two dichalcogenide Q_2^{2-} units in these clusters have different coordination modes. The methylated monochalcogenide CH_3Q^- acts as a μ_2-type ligand. Its formation probably originates from electrophilic attack of the solvent molecule (i.e. CH_3OH) on the monochalcogenide ligand under solvothermal conditions. The metal centers are octahedrally coordinated with formal oxidation state 1+, and possess idealized

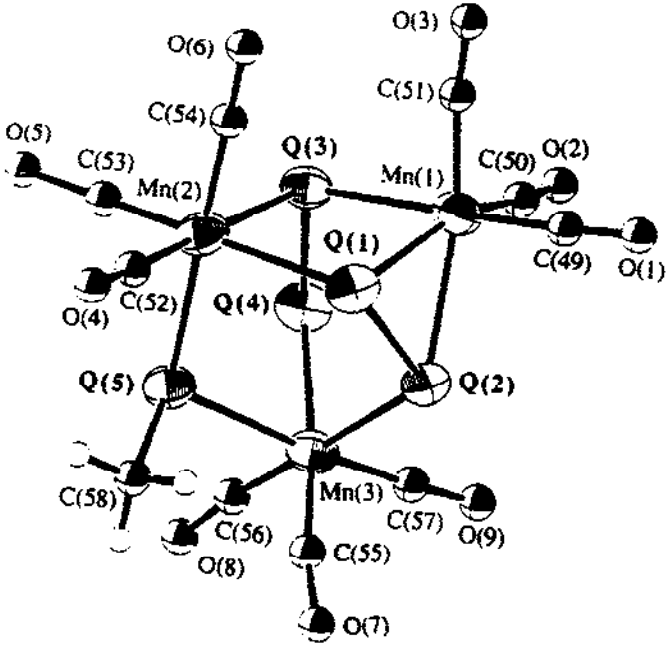

Fig. 92. The structure of $[Mn_2(Q_2)_2(QCH_3)(CO)_9]^{2-}$ (Q = S, Se or Te).

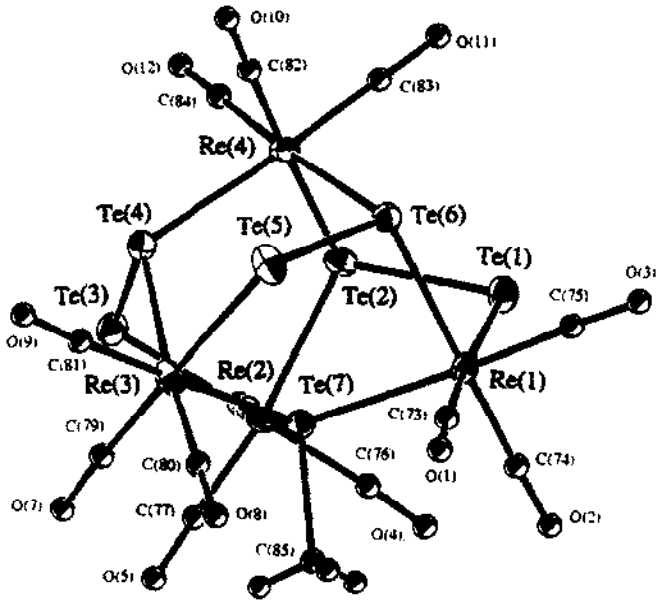

Fig. 93. The structure of $[Re_4(Te_2)_3(TeCH_3)(CO)_{12}]^{3-}$.

C_{3v} local symmetry. It should be noted that these compounds are metastable under the reaction conditions. The methylation of the chalcogenide ligands continues upon further heating of the above reactions. The final products are the dimeric methylchalcogenides $(Ph_4P)[Mn_2(QCH_3)_3]$ [163].

Interestingly, the reaction of $CpRe(CO)_3$ with Na_2Te_2 under the same conditions gave $(Ph_4P)_3[Re_4(Te_2)_3(TeCH_3)(CO)_{12}]\cdot CH_3OH$ (**140**) [163]. Although the reaction is now metathetical, methylation of the monotelluride ligand in the cluster also takes place under these conditions. Figure 93 shows the structure of the $[Re_4(Te_2)_3(TeCH_3)(CO)_{12}]^{3-}$ anion. The molecule possesses a pseudo-C_3 axis, i.e. passing through Te(7) and Re(4), that divides four rhenium atoms into two different types. Three of them are in the triangular base of a tetrahedron bridged by the μ_3-CH_3Te^- ligand. Three Te_2^{2-} ligands then each connect two of these basal rhenium atoms, creating a cavity of Te atoms all pointing in the same direction. This cavity is capped by a $Re(CO)_3$ fragment to form the tetranuclear cluster. All metal centers have the formal oxidation state 1+, and are octahedrally surrounded by three Te atoms and three CO groups, possessing idealized C_{3v} local symmetry.

(e) The chemistry of Group 8 elements (Fe, Ru and Os)

Compounds of this group, represented by the dichalcogen-containing iron carbonyls, are probably among the earliest chalcogen-containing organometallic species whose structures and reactivities have been thoroughly investigated.

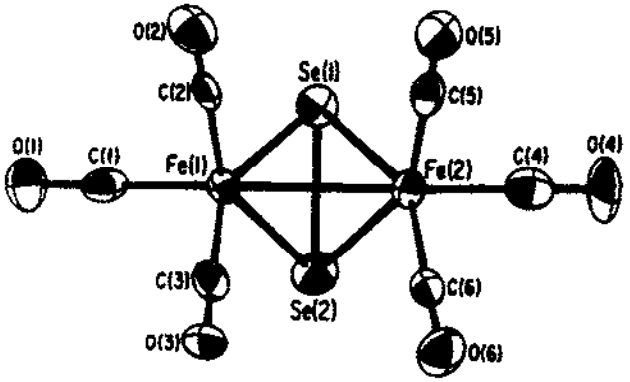

Fig. 94. The structure of $[Fe_2(Se_2)(CO)_6]$.

The binuclear iron carbonyl dichalcogenides $[Fe_2(Q_2)(CO)_6]$ (Q = S, Se) (**141**,**142**) were first prepared by Hieber and Gruber in 1958 by the reaction of $[Fe(CO)_4]^{2-}$ with SO_3^{2-} and SeO_3^{2-}, respectively [164]. Although the structure of this molecule was proposed to be analogous to the $[Fe_2(SC_2H_5)_2(CO)_6]$ based on IR spectroscopic and dipole moment studies [165], an X-ray single-crystal structure determination showed the presence of Q–Q bonding in the structure [166]. Figure 94 shows the structure of **142** which possesses C_{2v} symmetry. The $[Fe_2(Te_2)(CO)_6]$ (**143**) proved to be elusive until some 20 years later [167].

The $(Ph_4P)_2[Fe_4Se_2(Se_2)(CO)_{12}]$ (**144**), obtained from the methanothermal reaction of $Fe(CO)_5$ with Na_2Se_2, can be regarded as a reductive coupling product of two

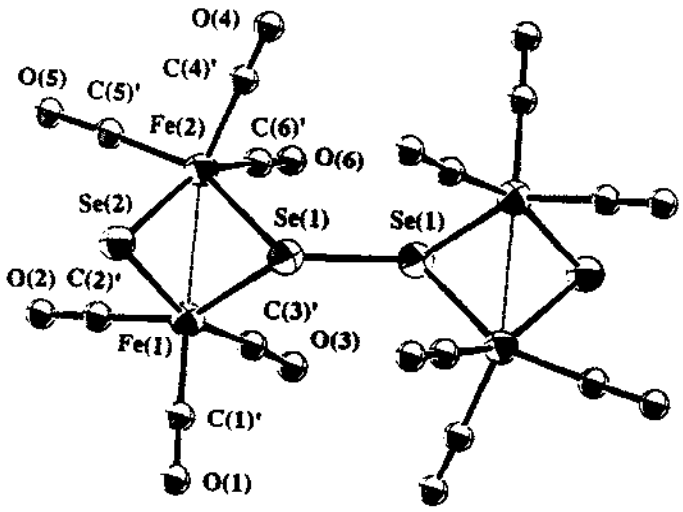

Fig. 95. The structure of $[Fe_4Se_2(Se_2)(CO)_{12}]^{2-}$.

$[Fe_2(Se_2)(CO)_6]$ molecules [168]. In fact, the isostructural sulfur analog $(Ph_4P)_2[Fe_4S_2(S_2)(CO)_{12}]$ (**145**) was synthesized by reduction of $[Fe_2(S_2)(CO)_6]$ with $LiEt_3BH$ [169]. The structure of the $[Fe_4Se_2(Se_2)(CO)_{12}]^{2-}$ anion, as shown in Fig. 95, can be viewed as two butterflies joining their wings in a side-by-side fashion. This is caused by breaking two intra-molecular Se–Se bonds and forming one inter-molecular Se-Se bond between two $Fe_2Se_2(CO)_6$ units. However, the distance of the inter-molecular Se–Se linkage is long at 2.467(7) Å, approaching the upper limit of a single Se–Se bond, while the intra-molecular Se–Se distance of 2.847(5) Å is significantly shorter than their van der Waals contact (i.e. 3.8–4.0 Å). This indicates that the valence electrons in the selenium atoms are more or less delocalized among these four atoms. It appears that Se(1) and Se(2) form a partial bond by removal of electron density from these atoms and transfer to the Se(1)–Se(1)

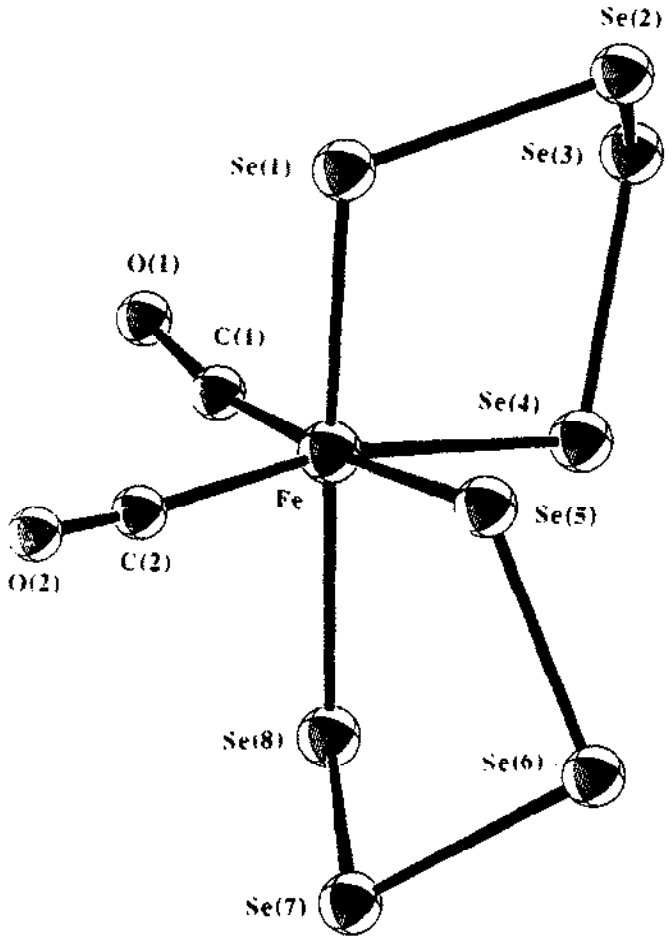

Fig. 96. The structure of $[Fe(Se_4)_2(CO)_2]^{2-}$.

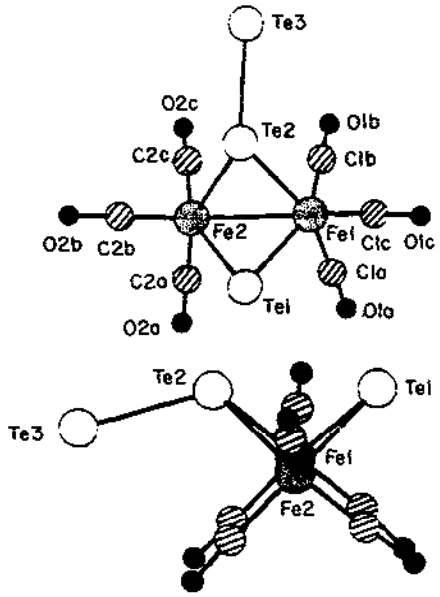

Fig. 97. The structure of $[Fe_2(Te)(Te_2)(CO)_6]^{2-}$.

bond and to the CO ligands. Finally, the coordination geometry around the iron atoms is best described as distorted octahedral because, in addition to the normal chemical bonds to selenium atoms and CO groups, the iron atoms are very close to each other at 2.555(6) Å, forming a metal–metal bond.

Two different routes are available to prepare the diamagnetic octahedral Fe^{2+} polyselenide $[Fe(Se_4)_2(CO)_2]^{2-}$. When $Fe(CO)_5$ reacts with Na_2Se_5 in DMF in the presence of Ph_4PCl, $(Ph_4P)_2[Fe(Se_4)_2(CO)_2]$ (**146**) is obtained in high yield [170]. Whereas the reaction of $Fe(CO)_5$ with N-MeIm suspension of grey selenium leads to $[Fe(N\text{-}MeIm)_6][Fe(Se_4)_2(CO)_2]$ (**147**) [171]. Both anions in these two compounds have essentially the same structure, i.e. two CO groups occupy the cis positions with respect to two $FeSe_4$ rings (Fig. 96).

Reaction of $Fe(CO)_3(\eta^4\text{-butadiene})$ with excess K_2Te_4 in ethylenediamine in the presence of crypt gave $[(K\text{-crypt})_2][Fe_2(Te)(Te_2)(CO)_6]\cdot\frac{1}{2}en$ (**148**) [172]. This peculiar molecule contains a μ_2-Te^{2-} and a μ_2-η^1-Te_2^{2-} ligand which bridges two iron centers using one tellurium atom while another tellurium atom assumes a terminal position. The whole molecule has a "butterfly" structure as shown in Fig. 97. The Te–Te distance for the Te_2^{2-} is 2.71(2)Å, representing a typical single bond, while the Te–Te distance between the Te^{2-} and Te_2^{2-}, i.e. Te(1)–Te(2) is 3.23(2) Å, can be considered non-bonding. The Fe–Fe bond is 2.626(12) Å.

The reaction of $Cp_2Fe_2(CO)_4$ with 2 equiv. of Et_3PTe in refluxing toluene gave $[Cp_2Fe_2(Te_2)(Et_3P)_2(CO)_2]$ (**149**) [173]. Compound **149** is a stable, crystalline material.

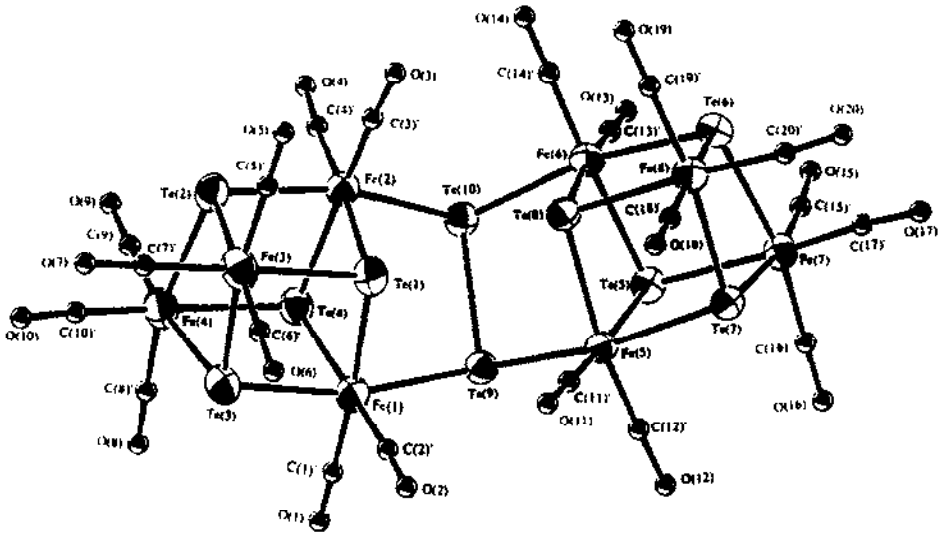

Fig. 98. The structure of $[Fe_8Te_8(Te_2)(CO)_{20}]^{2-}$.

The ^1H, ^{31}P and ^{125}Te NMR spectroscopic studies showed that this compound is a mixture of two diastereomers.

The largest structurally characterized cluster in the iron telluride system thus far is $(Ph_4P)_2[Fe_8Te_8(Te_2)(CO)_{20}]$ (**150**). This compound is accessible by either hydrothermal synthesis using $Fe(CO)_5$, Na_2Te_2 and Ph_4PCl as starting materials at 110°C [168] or conventional solution method of reacting $Fe(CO)_5$ with $(Ph_4P)_2Te_4$ in DMF at 85°C [174]. The $[Fe_8Te_8(Te_2)(CO)_{20}]^{2-}$ anion contains two Fe_4Te_4 cubane-like cages bridged by a Te_2^{2-} unit, as shown in Fig. 98. The octahedral coordination geometry of all the iron atoms in this compound, being completed by μ_3-Te^{2-} ligands and terminal CO groups, differs from many iron-sulfur cubanes which are omnipresent in iron-sulfur chemistry [175]. The Te–Te distance in the bridging unit is 2.829(2) Å and considered a normal single bond. If the charge of both the ditelluride and the monotelluride ligands in this structure is taken as 2–, the eight iron atoms would have a formal oxidation state 2+. Consistent with this oxidation state, the observed long Fe–Fe distances in both cubanes (the shortest distance is 3.75 Å) exclude any possible M–M bonding in **150**. The average Fe–Te bond distance is 2.619(4) Å.

$(Et_4N)_{1.5}Na_{0.5}[Ru(Se_4)_2(CO)_2]$ (**151**), the first structurally characterized ruthenium polyselenide complex, was obtained from $Ru_3(CO)_{12}$ with Na_2Se_5 in the presence of Et_4NCl in acetone [176]. The anion in this compound has a similar molecular structure to its iron analog, i.e. $[Fe(Se_4)_2(CO)_2]^{2-}$, as shown in Fig. 99. However, in the crystal lattice, a Na^+ ion (situated on an inversion center) is found to be encapsulated in an octahedral pocket created by two $[Ru(Se_4)_2(CO)_2]^{2-}$ anions. Figure 100 shows the interactions between this Na^+ ion and the Se(2), Se(4) and Se(8) atoms. Important bond distances are Ru–Se 2.55 Å, Se–Se 2.34 Å, and Na···Se from 2.921(1) to 3.148(1) Å.

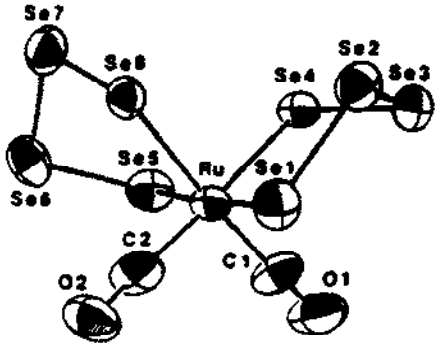

Fig. 99. The structure of $[Ru(Se_4)_2(CO)_2]^{2-}$.

Oxidative addition of elemental selenium to $CpRu(Ph_3P)_2OTf$ or $(MeCp)Ru(Ph_3P)_2OTf$ in CH_2Cl_2 resulted in two cationic species [177], $[\{CpRu(Ph_3P)_2\}_2Se_2](OTf)_2$ (**152**) and $[\{(MeCp)Ru(Ph_3P)\}_2(Se_2)_2](OTf)_2$ (**153**) (using excess Se). The structure of $[\{CpRu(Ph_3P)_2\}_2Se_2]^{2+}$, as shown in Fig. 101, contains an end-on *trans*-μ-η^1,η^1-Se_2 unit. This type of bonding mode was also observed in $K_6[Nb_4Se_4(Se_2)_9]$ (**15**). The Ru–Se bond distances are 2.377(2) and 2.341(2) Å, while the Se–Se distance is 2.492(2) Å. Figure 102 shows the structure of $[\{(MeCp)Ru(Ph_3P)\}_2(Se_2)_2]^{2+}$. The two μ-η^1,η^2-Se_2 ligands in this molecule are relatively common, as already encountered in several other compounds, such as $[(\eta^5\text{-}Cp^*)_2Re_2(Te_2)(CO)_4]$ and $[Mn_2(Se_2)_2(CO)_6]^{2-}$. The Ru–Se bond distances are 2.473(1) and 2.556(1) Å, and the Se–Se distance is 2.279(1) Å in this structure.

A novel Ru^{2+}/Te_2^{2-} cluster has been obtained by hydrothermal synthesis in this laboratory. The reaction of $Ru_3(CO)_{12}$ with Na_2Te_2, Ph_4PCl and H_2O at 110°C in a sealed Pyrex tube gave $(Ph_4P)_2[Ru_6(Te_2)_7(CO)_{12}]$ (**154**) [178]. The $[Ru_6(Te_2)_7(CO)_{12}]^{2-}$ anion features a hexanuclear cluster whose framework is established by an octahedral array of six Ru atoms upheld by a central ditelluride Te_2^{2-} unit and bridged by seven other Te_2^{2-}

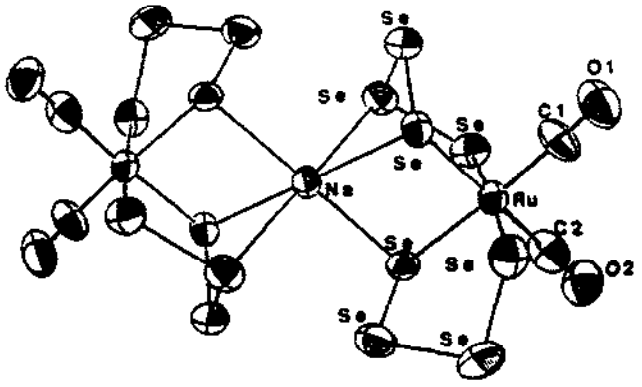

Fig. 100. Interactions of the Na^+ with two $[Ru(Se_4)_2(CO)_2]^{2-}$ anions in the crystal lattice.

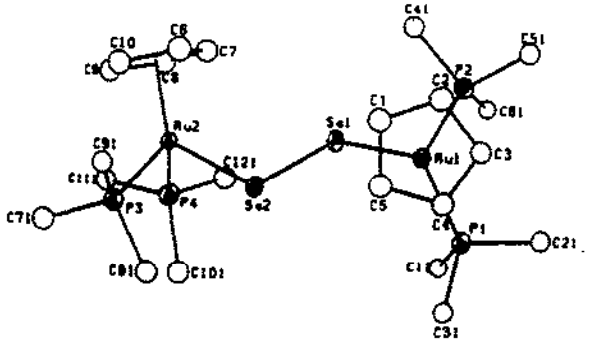

Fig. 101. The structure of $[(CpRu(Ph_3P)_2)_2Se_2]^{2+}$.

ligands in the periphery as shown in Fig. 103. In addition, each ruthenium is capped by two *cis* CO groups, resulting in octahedral coordination. The molecule bears a remarkable structural resemblance to the fundamental building block of pyrite-type $RuTe_2$, i.e. its central $\{Ru_6(Te_2)_7\}^{2-}$ core is reminiscent of an excised fragment of the $RuTe_2$ pyrite-type lattice. A comparison of this $\{Ru_6(Te_2)_7\}^{2-}$ core with a small fragment of $RuTe_2$ is given in Fig. 104. The relationship between the Ru_3Te–$TeRu_3$ fragment in this compound and the W_3Te–TeW_3 in $(Ph_4P)_2[W_6(Te_2)_4(CO)_{18}]\cdot CH_2Cl_2$ (**127**) is that the six metal atoms are arranged either octahedrally (for Ru atoms) or prismatically (for W atoms) around the Te_2^{2-} unit, resulting in a staggered or eclipse conformation. All ruthenium atoms in **154** have a formal oxidation state 2+. The mean Te–Te and Ru–Te bond distances are 2.748(10) Å and 2.709(80) Å, respectively.

Only one structurally characterized compound is known for osmium. The $(Ph_3P)_2Os(Se_2)(CO)_2$ (**155**), prepared from the reaction of $Os(CO)_2(Ph_3P)_3$ with red selenium in benzene, contains a side-on η^2-Se_2^{2-} ligand, two *cis*-CO and two *trans*-Ph_3P

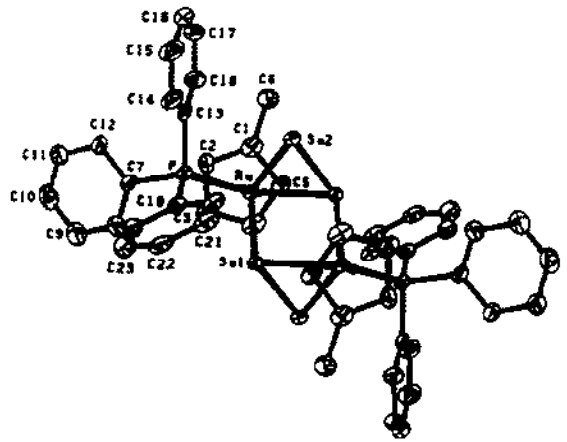

Fig. 102. The structure of $[((MeCp)Ru(Ph_3P)_2(Se_2)_2]^{2+}$.

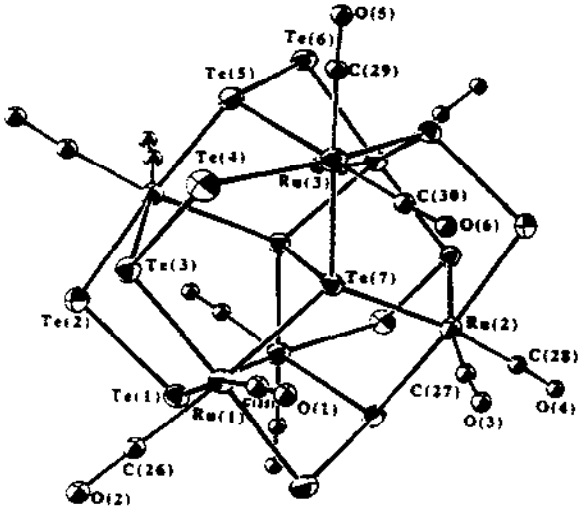

Fig. 103. The structure of $[Ru_6(Te_2)_7(CO)_{12}]^{2-}$.

groups as shown in Fig. 105 [179]. The Os–Se bond distances are 2.540(1) and 2.553(1) Å, while the Se–Se distance is 2.321(1) Å.

(f) The chemistry of Group 9 elements (Co, Rh and Ir)

Although some polychalcogenide chemistry is known for Rh and Ir, very little is known for Co. The $Me–C(CH_2PPh_2)_3Co(Se_4)$ (**1**) can be readily formed by reaction of

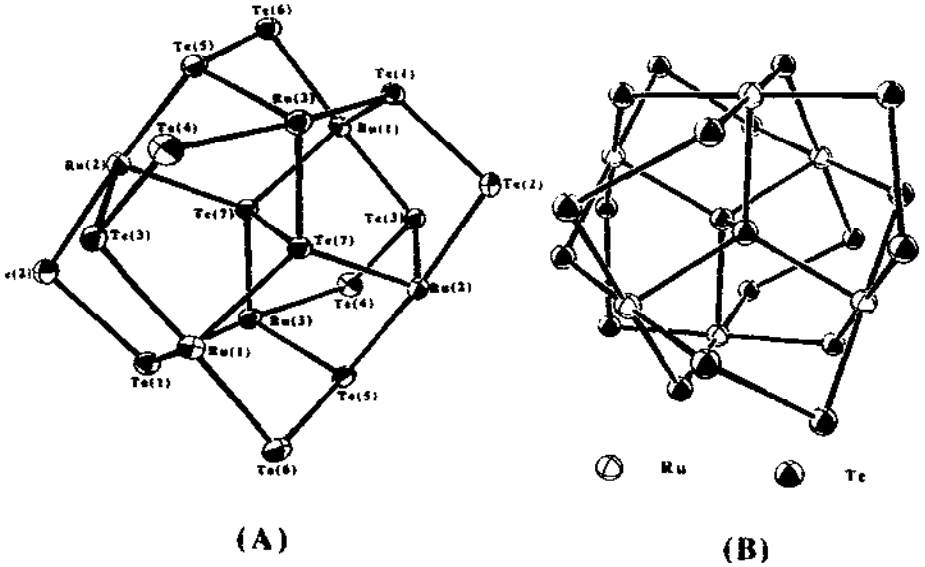

Fig. 104. Comparison between the $\{Ru_6(Te_2)_7\}^{2-}$ core (left) and a small-core fragment of $RuTe_2$ (right).

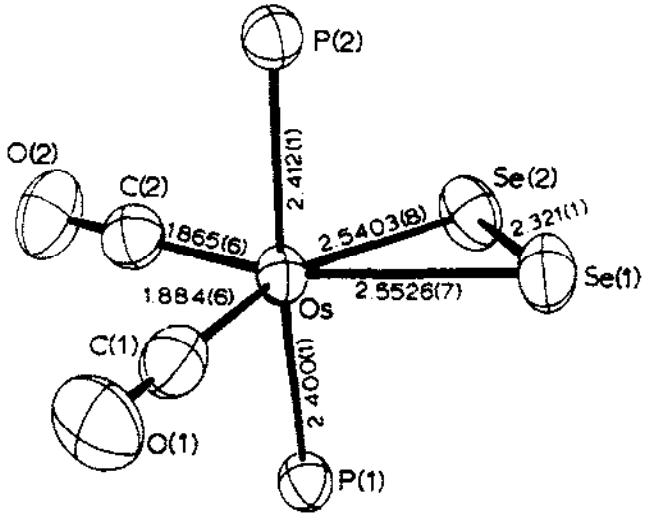

Fig. 105. The structure of $(Ph_3P)_2Os(Se_2)(CO)_2$.

$Me–C(CH_2PPh_2)_3Co(NCS)_2$ with Na_2Se_x [29]. However, its structural identity has never been revealed, except that a five-membered $CoSe_4$ ring was proposed to occur based on IR and elemental analytical data. Recently, a dimeric cobalt telluride compound has been synthesized and structurally characterized [180]. The reaction of $Co_2(CO)_8$ with 2 equiv. of Et_3PTe in toluene at 100°C in the presence of Et_3P gave $[(Et_3P)_4Co_2(Te_2)(CO)_4]$ (**156**). The structure of **156** consists of two distorted trigonal bipyramidal Co^+ centers as shown in Fig. 106. Two phosphine ligands on each metal are in axial positions. The Co–Te distance is 2.614(2) Å, and the Te–Te distance is 2.765(2) Å.

Two selenium-rich compounds, $[(\eta^5\text{-}Cp^*)_2M_2(Se)(Se_4)]$ (M = Co, Rh) (**157–158**), are formed as the final products of stepwise addition of elemental selenium to the M–M

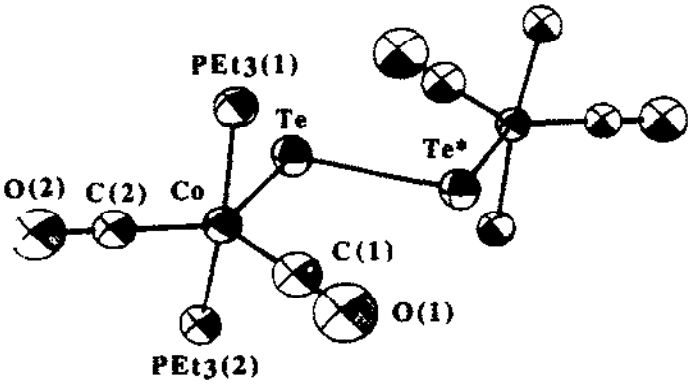

Fig. 106. The structure of $[(Et_3P)_4Co_2(Te_2)(CO)_4]$.

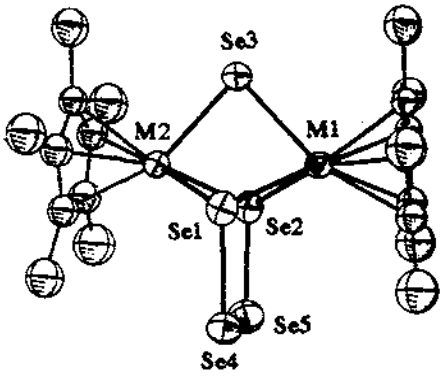

Fig. 107. The structure of $[(Cp^*)_2M_2(Se)(Se_4)]$ (M = Co, Rh).

double bond of $[(\eta^5\text{-}Cp^*)_2M_2(CO)_2]$ (M = Co, Rh) [181]. In these two compounds, a Se^{2-} and a Se_4^{2-} ligand form a nearly planar pseudo five-membered Se_5 ring, which intersects the M···M vector and is perpendicular to this axis as shown in Fig. 107. Two terminal selenium atoms in the Se_4^{2-} ligand and the Se^{2-} ligand form an almost equilateral triangle with separations of about 3.06 Å (in Co compound) and 3.10 Å (in Rh compound), much shorter than the sums of the van der Waals radii of two selenium atoms (3.80 Å). This indicates a significant electron delocalization among this pseudo five-membered ring. The M–Se and Se–Se bond distances average 2.35 and 2.36 Å (for Co compound), and 2.47 and 2.37 Å (for Rh compound).

The structure of the cationic $[(triphos)_2Rh_2(Se_2)_2]^{2+}$ **(159)** [182] features a similar bonding mode for two Se_2^{2-} ligands as found in $[\{(MeCp)Ru(Ph_3P)\}_2(Se_2)_2](OTf)_2$ **(153)**. Two $\mu\text{-}\eta^1,\eta^2\text{-}Se_2^{2-}$ ligands in this molecule are related to each other by a crystallographic inversion center as shown in Fig. 108. The average Rh–Se bond distance is 2.53 Å, and the Se–Se distance 2.298(1) Å.

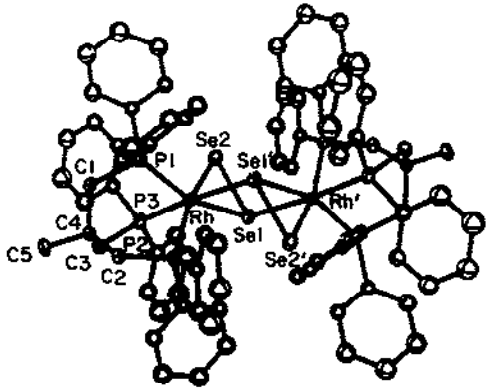

Fig. 108. The structure of $[(triphos)_2Rh_2(Se_2)_2]^{2+}$.

(A)

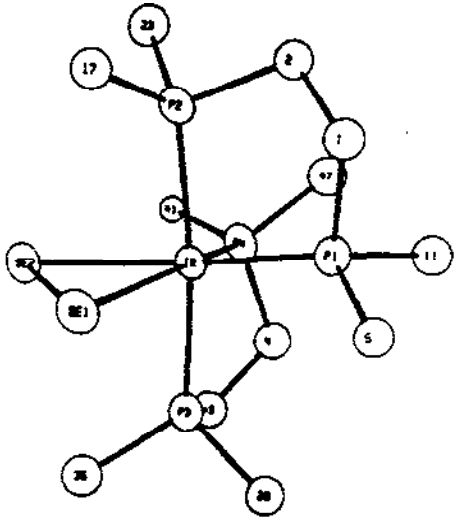

(B)

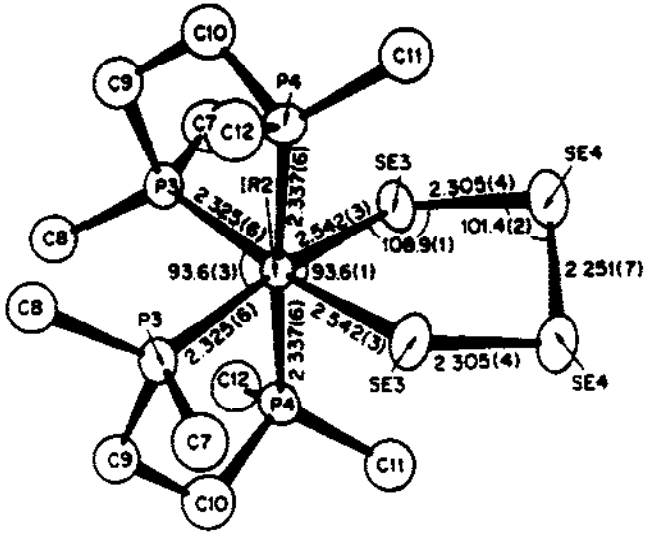

Fig. 109. The structures of (a) $[(dppe)_2Ir(Se_2)]^+$ and (b) $[(dmpe)_2Ir(Se_4)]^+$.

Oxidative addition of elemental selenium to $[Ir(dppe)_2]Cl$ gave $[(dppe)_2Ir(Se_2)]Cl$ (**160**) [183], while the reaction yielded a mixture of $[(dmpe)_2Ir(Se_4)]Cl$ (major product) and $[(dmpe)_2Ir(Se_2)]Cl$ (**161**) (minor product) if $[Ir(dmpe)_2]Cl$ was used [30]. Both structures were established by X-ray single-crystal structure studies. Except for the different $IrSe_x$ ring sizes, the two structures are very similar, featuring an octahedral iridium atom chelated by three bidentate ligands as shown in Fig. 109. The $IrSe_4$ ring in **160**

adopts a half-chair conformation. The average Ir–Se bonding distances are 2.54 Å in **160** and 2.53 Å in **161**, while the Se–Se distances are 2.32 Å (average) and 2.312 Å in **161**. SCF-X_α-SW calculations on $[(dmpe)_2Ir(Se_4)]^+$ indicate that the Se_4 group in the complex is best described as an excited Se_4 molecule. Ir–Se bonding is mainly via the overlap of Ir $5d_{yz}$, $5d_{z^2}$ and $6p_x$ orbitals with Se 4p orbitals, while the Se–Se bonding in the Se_4 ligand is σ_p type [30].

(g) The chemistry of Group 10 elements (Ni, Pd and Pt)

Organometallic compounds of heavy polychalcogenides are scarce for metals in this group. Two nickel telluride clusters from a family of metal-centered or empty icosahedral

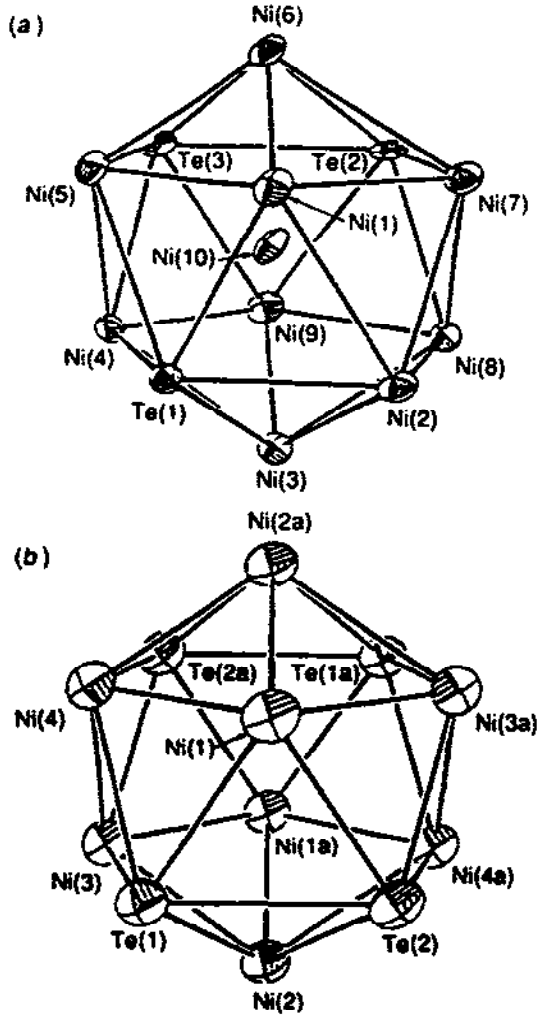

Figure 110. The structures of (a) $[NiNi_9Te_3(CO)_{15}]^{2-}$ and (b) $[Ni_8Te_4(Co)_{12}]^{2-}$

cages $[Ni_nNi_{12-x}Q_x(CO)_y]^{2-}$ (Q = Se, Te; $n = 1, 0$) seem to meet our criterion of having Q–Q bonding in the molecule. The $[NiNi_9Te_3(CO)_{15}]^{2-}$ (**162**) and $[Ni_8Te_4(CO)_{12}]^{2-}$ (**163**), both obtained from reaction of $[Ni_6(CO)_{12}]^{2-}$ with Ph_2Te_2 in THF, contain tellurium atoms in adjacent positions in the icosahedron, thus forming a Te_2^{2-} fragment in the cluster [184]. Figure 110 shows the structures of these two clusters. The metal-centered cluster $[NiNi_9Te_3(CO)_{15}]^{2-}$ possesses one Te–Te contact at 3.13 Å, while the empty cluster $[MgTe_4(CO)_{12}]^{2-}$ has two Te–Te contacts at 2.88 Å. It appears the longer Te–Te distance in **158** is the result of electron donation to an antibonding Te–Te orbital from the low valent Ni atoms in the cluster.

C. SUMMARY OF SYNTHETIC METHODS

(i) Use of polychalcogenide anions generated in situ as reagents

The simplest method of producing polysulfide ligands is to pass a stream of H_2S through an aqueous NH_3 solution in the presence of elemental sulfur. The polysulfide anions generated from such a procedure can then react with appropriate metal salts. This has been very successful in preparing metal polysulfides. Thus, the most rational synthetic approach for metal heavy polychalcogenides would be to duplicate this reaction. However, H_2Se gas is expensive and poisonous, and H_2Te is highly unstable. Such a preparative route is actually impractical, and potentially irreproducible.

In non-protic solvents, reactions of alkali metals with elemental chalcogens can also generate the polychalcogenide anions in situ. Another advantage of using non-aqueous solvents is to allow the use of various organic counterions. When appropriate metal salts are added to these solutions, metal complexes will form. The first compound prepared by this method was $(Ph_4P)_2[Fe_2Se_2(Se_5)_2]$ [34]:

$$6Na + 12Se + 2FeCl_2 \xrightarrow[Ph_4PCl]{DMF,\ 70°C} [Ph_4P]_2[Fe_2Se_2(Se_5)_2] + 6NaCl \quad (2)$$

Many other metal complexes have now been prepared in a similar manner, they include $(Ph_4P)_2[Sn(Se_4)_3]$ [135b], $(Ph_4P)_2[M(Se_4)_2]$ (M = Ni, Zn, Cd, Hg and Pb) [92a], $(Ph_2P)_2[Cu_4(Se_4)_{2.4}(Se_5)_{0.6}]$ [104], $(Ph_2P)_2[Ag_4(Se_4)_{2.1}(Se_5)_{0.9}]$ [104], $(Ph_4P)[(\eta^5\text{-Cp})Mo(Se_4)_2]$ [135b]. Although the current preparative examples all involve polyselenide compounds, the method itself is extendible to the polytelluride system. The only drawback seems to be the use of reactive alkali metals, which makes the reaction heterogeneous and control of stoichiometry difficult. A synthetic modification of using A_2Se_x (A = alkali metal, $x = 1, 2$) and elemental selenium is often used (eqn. (3) [115], eqn (4)([14d]):

$$2Na_2Se + 6Se + M(Ac)_2 \xrightarrow[15\text{-crown-5}]{DMF} [Na(15\text{-crown-5})_2]_2[M(Se_4)_2] + 2NaAc \quad (3)$$

(M = Zn, Cd and Hg)

$$2Na_2Se_2 + 4Se + PdCl_2 \xrightarrow[2Ph_4PCl]{DMF} (Ph_4P)_2[Pd(Se_4)_2] + 4NaCl \quad (4)$$

(ii) Use of alkali metal polychalcogenides as reagents

By far, this is the most successful synthetic method for making metal heavy polychalcogenide compounds. It is generally applicable to sulfide, selenide and telluride systems. Many of these phases can be obtained from either high-temperature or liquid ammonia reactions of alkali metals and chalcogens.

The extraction of the A_2Q_n (A = alkali metal; Q = Se, Te; n = 2–6) phases into polar organic solvents such as en, CH_3CN, and DMF generates polychalcogenide anions suitable for the preparation of metal complexes. When simple metal salts such as halides or oxides are used as starting materials, the reactions leading to metal complexes are mostly metathetical (eqn. (5) [113], eqn. (6) [106]).

$$ZnCl_2 + 2Na_2Se_4 + 2Ph_4PCl \xrightarrow{DMF} (Ph_4P)_2[Zn(Se_4)_2] + 4NaCl \quad (5)$$

$$K_2Te_4 + (Ph_3P)_3CuCl \xrightarrow[Me_4NCl]{DMF} (Me_4N)[Cu(Te_4)] + 2KCl + 3Ph_3P \quad (6)$$

Occasionally, redox processes can also occur [108]:

$$2AuCN + 2Na_2Se_5 + 2PPNCl \xrightarrow{DMF/Et_2O} (PPN)_2[Au_2Se_2(Se_4)_2] + 2NaCl + 2NaCN \quad (7)$$

Oxidative or metathetical decarbonylation of metal carbonyls by polychalcogenide ligands Q_n^{2-} (Q = S, Se and Te; n = 2–6) provides another convenient route for introducing chalcogen-atoms into metal centers [41]. Depending on the reactivity of the metal carbonyl and the polychalcogenide ligand, the product isolated can be either homoleptic or CO-containing complexes (eqn (8) [71], eqn. (9) [153]):

$$M(CO)_6 + nK_2Se_3 \xrightarrow{DMF} [MSe_4]^{2-} \text{ or } [MSe(Se_4)_2]^{2-} + 6CO \quad (8)$$

M = Mo, W

$$M(CO)_6 + K_2Te_4 + 2Ph_4PBr \xrightarrow{DMF/THF} (Ph_4P)_2[M(Te_4)(CO)_4] + 2CO + 2KBr \quad (9)$$

M = Cr, Mo, W

This shows that the reactions are often controlled by redox interplay between the metal center and the polychalcogenide ligand. Since most of the transition metal carbon-

yls are readily available, this synthetic method has been successfully applied to the preparations of many transition metal polychalcogenide compounds.

(iii) Hydro(solvo)thermal reactions

Despite the successful application of hydrothermal techniques to the preparation of many technologically important materials, such as α-quartz and zeolites, the hydrothermal synthesis of chalcogenides is little studied [78,79]. Several examples of preparing monochalcogenides under hydro(methano)thermal conditions are known [79]. These reactions often employ alkali carbonates as "mineralizers" (complexing agents) to increase dissolution of reactants as well as to facilitate crystal growth [79]. We have found that under hydro(solvo)thermal conditions, alkali metal polychalcogenides can act as reagents as well as "mineralizers". The latter help or promote crystal growth. These reactions provide a unique route to novel metal polyselenide clusters, most of which have, thus far, proven to be inaccessible by other synthetic methods [78]:

$$Mo + 2K_2Se_4 \xrightarrow[\text{sealed tube}]{H_2O,\ 140^\circ C \text{ for } 60\ h} K_{12}[Mo_{12}Se_8(Se_2)_{18}(Se_3)_4] \quad (10)$$

In addition, such a synthetic method is also applicable to metal carbonyl/polychalcogenides. Many interesting clusters have been synthesized by this technique (eqn. (11) [178], eqn. (12) [163]:

$$Ru_3(CO)_{12} + 5Na_2Te_2 \xrightarrow[6Ph_4PCl,\ \text{sealed tube}]{H_2O,\ 110^\circ C \text{ for } 65\ h} (Ph_4P)_2[Ru_6(Te_2)_7(CO)_{12}] \quad (11)$$

$$CpRe(CO)_3 + 2Na_2Te_2 \xrightarrow[4Ph_4PCl,\ \text{sealed tube}]{MeOH,\ 80^\circ C \text{ for } 48\ h} (Ph_4P)_3[Re_4(Te_2)_3(TeCH_3)(CO)_{12}] \quad (12)$$

(iv) Molten salt techniques

The use of molten alkali metal polychalcogenides for making solid-state compounds is a very active area of research [39]. As far as the synthesis of molecular compounds is concerned, the molten salt method differs from conventional, non-aqueous reactions in many respects. For example, reaction temperatures attainable by molten salts are higher than those using organic solvents. This tends to affect reaction pathways. The highly ionic nature of the melts provides enhanced solubility for many otherwise insoluble compounds. A significant advantage is the elimination of any "wet" solvent which could make the system oxygen-free. This may prove to be important in the synthesis of early transition metal, or lanthanide and actinide compounds, which tend to abstract oxygen atoms from solvent molecules (e.g. DMF, THF). Thus far, we have seen several such examples (eqn. (13) [60], eqn. (14) [68]):

$$U + 2K_2Se + 8Se \xrightarrow[10\ days]{300°C} K_4[U(Se_2)_4] \quad (13)$$

$$Nb + 3K_2Se + 10Se \xrightarrow[100\ h]{375°C} K_6[Nb_4Se_4(Se_2)_9] \quad (14)$$

The recent application of polychalcogenide salts of large organic cations (e.g. Ph_4P^+) as reactive fluxes opened up a new synthetic dimension in this research area. The use of organic counterions in place of alkali metal ions not only lowers the melting point, but also results in new and often open structure types (i.e. size or template effect). For example, three isomorphous compounds with a layered structure have been prepared as follows [134]:

$$M + (Ph_4P)_2Se_x \longrightarrow (Ph_4P)[M(Se_6)_2] \quad (15)$$

M = Ga, In or Tl

Large channels caused by the presence of Ph_4P^+ cations are found in the compounds. However, it should be noted that these compounds have an extended polymeric structure. In general, the molten salt technique favors formation of solid-state compounds. The synthesis of molecular compounds by molten salt methods has been occasional, and little is known about how to control the reactions from which small molecular anions can be reproducibly obtained.

(v) Use of elemental chalcogens as reagents

In order to achieve a successful addition of elemental chalcogen to a metal ion, the reaction requires that a coordinatively unsaturated electron-rich metal complex, or a compound containing metal–metal bonds be used as the starting material. Such a process often results in change of the metal oxidation state, and is bound to produce compounds with a partial chalcogenide-coordination environment. This is usually because no metathesis can take place between the all ancillary groups and the elemental chalcogen atoms. Thus, this method is responsible for the syntheses of most organometallic compounds. Examples are given in eqns. (16) [30] and (17) [152]:

$$[(dmpe)_2Ir]Cl + \tfrac{1}{2}Se_8 \xrightarrow[THF/benzene]{r.t.\ for\ 8\ days} [(dmpe)_2Ir(Se_4)]Cl \quad (16)$$

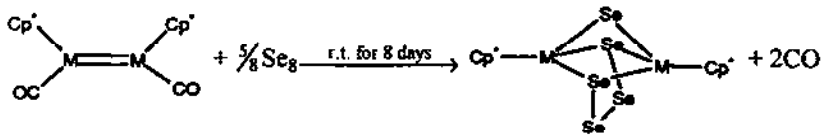

(17)

M = Co, Rh

However, due to the lack of suitable starting metal complexes, which possess enough reactivity towards elemental chalcogen, this method is not general. Organometallic compounds of polytellurides have not been prepared from this route, either because the reactivity of elemental tellurium is lower than that of selenium or, perhaps, because no such reactions have been extensively pursued.

Elemental selenium is readily incorporated into some metal monoselenide compounds, forming metal polyselenide rings via a redox process (eqn. (18) [64a,76], eqn. (19) [71]):

$$2[WSe_4]^{2-} + \tfrac{1}{4}Se_8 \xrightarrow{CH_3CN,\ 85°C} [W_2Se_{10}]^{2-}\ \text{(two isomers)} \qquad (18)$$

$$[MoSe_4]^{2-} + 5Se \xrightarrow[2\ h]{DMF,\ \text{at r.t.}} [MoSe(Se_4)_2]^{2-} \qquad (19)$$

The above results are analogous to those known earlier for sulfur [63,66].

Similar reactions between complexes containing Se–Se bonds and elemental selenium can also take place, resulting in MSe_x ring augmentation [84]:

$$[Mn(Se_2)_2(CO)_6]^{2-} + 4Se \xrightarrow{DMF} [Mn(Se_4)_2(CO)_6]^{2-} \qquad (20)$$

Recently, Rauchfuss and co-workers have discovered that *N*-alkylimidazoles can greatly promote the reactivity of elemental chalcogens (i.e. S and Se) towards low valent metal species, particularly metal powders and metal carbonyls. Thus, the *N*-alkylimidazole suspension of elemental selenium is found to react with $Fe(CO)_5$ or even zinc dust to produce polyselenide complexes:

$$2Fe(CO)_5 + Se_8 \xrightarrow{N\text{-MeIm},\ 25°C} [Fe(N\text{-MeIm})_6][Fe(Se_4)_2(CO)_2] + 8CO \qquad (21)$$

$$Zn + \tfrac{1}{2}Se_8 \xrightarrow{N\text{-MeIm},\ 100°C} [Zn(Se_4)(N\text{-MeIm})_2] \qquad (22)$$

The mixed-ligand coordination of zinc in $[Zn(Se_4)(N\text{-MeIm})_2]$ is the result of competition of the solvent *N*-methylimidazole which is a strong σ-donor ligand. This approach seems to be widely applicable to most metals and chalcogens. The five membered $ZnSe_4$ ring found in the structure is similar to that of $[Zn(Se_4)_2]^{2-}$.

(vi) Extraction of transition metal/chalcogen-containing alloys

Some ternary or quaternary alkali metal alloys can be "solubilized" in polar organic solvents (e.g. en). Such a process often involves the disruption of solid-state bonding with the assistance of a strongly coordinating solvent. As a result, metal polychalcogenide clusters can be isolated by addition of organic counterions (eqn. 23 [35], eqn. (24) [111]):

$$K_2Hg_2Te_3 \xrightarrow{en} \begin{cases} \xrightarrow{Bu_4NBr(MeOH)} (Bu_4N)_4[Hg_4(Te)_2(Te_2)_2(Te_3)_2] \\ \xrightarrow{Ph_4PBr(MeOH)} (Ph_4P)_2[Hg_2(Te)(Te_2)_2] \end{cases}$$

$$KAuTe_2 \text{ (or } K_2AuAsTe_3, K_3AuGeTe_3) \xrightarrow{en,\ PPNCl} (PPN)_2[Au_2(Te_2)_2] \quad (24)$$

(vii) Use of other reagents

(a) Bis(trialkylsilyl)selenides

It is known that bis(trimethylsilyl)sulfide $(Me_3Si)_2S$ can be used in place of H_2S to synthesize sulfido complexes [186]. However, this reagent and its Se analog, despite being highly reactive, are extremely malodorous and must be handled with great care. Ibers and co-workers explored the use of several bis(trialkylsilyl)selenides as possible "selenization" agents, and found that $[(CH_3)_2C_8H_{17}Si)]_2Se$ provides the best compromise between reactivity and odor control [61,64b]. Use of this reagent as well as the other bis(trialkylsilyl)selenides (mainly $[Me_3Si]_2Se$) was found in the synthesis of $(Et_4N)_2[V_2(Se_2)_4(Se_5)]$ [61], $[MSe_4]^{2-}$ (M = Mo, W) [64b], $[(\eta^5\text{-Cp})_4Ti_4(\mu_4\text{-O})(\mu_2\text{-Se})(\mu_3\text{-Se})_2(\mu_3\text{-Se}_2)_2]$ [146], $[\eta^5\text{-MeCp}_2V_2(\mu_2\text{-Se})(\mu_2\text{-Se}_2)(\mu_2\text{-}\eta^2\text{-Se}_2)]$ [148]. It should be pointed out that bis(trialkylsilyl)selenides are monoselenide-transfer agents, as can be seen in the synthesis of a large number of metal monoselenide clusters by Fenske et al. [148].

(b) Hydrogen chalcogenides

H_2Se was employed to synthesize $[(\eta^5\text{-MeCp})_2V_2(\mu_2\text{-Se})(\mu_2\text{-Se}_2)(\mu_2\text{-}\eta^2\text{-Se}_2)]$ [148]. Because of its poor stability, H_2Te was generated from reaction of Al_2Te_3 with HCl and used in situ to prepare $[(\eta^5\text{-Cp}^*)_2Re_2(Te_2)(CO)_4]$ [161]. Again, hydrogen chalcogenides are conceivably monoselenide-transfer agents. Generation of Q–Q bonds in the products must rely on a redox process during the reaction.

(c) Reactivity of Q_x^{2-} ligands towards organic phosphines

With abstraction of internal selenium atoms from MSe_x rings, this reaction can lead to compounds with shorter Se_x^{2-} ligands [30].

$$[(dmpe)_2Ir(Se_4)]Cl + 2Ph_3P \xrightarrow{CH_3CN} [(dmpe)_2Ir(Se_2)]Cl + 2Ph_3PSe \quad (25)$$

Sometimes these shorter ligands are highly reactive and can only be generated in situ. They often condense to give rise to larger clusters. For instance [145]:

(26)

R = H, Me, ^{i}Pr

(d) Other chalcogen-containing agents

Many other chalcogen-containing reagents, such as SeO_3^{2-}, TeO_3^{2-}, COSe and CSe_2, have all been occasionally used to synthesize metal chalcogenide complexes [164,167]. Reactions involving these reagents lack rationale, so their synthetic value is limited.

(viii) Thermolysis

Thermal rearrangement reactions have been used to prepare new compounds. The $(\eta^5\text{-MeCp})_2V(Se_5)$ is transformed to $[(\eta^5\text{-MeCp})_2V_2(\mu_2\text{-Se})(\mu_2\text{-Se}_2)(\mu_2\text{-}\eta^2\text{-Se}_2)]$ at reflux in THF [147]:

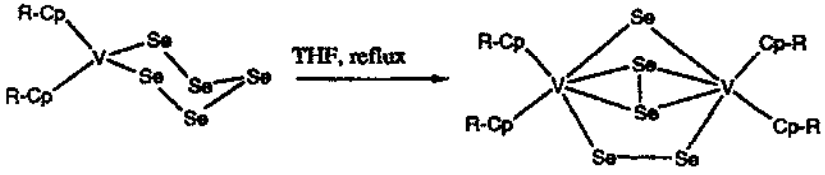

(28)

Heating a DMF solution of $[Mn_2(Se_4)_2(CO)_6]^{2-}$ at 90°C leads to the homoleptic complex $[Mn(Se_4)_2]^{2-}$. IR spectroscopic studies suggest that the process is a thermally induced disproportionation reaction [84]:

$$[Mn_2(Se_4)_2(CO)_6]^{2-} \xrightarrow{\text{DMF, 90°C}} [Mn(Se_4)_2]^{2-} + \tfrac{1}{2}Mn_2CO_{10} + CO \qquad (29)$$

D. SPECTROSCOPY

(i) IR and UV/vis spectroscopy

Both IR and UV/vis spectroscopic studies are not very informative in the structural characterization of metal heavy polychalcogenides. Unless CO groups are present in the molecules, the mid-IR region is invariably dominated by the hydrocarbon skeletons of ancillary ligands or the organic counterions. In the far-IR region, M–Se and Se–Se often show absorptions in the range 200–400 cm^{-1} with the corresponding M–Te and Te–Te bands shifting to even lower energies. IR spectroscopy could be used to confirm the presence of Q–Q bonds in the compound. However, one should be cautious in assigning these bands in view of the absence of any systematic studies using isotope labeling.

The problem associated with UV/vis spectroscopy is twofold. First, some metal complexes do not retain their identity in polar solvents such as DMF or CH_3CN. If monovalent M^+ ions are involved, such a dissociation is likely. In this case, the UV/vis spectrum of the metal complex is similar to that of the free polychalcogenide ligand. Second, most compounds that remain intact in polar solvents, show featureless UV/vis spectra yielding no information about the coordination environment of the metal ions. The following example is one of the very few occasions when the UV/vis spectra are useful in

identifying the different species present in solution. DMF solutions of $[Fe_2Se_2(Se_5)_2]^{2-}$ give five absorption maxima at 312(sh), 386(sh), 415(sh), 498 and 670(sh) nm, which are characteristic of this Fe^{III} species[34], while the UV/vis spectrum of $[Fe(Se_4)_2]^{2-}$ in the same solvent is featureless [90].

(ii) NMR spectroscopy

Both selenium and tellurium have spin-half nuclei with moderate NMR receptivity. ^{77}Se ($I = 1/2$, natural abundance = 7.58%, receptivity relative to $^{13}C = 2.98$), ^{125}Te ($I = 1/2$, natural abundance = 6.99%, receptivity relative to $^{13}C = 12.5$) and ^{123}Te ($I = 1/2$, natural abundance = 0.87%, receptivity relative to $^{13}C = 0.89$) are all NMR active, but ^{123}Te is seldom used because of its lower natural abundance [187]. In ^{77}Se and ^{125}Te NMR studies, the convention is that their chemical shifts are referenced to $(CH_3)_2Se$ and $(CH_3)_2Te$, respectively, at $\delta = 0$ ppm with the downfield shift associated with positive ppm values. ^{77}Se NMR spectroscopy has been applied to a larger extent than ^{125}Te, although both have the potential for characterizing metal complexes in solutions. The chemical shifts of both ^{77}Se and ^{125}Te are found to be extremely sensitive to their chemical environments. Due to low natural abundance of these two nuclei, the Se–Se, or Te–Te coupling is often unobservable. Occasionally, M–Q bond coupling to an NMR active metal can be observed. In a typical metal polychalcogenide complex, the ligand atoms are often in very different chemical environments (metal-bound, internal or bridging, etc.), thus the resonance pattern in its NMR spectrum can be very complex. In the absence of any homo-nuclear coupling information, the assignment of the different NMR resonances is not easy but several assignments have been made. For example, in the series of $[MX(Q_4)_2]^{2-}$ (M = Mo, W; X = O, Se; Q = Se, Te) and $[M(Se_4)_2]^{2-}$ (M = Ni, Pd, Pt, Zn, Cd, Hg) complexes, the NMR spectra have been completely assigned.

Within the $[WQ(Se_4)_2]^{2-}$ (Q = O, S, Se) series, the resonances corresponding to the metal-bound selenium atoms all exhibit couplings to W (^{183}W, $I = 1/2$, natural abundance = 14.3%) [64a,b]. This observation helps in assigning the resonances of the both the terminal and internal selenium atoms in the compounds. By analogy, similar assignments are then extended to the Mo (two quadrupolar nuclei: ^{95}Mo, $I = 5/2$, natural abundance = 15.7%; ^{97}Mo, $I = 5/2$, natural abundance = 9.5%) analogs of the above compounds [64b], as well as to the $[MO(Te_4)_2]^{2-}$ (M = Mo, W) system, where the Mo–Se, Mo–Te or W–Te couplings are not observed [72]. Table 2 gives the NMR data of these compounds.

Within the $[M(Se_4)_2]^{2-}$ (M = Ni, Pd, Pt) series, Pt has a spin-half nucleus (^{195}Pt, $I = 1/2$, natural abundance = 33.8%). In solution the $[Pt(Se_4)_2]^{2-}$ species generated in situ gives a two-line ^{77}Se NMR spectrum with $\delta = 727$ and 642 ppm. The resonance at 727 ppm shows coupling to ^{195}Pt, and is assigned to metal-bound selenium and the 642 ppm signal to the inner two selenium atoms of the Se_4^{2-} ligand. By analogy, similar assignments are made for the Ni and Pd analogs [86]. Detailed data are given in Table 2.

TABLE 2

^{77}Se and ^{125}Te NMR data for the $[MX(Q_4)_2]^{2-}$ (M = Mo, W; X = O, S, Se; Q = Se, Te) and $[M(Se_4)_2]^{2-}$ (M = Ni, Pd, Pt, Zn, Cd, Hg) series

Compound	Metal d electron configuration	δ (^1J(Q–M) Hz) (ppm)			Reference
		Metal-bound	Ring	Apical	
$[WO(Se_4)_2]^{2-}$	d^2	828(98)	280	–	[64b]
$[WS(Se_4)_2]^{2-}$	d^2	993(106)	313	–	[64b]
$[WSe(Se_4)_2]^{2-}$	d^2	1034(108)	324	1787	[64b]
$[MoO(Se_4)_2]^{2-}$	d^2	946	380	–	[64b]
$[MoS(Se_4)_2]^{2-}$	d^2	1122	396	–	[64b]
$[MoSe(Se_4)_2]^{2-}$	d^2	1163	403	2357	[64b]
$[WO(Te_4)_2]^{2-}$	d^2	903	120	–	[72]
$[MoO(Te_4)_2]^{2-}$	d^2	717(98)	89	–	[72]
$[Ni(Se_4)_2]^{2-}$	d^8	820	748	–	[86]
$[Pd(Se_4)_2]^{2-}$	d^8	893	758	–	[86]
$[Pt(Se_4)_2]^{2-}$	d^8	727(384)	642	–	[86]
$[Zn(Se_4)_2]^{2-}$	d^{10}	127	598	–	[86]
$[Cd(Se_4)_2]^{2-}$	d^{10}	62(255)	608	–	[86]
$[Hg(Se_4)_2]^{2-}$	d^{10}	76(1265)	594	–	[86]

Within the $[M(Se_4)_2]^{2-}$ (M = Zn, Cd, Hg) series, both Cd and Hg have spin-half nuclei (^{111}Cd, $I = 1/2$, natural abundance = 12.3%; ^{113}Cd, $I = 1/2$, natural abundance = 12.8% and ^{119}Hg, $I = 1/2$, natural abundance = 16.8%). The observed couplings in these two complexes allow unequivocal assignments for their ^{77}Se NMR spectra. The ^{77}Se NMR spectrum of the $[Zn(Se_4)_2]^{2-}$ is then assigned by analogy as shown in Table 2 [86].

By comparing the above assignments, a general shielding argument based on the metal d electron configuration has been advanced [86]. In the free Q_4^{2-} ligands, shielding arguments would predict that the terminal atoms resonate upfield of the internal atoms in accordance with the formal charge assignments on these atoms. Upon chelating to a metal ion with partially filled d orbitals, the electron density of these terminal (now metal-bound) atoms will decrease because of electron donation from the Q_4^{2-} ligand to the d orbitals of the metal. This will lead to NMR signals downfield of the resonances due to non-metal bound selenium atoms (see Table 2). However, if the metal ion has filled d orbitals (i.e. Zn, Cd or Hg), the electron donation from the ligand to the metal is claimed to be negligible leading to resonances upfield of the non-metal bound selenium atoms (Table 2).

It should be noted that the ^{77}Se NMR spectrum of $[Pt(Se_4)_3]^{2-}$ gives two signals at 680 and 790 ppm. The resonance at 680 ppm is assigned to the metal-bound Se atoms because of the observed Se–Pt coupling [98]. This is opposite to the trend defined above. Apparently, other factors must also be operative in affecting the resonance positions of Se atoms in polyselenides.

^{77}Se NMR spectroscopy was used to characterize the solution behavior of the In/Se_x^{2-} family of compounds. The ^{77}Se NMR spectra of $[In_2(Se_4)_4(Se_5)]^{4-}$, $[In_3Se_3(Se_4)_3]^{3-}$ and $[In_2Se_2(Se_4)_2]^{2-}$ in DMF solutions are all identical and show three peaks in 2:2:1 ratio at 643 ppm, 197 ppm and -244 ppm, respectively. This suggests that all complexes give rise to the same species in solution. It has been proposed that the most stable complex in solution is $[In_3Se_3(Se_4)_3]^{3-}$. The peak at 643 ppm can be tentatively assigned to resonance from the terminal Se atoms of the chelating Se_4^{2-} ligands and 197 ppm from the inner atoms of the Se_4^{2-} ligands while the –244 ppm is more reasonably assigned to the bridging Se^{2-} ligand. This assignment is consistent with the ^{77}Se NMR results reported for other metal polyselenide complexes discussed above. Intuitively, one would expect the dimeric $[In_2Se_2(Se_4)_2]^{2-}$ anion to possess higher energy ring-strain compared to the trimeric homologue, and therefore anticipate the latter to be the final solution product. Another destabilizing factor for the $[In_2Se_2]^{2+}$ core relative to the $[In_3Se_3]^{3+}$ core would be the stronger In---In Coulombic repulsion due to the closer proximity of the two In^{3+} atoms in the former. This repulsive force is somewhat dissipated in $[In_3Se_3(Se_4)_3]^{2-}$ due to the longer In---In distances in the corresponding $[In_3Se_3]^{3+}$ core (3.336 Å versus 3.69 Å, vide supra). Thus, it is reasonable to propose a solution rearrangement of $[In_2Se_2(Se_4)_2]^{2-}$ to the more stable $[In_2Se_2(Se_4)_3]^{2-}$ [130,131].

E. APPLICATIONS

(i) Thermal decomposition reactions

Conceptually, thermal decomposition of homoleptic complexes should eventually lead to binary metal chalcogenides. However, our thermal decomposition studies on various metal polyselenide compounds, using thermal gravimetric analysis (TGA), show that the final decomposition products sometimes depend on the decomposition properties of the precursor complexes. In addition to the bonding energetics in the different metal complexes, which affect the decomposition pathways, the counterions also have important influence. The leaving mechanism of these R_4N^+ (or R_4P^+) cations is provided by nucleophilic attack to an R– group by polyselenide to form volatile R_2Se_x (x = 1,2) species. Thus, some compounds give clean binary solid-state phases by thermal decomposition, others do not. For example, thermal decomposition of $(Ph_4P)_2[M(Se_4)_2]$ (M = Zn, Cd), $(Ph_4P)_2[Sn(Se_4)_3]$, $(Ph_4P)_2[Cu_4(Se_4)_3]$, $(Ph_4P)_2[Cu_2(Se_5)_2(Se_4)]$, $(Ph_4P)_4[In_2(Se_4)_4(Se_5)]$ and $(Et_4N)_3[M_3Se_3(Se_4)_3]$ (M = In, Tl), under inert atmosphere, gave single-phase products of their corresponding binary compounds, ZnSe, CdSe, $SnSe_2$, $Cu_{2-x}Se$, β-In_2Se_3 and TlSe, while $(Ph_4P)_2[Hg(Q_4)_2]$ (Q = Se, Te) decomposes to Hg vapor and Se or Te.

Figure 111 shows typical TGA diagrams of $(Ph_4P)_2[Cd(Se_4)_2]$, $(Ph_4P)_2[Cu_4(Se_4)_3]$ and $(Ph_4P)_2[Cu_2(Se_5)_2(Se_4)]$, while eqn. (30) gives a possible reaction route for the thermal decomposition of $(Ph_4P)_2[Cd(Se_4)_2]$ [131]:

$$(Ph_4P)_2[Cd(Se_4)_2] \xrightarrow{\Delta} CdSe + Ph_2Se + Ph_3P + Ph_3PSe + Se \quad (30)$$

In the cases where the thermal decomposition yields single phases of binary compounds, the metal complexes can be used as single source precursors for making thin films of solid-state chalcogenides. Investigations were carried out in this laboratory to fabricate crystalline films of CdSe, $Cu_{2-x}Se$, β-In_2Se_3, TlSe, and $CuInSe_2$ (co-thermolysis of Cu^+/Se_x^{2-} and In^{3+}/Se_x^{2-} complexes in appropriate molar ratio) from the following procedure [131]:

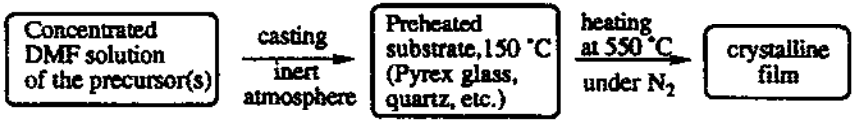

The phase identification and characterization of these metal chalcogenide films have been carried out by X-ray diffraction, scanning electron microscope (SEM), transmission electron microscope (TEM) and infrared spectroscopy [131]. One of the limitations of the molecular precursor method is the large weight-loss associated with pyrolysis which can result in cracked and discontinuous films. Although this can be avoided by preparing good precursor films, molecular precursors with high M/Se ratio are desired to help solve this problem.

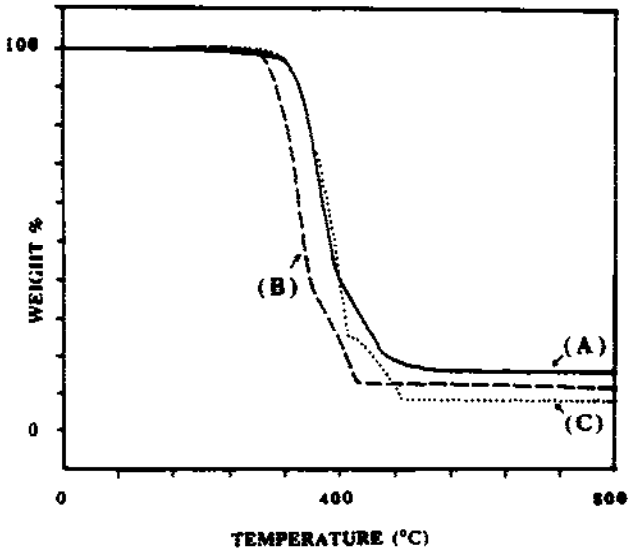

Figure 111. Typical TGA diagrams of $(Ph_4P)_2[Cd(Se_4)_2]$, $(Ph_4P)_2[Cu_4(Se_4)_3]$ and $(Ph_4P)_4[Cu_2(Se_5)_2(Se_4)]$.

(ii) Chalcogen-abstraction reactions

It is well known that Ph_3P, Bu_3P and CN^- can abstract sulfur atoms from polysulfide compounds. This type of reaction has also been extended to polyselenide complexes. Except for the aforementioned reactions of $(RCp)_2TiSe_5$ with Ph_3P (or Bu_3P) to give $[\{(\eta^5\text{-}RCp)_2Ti\}_2(\mu_2\text{-}Se_2)_2]$, and $[(dmpe)_2Ir(Se_4)]^+$ with Ph_3P to give $[(dmpe)_2Ir(Se_2)]^+$, other examples involving transformations of different polyselenide complexes are rare. However, the use of chalcogen-abstracting agents for removing all excess selenium atoms in a metal polyselenide complex should, in principle, lead to the binary solid-state compound. This chemistry has been extensively studied at this laboratory in hope of developing non-pyrolytic, low temperature routes to the technologically important metal chalcogenide semiconductors [46–48]. The virtue of this approach is that by controlling the reaction conditions, different particle sizes of semiconductors, ranging from quantum-size to bulk regime, can be obtained. This is because the growth of particles depends on the condensation of highly coordinatively unsaturated species generated during the reaction. The following is a general reaction scheme of this Se-abstracting chemistry:

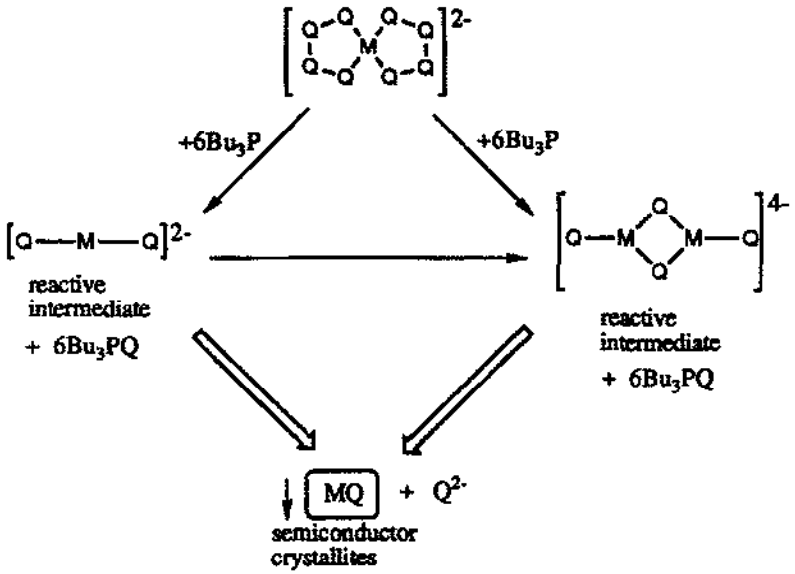

CdSe is formed from the exhaustive removal of Se by KCN or $(^nBu)_3P$ from $[Cd(Se_4)_2]^{2-}$ in DMF and DMSO. The particle size of CdSe is in the quantum size regime. The maximum crystallite size is obtained under reflux conditions. Tributylphosphine yields 60 Å crystallites, while KCN yields 120–150 Å crystallites. By comparison, other methods available for the synthesis of quantum-size CdSe yield particle sizes in the neighborhood of 35 Å [46,47].

The reaction of an appropriate mixture of $(Et_4N)_3[In_3Se_{15}]$ [130] and $(Ph_4P)_2[Cu_4Se_{12}]$ [104] with the appropriate amount of KCN (or $(^nBu)_3P$) in DMF at

60–155°C produces $CuInSe_2$ in 70% yield. Successive darkening of the solution is observed to form a colloidal suspension of $CuInSe_2$ which eventually precipitates. $CuInSe_2$ deposits directly in crystalline form and thus a subsequent annealing step is not required. When this Se-abstraction reaction is carried out individually with $[In_3Se_{15}]^{3-}$ or $[Cu_4Se_{12}]^{2-}$ the corresponding binary In_2Se_3 and CuSe are obtained. It is thus very interesting that a phase-separated mixture of In_2Se_3 and CuSe does not form. It is plausible that extremely small "embryo" clusters of In_2Se_3 and CuSe form first which immediately react to form $CuInSe_2$. The driving force for this would be the very high surface area of such small clusters, their intimate state of mixing, the favorable entropic component of the reaction (due to the formation of a ternary phase) and the considerable lattice energy gain from the formation of the very stable chalcopyrite structure. $CuInSe_2$ was uniquely identified by its X-ray powder diffraction pattern which is remarkably clean with regard to other crystalline phases. TEM studies reveal that the $CuInSe_2$ particles are in the submicrometer range.

The chalcogen-abstraction reaction is also suitable for the preparation of solid solutions (e.g. $Cd_{1-x}Hg_xSe$, $Cd_{1-x}Mn_xSe$) from which interesting materials such as dilute magnetic semiconductors could be obtained. Table 3 summarizes some nanocrystalline solid chalcogenides prepared by this method. In addition to being a mild and convenient route to solid chalcogenides this method also provides an opportunity to obtain and study many semiconductors in the quantum-size regime. This is especially useful in cases where the published methods (which work well for II–VI materials) cannot be generalized to other binary and particularly ternary semiconductors.

TABLE 3

Nanocrystalline solid chalcogenides prepared from molecular polychalcogenides

Compound	Structure	Precursor	Reagent	Max. particle size (Å)
CdSe	Wurtzite	$[Cd(Se_4)_2]^{2-}$	$(^nBu)_3P$	~60
			KCN	~150
HgSe	Sphalerite	$[Hg(Se_4)_2]^{2-}$	$(^nBu)_3P$	~100
			KCN	~10000[a]
CuSe	CuS type	$[Cu_4Se_{12}]^{2-}$	$(^nBu)_3P$	~240
			KCN	~450
SnSe	GeS type	$[Sn(Se_4)_3]^{2-}$	KCN	~1000[a]
MnSe	Wurtzite	$[Mn(Se_4)_2]^{2-}$	$(^nBu)_3P$	~500
HgTe	Sphalerite	$[Hg(Te_4)_2]^{2-}$	$(^nBu)_3P$	~5000[a]
$CuInSe_2$	Chalcopyrite	$[Cu_4Se_{12}]^{2-}/[In_3Se_{15}]^{3-}$	$(^nBu)_3P$	~100
			KCN	~5000[a]
$Cd_{1-x}Mn_xSe$	Wurtzite	$[Cd(Se_4)_2]^{2-}/[Mn(Se_4)_2]^{2-}$	$(^nBu)_3P$	~200–500

All particle size determinations were made using the Scherrer formula, except where indicated.
[a]Determined on a transmission electron microscope.

(iii) Reactions with activated acetylenes

Similar to the metal polysulfide complexes, reactions of MQ_n-containing (Q = Se, n = 2–5; Q = Te, n = 4) compounds with activated acetylenes give selenolene and tellurolene complexes (eqns. (31), (32) [188], eqn. (33) [189], eqn. (34) [72]):

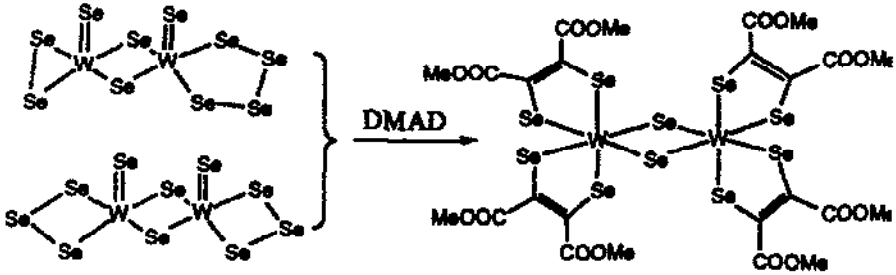

(31)

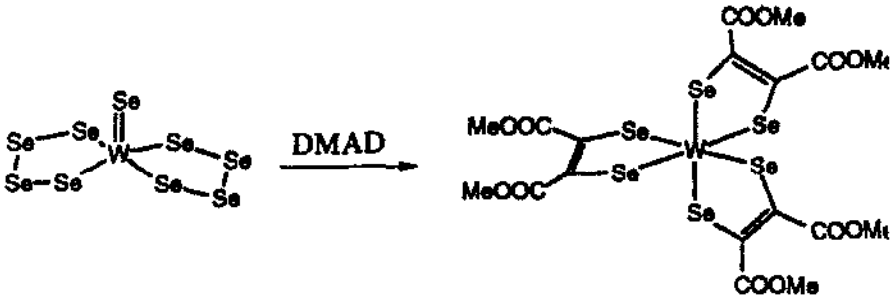

(32)

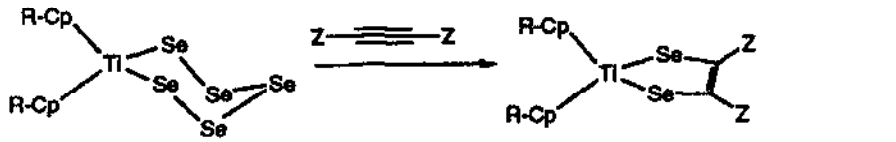

(33)

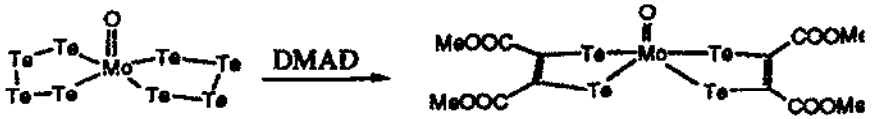

(34)

This type of chemistry closely parallels that of metal polysulfides reported earlier by Coucouvanis et al. [190].

F. OUTLOOK

Although great progress has been made in the last 6 years, we hope that the readers have been convinced that metal heavy polychalcogenide chemistry is still an emerging field with a great deal of questions remaining to be answered. This diversity can be

chiefly attributed to the fact that polychalcogenide ligands are keen to respond, by adjusting their coordination modes, to the demands of the metal ions, whether these demands are of electronic or steric nature. The versatile coordination abilities of these ligands are then manifested by the variety of structures exhibited by their metal complexes which can be discrete molecules, clusters and even polymeric networks. Of course, all this also undermines our ability to predict their structures at the current stage. On the other hand, different synthetic methods, such as conventional solution reactions, hydro(solvo)thermal techniques and molten salt syntheses are now beginning to emerge as powerful tools in this area The exploration of these different approaches promises to broaden the horizon of the coordination chemistry of metal polychalcogenides. Despite the large number of polychalcogenide compounds synthesized, many aspects of their reaction chemistry remain unexplored, and mechanistic issues have seldom been addressed thus far. Furthermore, the reactivity of these compounds towards other molecules also remains unexplored. Interest in this area, along with the synthesis of yet new metal heavy polychalcogenide compounds, is expected to grow.

NOTE ADDED IN PROOF

A nice review article dealing with the coordination chemistry of inorganic selenide and telluride ligands has recently been published [191]. A novel electrochemical synthesis of $(Bu_4N)_3[Au_3Te_4]$ and $(Ph_2P)_2[Au_2Te_4]$ was reported [192]. Several recent reports by Ibers et al. described the preparation of $(Ph_4P)_4[Ni_4Te_4(Te_2)_2(Te_3)_4]$ and $(Ph_4P)_4[Pt_4Te_4(Te_3)_6]$ [193] and the synthesis of the unusual metal polytelluride species $(Et_4N)_3[AuTe_7]$ [194]. The compounds $(Ph_4P)_2(Et_4N)[AgTe_7]$ and $(Ph_4P)_2[HgTe_7]$ [195] and the Et_4N^+ salts of $[M_2(Te_4)_3]^{4-}$ (M = Cu and Ag) [196] also appeared since the submission of the present review. The Ph_4P^+ salts of $[M_2(Te_4)_3]^{4-}$ anions were reported earlier by Dehnicke [105]. Finally, the X-ray single-crystal structures of $[Cs(18\text{-crown-}6)]_2Se_5 \cdot DMF$, $[Rb(222\text{-crypt})]_2Se_6$, $[Ba(15\text{-crown-}5)_2]Se_6 \cdot DMF$ and $[Na(12\text{-crown-}4)]_2Se_7$ were reported [197].

ACKNOWLEDGMENTS

Financial Support from the National Science Foundation, the Beckman Foundation and the Petroleum Research Fund is gratefully acknowledged. MGK is a NSF Presidential Young Investigator and an A.P. Sloan Fellow 1991–1993. We also thank our colleagues J.H. Liao, K.-W. Kim, S. Dhingra, Y. Park, T. McCarthy, A. Sutorik, A. Axtell, L. Hill for invaluable contributions to this work. We thank Professors Kurt Dehnicke, Ian Dance and Thomas Rauchfuss for making preprints available to us prior to publication.

REFERENCES

1 (a) N.N. Greenwood and A. Earnshaw, Chemistry of the Elements, Pergamon Press, Oxford UK, 1989, p. 757. (b) F. A. Cotton and G. Wilkinson, Advanced Inorganic Chemistry, 5th edition, Wiley, New York, 1988, p. 491.

2 Early investigations on the existence of the homopolychalcogenide anions in liquid ammonia solution can be found in: (a) C. Hugot, C.R. Hebd. Seances Acad. Sci., (1899) 219, 299, 388. (b) C. Hugot, Ann. Chim. Phys., 21 (1900) 72. (c) C. A. Kraus and C. Y. Chiu, J. Am. Chem. Soc, 14 (1922) 1999. (d) F.W. Bergstrom, J. Am. Chem. Soc., 48 (1926) 146. (e) E. Zintl, J. Goubeau and W. Dullenkopf, Z. Phys. Chem., Abt. A, 154 (1931) 1. (f) W. Klemm, H. Sodomann and P. Langmesser, Z. Anorg. Allg. Chem., 241 (1939) 281.

3 For recent spectroscopic studies of these species in polar solvents (i.e. en, NH_3 and DMF, etc.) see: (a) F. Seel, H.J. Guttler, G. Simon and A. Wieckowski, Pure Appl. Chem., 49 (1977) 45. (b) K.W. Sharp and W.H. Koehler, Inorg. Chem., 16 (1977) 2528. (c) L.D. Schultz and W.H. Koehler, Inorg. Chem., 26 (1987) 1989. (d) P. Dubois, J.P. Lelieur and G. Lepoutre, Inorg. Chem., 26 (1987) 1897. (e) P. Dubois, J.P. Lelieur and G. Lepoutre, Inorg. Chem., 27 (1987) 73. (f) P. Dubois, J.P. Lelieur and G. Lepoutre, Inorg. Chem., 27 (1988) 1883. (g) V. Pinon and J.P. Lelieur, Inorg. Chem., 30 (1991) 2260. (h) M. Bjorgvinsson and G.J. Schrobilgen, Inorg. Chem., 30 (1991) 2540.

4 Many anionic polychalcogenide chains have been isolated and structurally characterized as alkali salts, alkali-cryptates or using large organic counterions. These include S_n^{2-} ($n = 2$–7) [5–10], Se_n^{2-} ($n = 2$–9) [11–18], and Te_n^{2-} ($n = 2$–5) [19–22].

5 For S_2^{2-}, see: (a) H. Föppl, Angew. Chem., 70 (1958) 401. (b) H. Föppl, E. Busmann and F.-K. Frorath, Z. Anorg. Allg. Chem., 314 (1962) 12.

6 For S_3^{2-}, see: W.S. Miller and A.J. King, Z Kristallogr., Kristallgeom., Kristallphys., Kristallchem., 94 (1936) 439.

7 For S_4^{2-}, see: (a) S.C. Abrahams, Acta Crystallogr., 7 (1954) 423. (b) S. C. Abrabams and J. L. Bernstein, Acta Crystallogr., Sect. B, 25 (1969) 2365. (c) R. Tegman, Acta Crystallogr., Sect. B, 29 (1973) 1463.

8 For S_5^{2-}, see: (a) B. Leclerc and T.S. Kabre, Acta Crystallogr., Sect. B, 31 (1975) 1675. (b) B. Kelly and P. Woodward, J. Chem. Soc. Dalton Trans., (1976) 1314. (c) P. Böttcher, Kristallogr., 150 (1974) 651. (d) P. Böttcher and K. Kruse, J. Less-Common Metals, 83 (1982) 115.

9 For S_6^{2-}, see: (a) S.C. Abrahams and E. Grison, Acta Crystallogr., 6 (1953) 206. (b) A. Hordvik and E. Stetten, Acta Chem. Scand., 22 (1968) 3029. (c) R.G. Teller, L.J. Krause and R.C. Haushalter, Inorg. Chem., 22 (1983) 1809.

10 For S_7^{2-}, see: (a) H. Krebs and K.H. Müller, Z. Anorg. Allg. Chem., 275 (1954) 147. (b) M. G. Kanatzidis, N.C. Baenziger and D. Coucouvanis, Inorg. Chem., 22 (1983) 291.

11 For Se_2^{2-}, see: (a) G. Cordier, R. Cook and H. Schäfer, Angew. Chem. Int. Ed. Engl., 19 (1980) 324. (b) Ref. [5b].

12 For Se_3^{2-}, see: (a) H.G. Von Schnering and N.K. Goh, Naturwissenshaften, 61 (1974) 272. (b) P. Böttcher, Z. Anorg. Allg. Chem., 461 (1980) 13.

13 For Se_4^{2-}, see: (a) O. Foss and V. Janickis, J. Chem. Soc. Dalton Trans., (1980) 620. (b) T. König, B. Eisenmann and H. Schäfer, Z. Naturforsch., 37B (1982) 1245. (c) T. König, B. Eisenmann and H. Schäfer, Z. Anorg. Allg. Chem., 498 (1983) 99. (d) N.E. Brese, C.R. Randall and J.A. Ibers, Inorg. Chem., 27 (1988) 940.

14 For Se_5^{2-}, see: (a) U. Kretschmann and P. Böttcher, Z. Naturforsch., 40B (1985) 895. (b) C.-N. Chau, R.W.M. Wardle and J.A. Ibers, Acta Crystallogr., Sect. C, 44 (1988) 883. (c) W.S. Sheldrick and H.G. Braunback, Z. Naturforsch., 44B (1989) 1397. (d) G. Kräuter, K. Dehnicke and D. Fenske, Chem.-Ztg., 114 (1990) 7. (e) J. Dietz, U. Müller, V. Müller and K. Dehnicke, Z. Naturforsch., 46B (1991) 1293. (f) V. Müller, G. Frenzen, K. Dehnicke and D. Fenske, Z. Naturforsch., 47B (1992) 205. (g) Ref. [8c]. (h) Ref. [13d].

15 For Se_6^{2-}, see: (a) F. Weller, J. Adel and K. Dehnicke, Z. Anorg. Allg. Chem., 548 (1987) 125. (b) D. Fenske, C. Kraus and K. Dehnicke, Z. Anorg. Allg. Chem., 607 (1992) 109. (c)

R.G. Teller, L.J. Krause and R.C. Haushalter, Inorg. Chem., 22 (1983) 1809.
16 For Se_7^{2-}, see: V. Müller, K. Dehnicke, D. Fenske and G. Baum, Z. Naturforsch., 46B (1991) 63.
17 For Se_8^{2-}, see: R. Staffel, U. Müller, A. Ahle and K. Dehnicke. Z Naturforsch., 46B (1991) 1287.
18 For Se_9^{2-}, see: V. Müller, C. Grebe, U. Müller and K. Dehnicke, Z. Anorg. Allg. Chem., 619 (1993) 416.
19 For Te_2^{2-}, see: R.C. Burns and J.D. Corbett. J. Am. Chem. Soc., 103 (1981) 2627.
20 For Te_3^{2-}, see: (a) A. Cisar and J.D. Corbett, Inorg. Chem., 16 (1977) 632. (b) B. Eisenmann and H. Schäfer, Angew. Chem. Int. Ed. Engl., 17 (1978) 684. (c) P. Böttcher, J. Less-Common Metals, 70 (1980) 263.
21 For Te_4^{2-}, see: (a) J.C. Huffman and R.C. Haushalter, Z. Anorg. Allg. Chem., 518 (1984) 203. (b) L.A. Devereux, G.J. Schrobilgen and J.F. Sawyer, Acta Crystallogr., Sect. C, 41 (1985) 1730. (c) K.W. Klinkmammer and P. Böttcher, Z. Naturforsch., 45B (1990) 141. (d) H. Wolker, B. Schreiner, R. Staffel, U. Müller and K. Dehnicke, Z. Naturforsch., 46B (1991) 1015. (e) B. Schreiner and K. Dehnicke, Chem.-Ztg., 115 (1991) 326. (f) D. Fenske, G. Baum, H. Wolkers, B. Schreiner, F. Weller and K. Dehnicke, Z. Anorg. Allg. Chem., 619 (1993) 489.
22 For Te_5^{2-}, see: (a) P. Böttcher and U. Kretschmann, J. Less-Common Metals, 95 (1983) 81A. (b) P. Böttcher and U. Kretschmann, Z. Anorg. Allg. Chem., 491 (1982) 39. (c) Ref.[9c]. (d) Ref.[21f].
23 (a) R.R. Chianelli, Catal. Rev. Sci. Eng., 26 (1984) 361. (b) F.E. Massoth and G. Muralidhar, in H.P. Barry and P.C. Mitchell, Eds., Proceedings of the Climax Fourth International Conference on the Chemistry and Uses of Molybdenum, Climax Molybdenum Company, Ann Arbor, MI, 1982, p. 343.
24 M.R. Dubois, Chem. Rev., 89 (1989) 1.
25 D. Coucouvanis, D. Swenson, P. Stremple and C. N. Baenziger, J. Am. Chem. Soc., 101 (1979) 339.
26 (a) K.B. Krauskopf, Introduction to Geochemistry, McGraw Hill, New York, 1979. (b) T.B. Rauchfuss and E.R. Ramli, J. Am. Chem. Soc., 112 (1990) 4043.
27 M. Draganjac and T.B. Rauchfuss, Angew. Chem. Int. Ed. Engl., 24 (1985) 742.
28 (a) A. Müller, Polyhedron, 5 (1986) 323. (b) A. Müller and E. Diemann, Adv. Inorg. Chem., 31 (1987) 89.
29 M. Schmidt and R. Höller, Rev. Chim. Miner., 20 (1983) 763.
30 A.P. Ginsberg, W.E. Lindsell, C.R. Sprinkle, K.W. West and R.L. Cohen, Inorg. Chem., 22 (1983) 1781.
31 H. Köpf, B. Block and M. Schmidt, Chem. Ber., 101 (1968) 272.
32 H. Köpf, A. Wirl and W. Kahl, Angew. Chem. Int. Ed. Engl., 10 (1971) 137.
33 H. Köpf, W. Kahl and A. Wirl, Angew. Chem. Int. Ed. Engl., 9 (1970) 801.
34 H. Strasdeit, B. Krebs and G. Henkel, Inorg. Chim. Acta, 89 (1984) L11.
35 R.C. Haushalter, Angew. Chem. Int. Ed. Engl., 24 (1985) 433.
36 (a) W.A. Flomer and J.W. Kolis, J. Am. Chem. Soc., 110 (1988) 3682. (b) W.A. Flomer, S.C. O'Neal, W.T. Pennington, D. Jeter, A.W. Cordes and J.W. Kolis, Angew Chem. Int. Ed. Engl., 27 (1988) 1702.
37 B.W. Eichhorn, R.C. Haushalter, F.A. Cotton and B. Wilson, Inorg. Chem., 27 (1988) 4084.
38 (a) M.G. Kanatzidis and S.-P. Huang, J. Am. Chem. Soc., 111 (1989) 760. (b) M.G. Kanatzidis and S.-P. Huang, Angew. Chem. Int. Ed. Engl., 28 (1989) 1513.
39 M.G. Kanatzidis, Comments Inorg. Chem., 10 (1990) 161.
40 M.A. Ansari and J.A. Ibers, Coord. Chem. Rev., 100 (1990) 223.

41 J.W. Kolis, Coord. Chem. Rev., 105 (1990) 195.
42 H. Vahrenkamp, Adv. Organomet. Chem., 22 (1983) 169.
43 W.A. Herrmann, Angew. Chem. Int. Ed. Engl., 25 (1986) 56.
44 K.H. Whitmire, J. Coord. Chem., 17 (1988) 95.
45 J. Wachter, Angew. Chem. Int. Ed. Engl., 28 (1989) 1613.
46 S. Dhingra and M.G. Kanatzidis, in Better Ceramics Through Chemistry IV, Mater. Res. Soc. Symp. Proc., 204 (1991) 825.
47 S. Dhingra, K.-W. Kim and M.G. Kanatzidis, in Chemical Perspectives in Microelectronic Materials, Mater. Res. Soc. Symp. Proc., 204 (1991) 163.
48 K.-W. Kim, J.A. Cowen, S. Dhingra and M.G. Kanatzidis, in Chemical Processes in Inorganic Materials: Metal and Semiconductor Clusters, Mater. Res. Soc. Symp. Proc., 272 (1992) 27.
49 (a) R.A. Smith, Semiconductors, Cambridge University Press, Cambridge, UK, 1978, p. 438. (b) B.E. Bartlett et al., Infrared Phys., 9 (1969) 35.
50 Z.K. Kun, Solid State Technology, 31 (1988) L77.
51 A.A. Ballman, R.L. Byer, D. Eimerl, R.S. Feigelson, B.J. Feldman, L.S. Goldberg, N. Menyuk and C.L. Tang, Appl. Opt, 26 (1987) 224.
52 (a) J.R. Tuttle, D.S. Albin and R. Noufi, Solar Cells 27 (1989) 231. (b) K. Zeibel, in D.Y. Goswami, Ed., The Potential of $CuInSe_2$ and CdTe for Space Applications, 23rd Intersociety Energy Conversion Engineering Conference, Vol. 3, ASME, 1988, p. 97.
53 (a) M.S. Whittingham, Science, 192 (1976) 1126. (b) M.S. Whittingham, J. Solid State Chem., 29 (1979) 303.
54 (a) A.F. Wells, Structural Inorganic Chemistry, 5th edition, Clarendon Press, Oxford, UK, 1984, p. 1. (b) T.A. Bither, R.J. Bouchard, W.H. Cloud, P.C. Donohue and W.J. Siemons, Inorg. Chem., 7 (1968) 2208. (c) S. Jobic, R. Brec and J. Rouxel, J. Solid State Chem., 96 (1992) 169.
55 (a) J. Rouxel, A. Meerschaut, L. Guemas and P. Gressier, Ann. Chim. Fr., 7 (1982) 445. (b) A. Meerschaut, Ann. Chim. Fr. 7 (1982) 131.
56 J.D. Corbett, Chem. Rev., 85 (1985) 383.
57 K. Tatsumi, Y. Inoue, A. Nakamura, R.E. Cramer, W. VanDoorne and J.W. Gilje, Angew. Chem. Int. Ed. Engl., 29 (1990) 422.
58 Although exotic to the coordination chemist, the synthesis of solid-state compounds by using molten salts, such as alkali metal polychalcogenides, as solvents at mild temperatures (i.e. below 500 °C) is currently a very active area of research. For recent examples, see: (a) M.G. Kanatzidis, Chem. Mater., 2 (1990) 353. (b) P.M. Keane, Y.-J. Lu and J.A. Ibers, Acc. Chem. Res., 24 (1991) 223.
59 A.C. Sutorik and M.G. Kanatzidis, J. Am. Chem. Soc., 113 (1991) 7754.
60 A.C. Sutorik and M.G. Kanatzidis, Angew. Chem. Int. Ed. Engl. 31 (1992) 1594.
61 C.-N. Chau, R.W.M. Wardle and J.A. Ibers, Inorg. Chem., 26 (1987) 2740.
62 J.-H. Liao, L. Hill and M.G. Kanatzidis, Inorg. Chem., (1993) in press.
63 M. Draganjac, E. Simhon, L.T. Chan, M.G. Kanatzidis, N.C. Baenziger and D. Coucouvanis, Inorg. Chem., 21 (1982) 3321.
64 (a) R.W.M. Wardle, S. Bhaduri, C.-N. Chau and J.A. Ibers, Inorg. Chem., 27 (1988) 1747. (b) R.W.M. Wardle, C.H. Mahler C.-N. Chau and J. A. Ibers, Inorg. Chem., 27 (1988) 2790.
65 W.A. Flomer and J.W. Kolis, Inorg. Chem., 28 (1989) 2513.
66 (a) W. Clegg, G. Christou, C.D. Garner and G.M. Sheldrick, Inorg. Chem., 20 (1981) 1562. (b) W.-H. Pan, M.A. Harmer, T.R. Halbert and E.I. Stiefel, J. Am. Chem. Soc., 106 (1984) 459.
67 (a) A. Müller, M. Römer, C. Römer, U. Reinsch-Vogell, H. Bögge and U. Schimanski,

Monatsch. Chem., 116 (1985) 711. (b) S.A. Cohen and E.I. Stiefel, Inorg. Chem., 24 (1985) 4657.
68 S. Schreiner, L.E. Aleandri, D. Kang and J.A. Ibers, Inorg. Chem., 28 (1989) 392.
69 W. Tremel, Inorg. Chem., 31 (1992)1030.
70 A. Müller, E. Urichemeyer, H. Bögge, M. Penk and D. Rehder, Chimia, 40 (1986) 50.
71 S.C. O'Neal and J.W. Kolis, J. Am. Chem. Soc., 110 (1988) 1971.
72 W.A. Flomer and J.W. Kolis, Inorg. Chem., 28 (1989) 2513.
73 M. Draganjac, E. Simhon, L.T. Chan, M.G. Kanatzidis, N.C. Baenziger and D. Coucouvanis, Inorg. Chem., 21 (1982) 3321.
74 H.D. Block and R. Allmann, Cryst. Struct. Commun., 4 (1975) 53.
75 C.E. Briant, M.J. Calhorda, T.S.A. Hor, N.D. Howells and D.M.P. Mingos, J. Chem. Soc. Dalton Trans., (1983) 1325.
76 R.W.M. Wardle, C.-N. Chau and J.A. Ibers, J. Am. Chem. Soc., 109 (1987) 1859.
77 J.-H. Liao and M.G. Kanatzidis, unpublished results.
78 J.-H. Liao and M.G. Kanatzidis, J. Am. Chem. Soc., 112 (1990) 741.
79 Hydrothermal conditions have also been used to prepare metal monochalcogenides, see: (a) W.S. Sheldrick, Z. Anorg. Allg. Chem., 562 (1988) 23. (b) W.S. Sheldrick and H.-J. Häuser, Z. Anorg. Allg. Chem., 557 (1988) 98. (c) W.S. Sheldrick and H.-J. Häuser, Z. Anorg. Allg. Chem., 557 (1988) 105. (d) W.S. Sheldrick and J. Kaub, Z. Anorg. Allg. Chem., 535 (1986) 179. (e) J.B. Parise, Science, 251 (1991) 293. (f) J.B. Parise, J. Chem. Soc., Chem. Commun., (1990) 1553.
80 J.-H. Liao and M.G. Kanatzidis, Inorg. Chem., 31 (1992) 431.
81 J.-H. Liao and M.G. Kanatzidis, unpublished results.
82 A. Müller, S. Sarkar, R.G. Bhattacharyya, S. Pohl and M. Dartmann, Angew. Chem. Int. Ed. Engl., 17 (1978) 535.
83 H.P. Jensen and F. Woldbye, Coord. Chem. Rev., 29 (1979) 313.
84 S.C. O'Neal, W.T. Pennington and J.W. Kolis, Inorg. Chem., 29 (1990) 3134.
85 G. Kräuter, M.-L. Ha-Eierdanz, U. Müller and K. Dehnicke, Z. Naturforsch., 45B (1990) 695.
86 M.A. Ansari, C.H. Mahler, G.S. Chorghade, Y.-J. Lu and J.A. Ibers, Inorg. Chem., 29 (1990) 3832.
87 (a) A. Müller, E. Krickemeyer, H. Bögge, W. Clegg and G.M. Sheldrick, Angew. Chem. Int. Ed. Engl., 22 (1983)1006. (b) D. Coucouvanis, P.R. Patil, M.G. Kanatzidis, B. Detering and N.C. Baenziger, Inorg. Chem., 24 (1985) 24. (c) A. Müller, J. Schimanski, U. Schimanski and H. Bögge, Z. Naturforsch., 40B (1985) 1277.
88 D. Coucouvanis, D. Swenson, P. Stremple and N.C. Baenziger, J. Am. Chem. Soc., 101 (1979) 3392.
89 U. Müller, M.-L. Ha-Eierdanz, G. Kräuter and K. Dehnicke, Z. Naturforsch., 46B (1991) 175.
90 K.-W. Kim and M.G. Kanatzidis, unpublished results.
91 S.-P. Huang and M. G. Kanatzidis, unpublished results.
92 (a) R.M.H. Banda, J. Cusick, M.L. Scudder, D.C. Craig and I.G. Dance, Polyhedron, 8 (1989) 1995. (b) A. Ahle, B. Neumüller, J. Pebler, M. Atanasov and K. Dehnicke, Z. Anorg. Allg. Chem., 615 (1992) 1.
93 R.D. Adams, T.A. Wolfe, B.W. Eichhorn and R.C. Haushalter, Polyhedron, 8 (1989) 701.
94 (a) M.G. Kanatzidis, Acta Crystallogr., Sect. C, 47 (1991) 1193. (b) H. Wolkers, K. Dehnicke, D. Fenske, A. Khassanov and S. S. Hafner, Acta Crystallogr., Sect. C, 47 (1991) 1627.
95 (a) A.E. Wickenden and R.A. Kraus, Inorg. Chem., 8 (1969) 779. (b) M. Schmidt and G.G. Hoffmann, Z. Anorg. Allg. Chem., 452 (1979) 112.

96 (a) P.E. Jones and L. Katz, J. Chem. Soc. Chem. Commun., (1967) 8420. (b) P.E. Jones and L. Katz, Acta Crystallogr., Sect. B, 25 (1969) 745. (c) M. Schmidt, Angew. Chem. Int. Ed. Engl., 12 (1973) 445. (d) M. Spangenberg and W. Bronger, Z. Naturforsch., 33B (1978) 4821.
97 K.-W. Kim and M.G. Kanatzidis, Inorg. Chem. in press.
98 M.A. Ansari and J.A. Ibers, Inorg. Chem., 28 (1989) 4068.
99 (a) J.M. McConnachie, M.A. Ansari and J.A. Ibers, J. Am. Chem. Soc., 113 (1991) 7078. (b) J.M. McConnachie, M.A. Ansari and J.A. Ibers, Inorg. Chim. Acta, 198–200 (1992) 85.
100 P.S. Haradem, J.L. Cronin, R.L. Krause and L. Katz, Inorg. Chim. Acta, 25 (1977) 173 and refs. therein.
101 K.-W. Kim and M.G. Kanatzidis, J. Am. Chem. Soc., 114 (1992) 4878.
102 (a) C. Burschka, Z. Naturforsch, 35B (1980) 1511. (b) A. Müller and U. Schimanski, Inorg. Chim. Acta, 77 (1983) L187. (c) A. Müller, F.-W. Baumann, H. Bögge, M. Römer, E. Krickemeyer and K. Schmitz, Angew. Chem. Int. Ed. Engl., 23 (1984) 632. (d) A. Müller, N. H. Schlanderbeck, E. Krickemeyer, H. Bögge, K. Schmitz, E. Bill and A. X. Trautwein, Z. Anorg. Allg. Chem., 570 (1989) 7. (e) G. Kiel, G. Gattow and T. Dingeldein, Z. Anorg. Allg. Chem., 596 (1991) 111.
103 U. Müller, M.-L. Ha-Eierdanz, G. Kräuter and K. Dehnicke, Z. Naturforsch., 45B (1990) 1128.
104 J. Cusick, M.L. Scudder, D.C. Craig and I.G. Dance, Polyhedron, 8 (1989) 1139.
105 D. Fenske, B. Schreiner and K. Dehnicke, Z. Anorg. Allg. Chem., 619 (1993) 253.
106 K.-W. Kim and M.G. Kanatzidis, J. Am. Chem. Soc., 115 (1993) 5871.
107 S.-P. Huang and M.G. Kanatzidis, Inorg. Chem., 30 (1991) 1455.
108 M.G. Kanatzidis and S.-P. Huang, Inorg. Chem., 28 (1989) 4667.
109 B. Krebs, private communication to Böttcher 1986, see: P. Böttcher, Angew. Chem. Int. Ed. Engl., 27 (1988) 759.
110 S.-P. Huang and M.G. Kanatzidis, Inorg. Chem., 30 (1991) 3572.
111 R.C. Haushalter, Inorg. Chim. Acta, 102 (1985) L37.
112 M.G. Kanatzidis and S.-P. Huang, Phosphorus, Sulfur, Silicon, 64 (1992) 15.
113 S.-P. Huang and M.G. Kanatzidis, unpublished results.
114 S. Magull, B. Neumüller and K. Dehnicke, Z. Naturforsch., 46B (1991) 985.
115 J. Adel, F. Weller and K. Dehnicke, Z. Naturforsch., 43B (1988) 1094.
116 B. Neumüller, M.-L. Ha-Eierdanz, U. Müller, S. Magull, G. Kräuter and K. Dehnicke, Z. Anorg. Allg. Chem., 609 (1992) 12.
117 G. Kräuter, F. Weller and K. Dehnicke, Z. Naturforsch., 44B (1989) 444.
118 S. Magull, K. Dehnicke and D. Fenske, Z. Anorg. Allg. Chem., 608 (1992) 17.
119 S. Dhingra and M.G. Kanatzidis, unpublished results.
120 D. Fenske, S. Magull and K. Dehnicke, Z. Naturforsch., 46B (1991) 1011.
121 K.-W. Kim and M.G. Kanatzidis, Inorg. Chem., 30 (1991) 1967.
122 (a) K.-W. Kim and M.G. Kanatzidis, unpublished results. (b) K. Dehnicke et al., private communication. (c) K.-W. Kim, PhD Dissertation, Michigan State University, 1993.
123 U. Müller, C. Grebe, B. Neumüller, B. Schreiner and K. Dehnicke, Z. Anorg. Allg. Chem., 619 (1993) 500.
124 Among the first known soluble molecular species of Group 13 chalcogenides are the monochalcogenide compounds $[M_4Q_{10}]^{8-}$ (for M = Ga, Q = S and for M = In, Q = S or Se) see: B. Krebs, D. Voelker and K.-O. Stiller, Inorg. Chim. Acta, 65 (1982) L101.
125 S. Dhingra and M.G. Kanatzidis, Inorg. Chem., 32 (1993) 3300.
126 S. Dhingra and M.G. Kanatzidis, Polyhedron, 10 (1991) 1069.
127 M.G. Kanatzidis and S. Dhingra, Inorg. Chem., 28 (1989) 2024.

128 A.I. Hadjikyriacou and D. Coucouvanis, Inorg. Chem., 26 (1987) 2400.
129 (a) C. Burschka, Z. Naturforsch, B35 (1980) 1511. (b) A. Müller, F.-W. Baumann, H. Bögge, M. Römer, E. Krickemeyer and K. Schmitz, Angew. Chem. Int. Ed. Engl., 23 (1984) 632.
130 S. Dhingra and M.G. Kanatzidis, Inorg. Chem., 32 (1993) 1350.
131 S. Dhingra, Ph.D. Thesis, Michigan State University, 1992.
132 S. Dhingra and M. G. Kanatzidis, unpublished results.
133 S. Dhingra, F. Liu and M.G. Kanatzidis, Inorg. Chim Acta, 210 (1993) 237.
134 S. Dhingra and M.G. Kanatzidis, Science, 258 (1992) 1769.
135 (a) S.-P. Huang, S. Dhingra and M.G. Kanatzidis, Polyhedron, 9 (1990) 1389. (b) R.M.H. Banda, J. Cusick, M.L. Scudder, D.C. Craig and I.G. Dance, Polyhedron, 8 (1989) 1999.
136 (a) B. Krebs, H.-U. Mürter, J. Enaxl and R. Fröhlich, Z. Anorg. Allg. Chem., 581 (1990) 141. (b) C.H. Belin and M.M. Charbonnel, Inorg. Chem., 21 (1982) 2504. (c) M.A. Ansari, J.A. Ibers, S.C. O'Neal, W.T. Pennington and J.W. Kolis, Polyhedron, 11 (1992) 1877. (d) C.H. Belin, C. R. Acad. Sci., t. 298, 16 (1984) 691. (e) W.S. Sheldrick and J. Kaub, Z Naturforsch., 40B (1985) 1020. (f) E.J. Porter and G.M. Sheldrick, J. Chem. Soc. A, (1971) 3130. (g) V. Angilella, H. Mercier and C. Belin, J. Chem. Soc., Chem. Commun., (1989) 1654. (h) C. Belin, V. Angilella and H. Mercier, Acta Crystallogr., Sect. C, 47 (1991) 61. (i) R. Haushalter, J. Chem. Soc., Chem. Commun., (1987) 19.
137 S.-P. Huang, S. Dhingra and M.G. Kanatzidis, Polyhedron, 11 (1992) 1869.
138 B. Krebs, E. Lührs, R. Willmer and F.-P. Ahlers, Z Anorg. Allg. Chem., 592 (1991) 17.
139 R. Zagler and B. Eisenmann, Z. Naturforsch., 46B (1991) 593.
140 D. Fenske, G. Kräuter and K. Dehnicke, Angew. Chem. Int. Ed. Engl., 29 (1990) 390.
141 W.S. Sheldrick and H.G. Braunbeck, Z. Naturforsch., 44B (1989) 1397.
142 D. Fenske, J. Adel and K. Dehnicke, Z. Naturforsch., 42B (1987) 931.
143 N. Albrecht and E. Weiss, J. Organomet. Chem., 355 (1988) 89.
144 P. Pekonen, Y. Hiltunen, R.S. Laitinen and J. Valkonen, Inorg. Chem., 30 (1991) 1874.
145 D.M. Giolando, M. Papavassiliou, J. Pickardt, T.B. Rauchfuss and R. Steudel, Inorg. Chem., 27 (1988) 2596.
146 P.G. Maué and D. Fenske, Z. Naturforsch., 43B (1988) 1213.
147 (a) C.M. Bolinger, T.B. Rauchfuss and A.L. Rheingold, Organometallics, 1 (1982) 1551. (b) A.L. Rheingold, C.M. Bolinger and T.B. Rauchfuss, Acta Crystallogr., Sect. C, 42 (1986) 1878.
148 D. Fenske, J. Ohmer, J. Hachgenei and K. Merzweiler, Angew. Chem. Int. Ed. Engl., 27 (1988) 1277.
149 J. Adel, F. Weller and K. Dehnicke, J. Organomet. Chem., 347 (1988) 343.
150 S.C. O'Neal, W.T. Pennington and J.W. Kolis, Organometallics, 8 (1989) 2281.
151 L.Y. Goh, C. Wei and E. Sinn, J. Chem. Soc., Chem. Commun., (1985) 462.
152 W.A. Herrmann and J. Rohrmann, Chem. Ber., 119 (1986) 1437.
153 W.A. Flomer, S.C. O'Neal, J.W. Kolis, D. Jeter and A.W. Coraes, Inorg. Chem., 27 (1988) 969.
154 L.A. Roof, W.T. Pennington and J.W. Kolis, Inorg. Chem., 31 (1992) 2056.
155 O. Scheidsteger, G. Huttner, K. Dehnicke and J. Pebler, Angew. Chem. Int. Ed. Engl., 24 (1985) 428.
156 L.C. Roof, W.T. Pennington and J.W. Kolis, J. Am. Chem. Soc., 112 (1990) 8172.
157 S.-P. Huang and M. G. Kanatzidis, unpublished results.
158 M. Herberhold, D. Reiner and U. Thewalt, Angew. Chem. Int. Ed. Engl., 22 (1983) 1000.
159 M. Herberhold, D. Reiner and U. Thewalt, Z. Naturforsch., 35B (1980) 1281.
160 M.L. Steigerwald and C.E. Rice, J. Am. Chem. Soc., 110 (1988) 4228.

161 W.A. Herrmann, C. Hecht, E. Herdtweck and H.-J. Kneuper, Angew. Chem. Int. Ed. Engl., 26 (1987) 13.
162 S.C. O'Neal, W.T. Pennington and J.W. Kolis, Can. J. Chem., 67 (1989) 1980.
163 S.-P. Huang and M.G. Kanatzidis, unpublished results.
164 W. Hieber and J. Gruber, Z. Anorg. Allg. Chem., 296 (1958) 91.
165 W. Hieber and W. Beck, Z. Anorg. Allg. Chem., 305 (1969) 2651.
166 (a) C.H. Wei and L.F. Dahl, Inorg. Chem., 4 (1965) 16. (b) C.F. Campana, F.Y.-K. Lo and L.F. Dahl, Inorg. Chem., 18 (1979) 3060.
167 D.L. Lesch and T.A. Rauchfuss, Inorg. Chem., 20 (1981) 3583.
168 S.-P. Huang and M.G. Kanatzidis, Inorg. Chem., 32 (1992) 82.
169 K.S. Rose, E. Sinn and B.A. Averill, Organometallics, 3 (1984) 1.
170 S.-P. Huang and M.G. Kanatzidis, unpublished results.
171 T.A. Rauchfuss, S. Dev and S.R. Wilson, Inorg. Chem., 31 (1992) 153.
172 B.W. Eichhorn, R.C. Haushalter and J.S. Merola, Inorg. Chem., 29 (1990) 728.
173 M.L. Steigerwald, Chem. Mater., 1 (1989) 52.
174 L.C. Roof, W.T. Pennington and J.W. Kolis, Angew. Chem. Int. Ed. Engl., 31 (1992) 153.
175 (a) J.M. Berg and R.H. Holm, in T.G. Spiro, Ed., Iron-Sulfur Proteins, Wiley, New York, 1982, Ch. 1. (b) B. Krebs and G. Henkel, Angew. Chem. Int. Ed. Engl., 30 (1991) 769.
176 M. Draganjac, S. Dhingra, S.-P. Huang and M.G. Kanatzidis, Inorg. Chem., 29 (1990) 590.
177 J. Amarasekera, E.J. Houser, T.A. Rauchfuss and C.L. Stern, Inorg. Chem., 31 (1992) 1614.
178 S.-P. Huang and M.G. Kanatzidis, J. Am. Chem. Soc., 114 (1992) 5477.
179 D.H. Farrar, K.R. Grundy, N.C. Payne, W.R. Roper and A. Walker, J. Am. Chem. Soc., 101 (1979) 6577.
180 M.L. Steigerwald, T. Siegrist and S. M. Stuczynski, Inorg. Chem., 30 (1991) 4940.
181 (a) H. Brunner, W. Meier, B. Nuber, J. Wachter and M.L. Ziegler, Angew. Chem. Int. Ed. Engl., 25 (1986) 907. (b) H. Brunner, N. Janietz, W. Meier, J. Wachter, E. Herdtweck, W.A. Herrmann, O. Serhadli and M.L. Ziegler, J. Organomet. Chem., 347 (1988) 237.
182 C. Bianchini, C. Mealli, A. Meli and M. Sabat, J. Am. Chem. Soc., 107 (1985) 5317.
183 A.P. Ginsberg, W.E. Lindsell, C.R. Sprinkle, K.W. West and R.L. Cohen, Inorg. Chem., 21 (1982) 3666.
184 A.J. Kahaian, J.B. Thoden and L.F. Dahl, J. Chem. Soc., Chem. Commun., (1992) 353.
185 S. Dev, E. Ramli, T.B. Rauchfuss and C.L. Stern, J. Am. Chem. Soc., 112 (1990) 6385.
186 J. Sola, Y. Do, J.M. Berg and R.H. Holm, Inorg. Chem., 24 (1985) 1706.
187 H.C.E. McFarlane and W. McFarlane, in R.K. Hanis and B.E. Mann, Eds., NMR and the Periodic Table, Academic Press, New York, 1978, p. 402.
188 M.A. Ansari, C.H. Mahler and J.A. Ibers, Inorg. Chem., 28 (1989) 2669.
189 C.M. Bolinger and T.A. Rauchfuss, Inorg. Chem., 21 (1982) 3947.
190 D. Coucouvanis, A. Hadjikyriacou, A. Toupadakis, S.-M. Koo, O. Ileperuma, M. Draganjac and A. Salifoglou, Inorg. Chem., 30 (1991) 754.
191 L.C. Roof and J.W. Kolis, Chem. Rev., 93 (1993) 1037
192 C.J. Warren, D.M. Ho, A.B. Bocarsly and R.C. Haushalter, J. Am. Chem. Soc., 115 (1993) 6416.
193 J.M. McConnachie, J.C. Bollinger and J.A. Ibers, Inorg. Chem., 32 (1993) 3923.
194 M.A. Ansari, J.M. McConnachie and J.A. Ibers, J. Am. Chem. Soc., 115 (1993) 3838.
195 J.M. McConnachie, M.A. Ansari, J.C. Bollinger, R.J. Salm and J.A. Ibers, Inorg. Chem., 32 (1993) 3201.
196 M.A. Ansari, J.C. Bollinger and J.A. Ibers, Inorg. Chem., 32 (1993) 1747.
197 V. Muller, A. Ahle, G. Frenzen, B. Neumuller and K. Dehnicke, Z. Anorg. Allg. Chem., 619 (1993) 1247.